Liprin-alpha Proteins Regulate Neuronal Development and Synapse Function

Liprin-alpha eiwitten reguleren neuronale ontwikkeling
en synaps functie

Proefschrift

ter verkrijging van de graad van doctor aan de
Erasmus Universiteit Rotterdam
op gezag van de rector magnificus
Prof.dr. H.G. Schmidt
en volgens besluit van het College voor Promoties

De openbare verdediging zal plaatsvinden op
woensdag 18 november 2009 om 15.30 uur

door

Samantha Ann Spangler
Geboren te Charlotte, NC, USA

ERASMUS UNIVERSITEIT ROTTERDAM

Promotiecommissie

Promotor: Prof.dr. C.I. de Zeeuw

Overige leden: Prof.dr. J.G.G. Borst
                      Prof.dr. Y. Elgersma
                      Dr. A. Akhmanova

Copromotor: Dr. C.C. Hoogenraad

Table of Contents

Chapter 1

Introduction

1.1. General introduction

Cells are the fundamental building blocks of life, yet there are innumerable processes that take place within a single cell. On average, the human body contains about 100 trillion cells, each of which has evolved to serve a specific purpose. Amongst the largest and most complex of these cells are those that make up the brain. The brain consists of two primary cell types, neurons and glia. Glial cells are responsible for supporting neurons in a variety of ways and are crucial for axon myelination, cleanup of cellular debris, neuronal migration, and formation of the blood-brain barrier, among other things[1]. Neurons are unique in that they communicate with each other at synapses, specialized sites of cell-cell contact of which the average human brain contains 100-500 trillion. The proper establishment of synaptic contacts and synaptic transmission is critical not only for the performance of basic, involuntary tasks such as breathing and the regulation of blood flow, but for carrying out both simple and complex behaviors including walking, talking, and learning. Synaptic transmission depends on the concentration of specific proteins on both sides of the synapse and their segregation between different kinds of synapses. Inhibitory and excitatory synapses, containing different sets of proteins, are present and functional within a few micrometers of each other along the same dendrite. Together, the signals received at these synapses determine the activity level of the entire neuron and ultimately its participation within complex neural networks. Cellular neuroscience as it currently exists owes its foundations to the work of Camillo Golgi and Santiago Ramón y Cajal in the late 1800s. Their discovery that the brain is made up of individual cells which function to signal to one another laid the basis for our understanding of brain organization, neuronal cell types, and intracellular signaling. Research in the years following those initial descriptions of brain cells has led to immense amounts of knowledge regarding the physiological communication between neurons, the roles of different brain regions and cell types in different behaviors, and the processes which take place within a single neuron.

1.2. Cell biology of neurons

During the last two decades major steps have been taken towards understanding the molecular and cellular mechanisms underlying brain function. Much progress has been made by the cloning of neurotransmitter receptors, the determination of SNARE

function at presynapses, the investigation of postsynaptic density (PSD) proteomics, and the elucidation of receptor trafficking mechanisms involved in long-term potentiation and long-term depression. Electrophysiological techniques such as extracellular and whole-cell patch clamp recordings *in vitro* and *in vivo* have yielded invaluable amounts of information critical to unraveling the mechanisms of synapse function and development. Additionally, genetic approaches have unique benefits to neuroscience research. The phenotypes of knock-out and mutant mice remain the best approximation of gene function in humans, and genetic screening in *C.elegans* and *Drosophila* is a powerful tool for the isolation of genes that affect synapse formation, growth, and stability.

Cell biological approaches have complemented genetics, biochemistry, and electrophysiology in the study of the mechanisms of neuronal function and development. This has led to the development of tools with which to investigate the workings of the brain at the systems and cognitive levels. Already we can visualize GFP-filled dendritic spines being altered by experience in the brain of transgenic mice[2], view the real-time activation of neuronal circuits in behaving animals[3], and visualize synaptogenesis with highly developed molecular tools[4]. Additionally, our understanding of neuronal structure and function has increased tremendously through the use of primary culture techniques that allow brain cells to develop their normal morphological characteristics and the specialization of subdomains, such as growth cones, axon initial segment, dendritic spines, and inhibitory and excitatory synapses, *in vitro*. Primary neuron culture has become an important tool in neuronal cell biology, especially when combined with the ability to transfect, stain, and live image neurons to address the function of specific proteins in their native cellular context.

1.2.1 Neuronal cultures as a model for how the brain works

Like several other specialized cell types, neurons consist of unique organelles (e.g., synaptic vesicles), cellular structures (e.g., chemical synapses), and activities (e.g., synaptic plasticity). But what makes neuronal cell biology so important, and how is it similar and different from general cell biology? The characteristics of the space in which a cell grows are very important for its development. Neurons serve as a prime example of this on account of their expansive morphology and complex intracellular organization. While other cell types establish polarity, neurons are the only cells that develop axons and dendrites which accumulate specific proteins and have distinct

physiological functions. Since axonal and dendritic compartments are easily identified and segregated from one another and neuronal signaling is clearly regulated temporally and spatially and in response to known extracellular signals, neurons are a unique environment that is especially suited to the study of cellular processes that are harder to investigate in non-neuronal cells. For example, most of our knowledge of regulated exocytosis[5], long distance microtubule-based transport[6], receptor scaffolding[7] and diffusion[8], and local mRNA translation[9, 10] comes from work done in neuronal cells rather than heterologous cell lines.

How useful, though, are neuronal cultures for understanding the function of the brain? Knowing about what goes on inside a single neuron will obviously not explain how the brain processes visual images or how it makes decisions. However, the relationship between cell biology of neurons and ultimate function of the entire brain has been shown on many occasions. It is still exceedingly difficult to study the molecular characteristics of individual neurons in an efficient and controlled manner within an intact and living brain. However, it is feasible to investigate the development and behavior of live CNS neurons in culture[11]. Some aspects of neuronal communication can be studied with much higher resolution and much greater control in neuron culture systems, where the underlying physiological processes and molecular mechanisms can be examined more precisely and thoroughly than in the intact brain. The more dynamic approaches and applications in neuronal cell biology (e.g., the turnover of synapses and synaptic receptors) allow for more accurate and direct study of the dynamic organization of the brain and remodeling of neural circuits. This has led to tremendous progress in our understanding of synaptic development, transmission, and signaling, which can then be translated into a more reliable and complete interpretation of electrophysiological and behavioral data from more intact model systems.

1.2.2 Development of neurons in culture

Primary culture of neurons has always been more difficult than culturing non-neural cells and did not become routine until the late 1980s[12]. Dissociated culture disperses neurons into a two-dimensional layer, making it easier to analyze specific morphological parameters (such as density of synapses, growth of axons and dendrites, and morphogenesis of dendritic spines), to identify the subcellular distribution of specific molecules, and to follow some processes over time by live cell imaging. Hippocampal neurons in culture are most often derived from the hippocampi of embryonic rats a few

DIV2	DIV5	DIV12	DIV19

Axon Differentiation	Axon Growth	Dendrite Growth	Spine Development
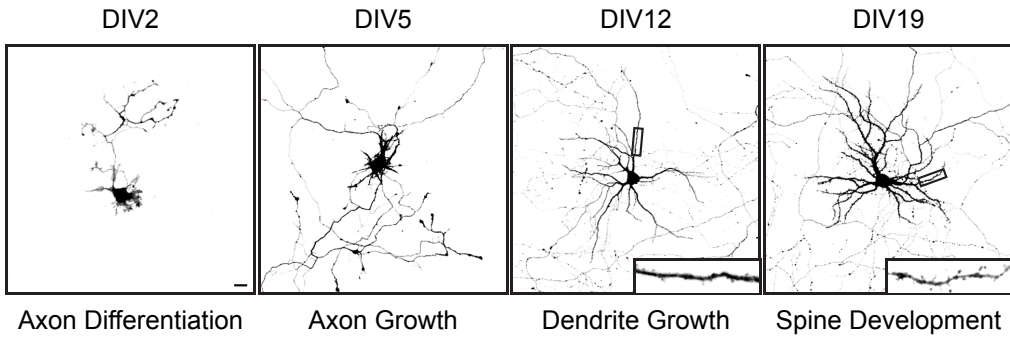
Figure 1.1. *Development of primary hippocampal neuron cultures.*
From left to right, representative images of neurons after 2, 5, 12, and 19 days *in vitro* (DIV2-DIV19). Box indicates zoomed in region. Scale bar, 10 μm.

days before birth (E16-E19). Once they are plated, neurons adhere to the culture dish and almost immediately begin to develop processes that will later become axons and dendrites. After only one to two days *in vitro* (DIV1-2, Figure 1.1), neurons appear asymmetrical, with one neurite having grown significantly more than the others. Over the next few days, this process continues to grow rapidly and begins to branch, eventually displaying the morphological characteristics of an axon. The other processes begin to grow and differentiate into dendrites around DIV4, with dendritic growth peaking from DIV5-7 (Figure 1.1)[13]. After this stage, neuronal polarity is considered to be completely established and neurons continue to grow and mature, forming elaborate networks of axonal and dendritic branches that communicate with each other at functional synapses.

1.2.3 Techniques – transfection, staining, and imaging of cultured neurons

As opposed to the hippocampus *in vivo*, hippocampal neurons in culture are easy to distinguish from one another and can be manipulated in a variety of different ways to facilitate the investigation of all manners of cellular processes that are vital to neuronal function. Exogenous genes can be easily introduced into neurons at any stage in culture, from just plated to fully mature, by electroporation, transfection, or viral infection[14]. These genes can encode full length proteins fused to a fluorescent tag to allow for visualization inside the cell, or truncated or mutated proteins that behave differently than the endogenous protein to highlight the importance of particular functions of a given protein. Moreover, the expression of endogenous proteins can be disrupted by the expression of short hairpin (sh) or small interfering (si) RNAs, a process known

as RNA interference (RNAi)[15]. Additionally, antibodies designed against native proteins inside the neurons can be used to illuminate their subcellular localizations. Since these tools are useful throughout the lifetime of cultured neurons, they allow for the isolated and rapid examination of most of the processes involved in the development, function, and plasticity of CNS neurons.

Perhaps most advantageous, since primary neuron cultures grow in a monolayer on a glass coverslip, they are easily accessible for fixed and live imaging. In the absence of the depth of tissue surrounding the densely packed neurons inside an intact brain, individual neurons are easily identified and can be imaged at high resolution and for extended periods of time. Confocal microscopy allows for the identification of small clusters of proteins and the observation of their trafficking within the cell with three-dimensional resolution. Furthermore, processes ranging from axon growth and branching to the release of synaptic vesicles in response to membrane depolarization can be imaged in real-time in living neurons. The discovery of fluorescent proteins[16-18] and the continuing development of more versatile and stable variants of fluorescent proteins[19, 20] provides numerous opportunities for the visualization of neuronal growth, development, and function in living cells, and in a reduced system such as primary neuron cultures, the degree of control that can be exerted over the neuron is immense. In all, these techniques make primary neuron cultures an ideal system for studying the fundamental cell biology of neurons, and greater understanding of the way an individual neuron works leads to better interpretation of the data obtained from more *in vivo* preparations.

1.3 Axon Growth, Guidance, and Targeting

As described above, there are multiple processes that characterize the development of a newly differentiated neuron into a fully mature one. Of these, four stand out as major and distinct components of neuronal maturation. In order to function properly as a member of a neuronal circuit, a neuron must send out an axon which can travel long distances and reliably make the correct synaptic contacts and develop a dendritic tree that is capable of integrating the signals received from synaptic contacts. It must build functional pre- and postsynaptic sites that release synaptic vesicles in response to an action potential and respond to the release of vesicles from connected neurons and modify these synaptic contacts in response to their activity.

The first to occur is the growth of the axon (Figure 1.1)[13], the neurite which will be responsible for the propagation of action potentials and the sending of signals to other neurons. *In vitro*, axons grow at an average rate of 60 μm per day[13]. Axons *in vivo* have to travel long distances to very specific targets, sometimes more than one meter in humans, thus necessitating rapid growth and efficient pathfinding[21]. The molecular cues responsible for axon growth, guidance, and turning, as well as eventual target selection are still under investigation, though some, for example semaphorins and netrins, are well studied[22, 23].

1.3.1 Growth cones

At the tip of each branch of an axon is a growth cone, an actin-rich structure that extends and retracts filopodia while exerting tension responsible for forward growth on the axon itself[21]. Growth cones consist of three domains – the peripheral (P), transitional (T), and central (C) domains (Figure 1.2). The outermost, P, domain is comprised primarily of actin filaments making up lamellipodia and filopodia, while the innermost, C, domain contains a large number of microtubules that are continuous with the rest of the axon, as well as organelles and membranous vesicles. The T domain is a small region at the border between the P and C domains[24]. Transmembrane proteins on the surface of the growth cone interact with the external environment of the cell and relay information about what they find to the cytoskeleton inside the cell, which in turn stimulates growth, retraction, or turning of the growth cone[21].

1.3.2 The cytoskeleton and axon growth

The characteristics of axon growth are primarily determined by the interplay and dynamics of the actin and microtubule cytoskeletons within the growth cone. Elongation
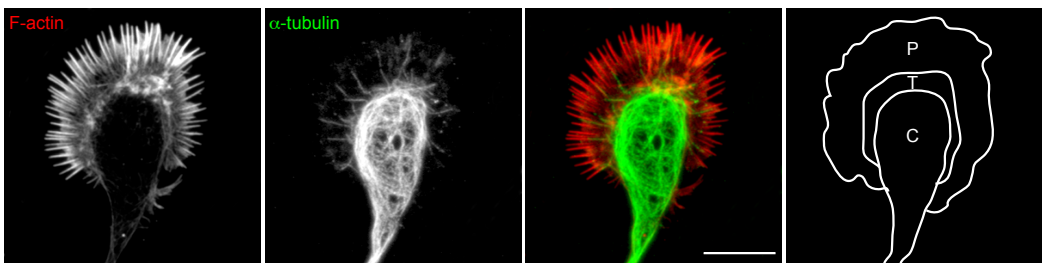
Figure 1.2. *Image of an axonal growth cone of a DIV3 neuron.*
Neurons were stained for F-actin (far left, red) and α-tubulin (second from left, green). Far right panel shows a cartoon depicting the regions of the growth cone that form the peripheral (P), transitional (T), and central (C) domains. Scale bar, 10 μm.

of an axon is thought to occur by the extensive repetition of three steps – formation of filopodia and lamellipodia at the leading edge of the growth cone (protrusion), thickening at the base of the filopodium and movement of vesicles and organelles into that space (engorgement), and reshaping the morphology of the filopodium to become continuous with the axon proper (consolidation)[24-26]. Importantly, axon growth occurs in a regulated, rather than constitutive, fashion[21]. The interaction of substrate receptors, extracellular matrix receptors, and cell adhesion molecules on the surface of the growth cone with signaling molecules outside of the cell induces an increase in the strength of their connection to the actin network within the growth cone[21]. This, in turn, results in a shift towards forward growth of actin filaments and less inhibition of microtubule polymerization, leading to growth of the entire axon[27].

1.3.3 Directed axon growth and guidance cues

In addition to controlling axon growth itself, the extracellular environment controls the direction in which the axon grows. Axon guidance is thought to be mediated by the presence of gradients of attractive and repulsive cues external to the cell[24]. Receptors in the growth cone respond to these cues by modulating the actin and microtubule cytoskeletons within the growth cone and activating or repressing a variety of secondary signaling pathways[28]. Some axon growth and guidance cues, such as semaphorins and netrins, are secreted by other cells near the developing axon[22, 23]. Semaphorins are generally considered to be chemorepellants, meaning that the growth cone will turn away from high amounts of semaphorin protein, while netrins are primarily chemoattractants, although it is important to note that, in both cases, specific axons behave in an opposite fashion[22, 28]. In addition to secreted guidance cues, axon growth and turning are also modulated by homo- and heterophilic interactions between transmembrane proteins on different cells. For example, both receptor protein tyrosine phosphatases (RPTPs)[29] and ephrins and their eph receptors[22] are necessary for axon growth, and perhaps more importantly, eventual target selection and synapse formation. Intriguingly, a single growth cone contains a set of receptors that respond to many guidance cues, and the net growth of an axon is dependent on the integration of the signals it receives[22]. This fact simultaneously increases the possible directions each axon can grow and allows each neuron to interpret the same cues in different ways.

1.4 Dendrite Development

At around DIV5, axon growth begins to slow and the other neurites begin to grow, branch, and develop into dendrites (Figure 1.1)[13]. Mature dendrites are the primary site on which a neuron receives synaptic input from other neurons[1]. Each neuron has a unique pattern of dendritic arborization, which, for hippocampal pyramidal neurons, is characterized by a long apical dendrite and many shorter basal dendrites[30]. In culture, this morphology is not as readily distinguishable, likely due to the absence of a regulated pattern of orienting signals as would be found *in vivo*[31]. However, the dendrites of cultured hippocampal neurons do display the other key morphological features necessary to carry out the process of receiving, distinguishing, and integrating synaptic signals, namely, an extensively branched network of tapered projections characterized by the presence of numerous shorter, mushroom-headed protrusions called spines[32].

1.4.1 Dendritic growth and branching

Although dendrites only grow at about one-fifth the speed of axons[13], they respond to similar growth cues[33-35]. These combined phenomena indicate that there may be an intrinsic switch within individual neurons between the support of axonal and dendritic growth[21]. However, the growth and maturation of axons and dendrites do differ in some key ways. For example, while axon morphology is fairly similar for most types of neurons, neurons in different parts of the brain often display radically different dendritic branching patterns[36]. Generally speaking, these patterns are thought to result from a combination of factors intrinsic to the neuron, diffusible growth and guidance cues in the cell's environment, contacts with other cells, and neuronal activity[37].

Similar to axon growth, dendritic growth is characterized by the extension and retraction of both the primary neurites originating at the cell soma and secondary neurites emanating from the primary neurites[31]. After a period of tremendous plasticity, certain branches become stabilized, and the structure of the dendritic arbor remains relatively constant for the remainder of the neuron's lifetime (Figure 1.1)[37]. In maturity, dendritic organization is likely critical for the integration of synaptic signals, as the location of synapses on the dendrite determines the degree to which those synapses influence action potential initiation in the neuron[30].

1.4.2 Dendritic spines

The large majority of excitatory postsynaptic sites in hippocampal neurons are found not on the dendritic shaft itself, but on small projections off of the main dendrite called dendritic spines (Figure 1.1)[38]. Developing neurons possess a large number of motile and dynamic filopodia[39, 40], which can, in cultured neurons, initiate contact with neighboring axons[40]. Though the mechanism by which they do so varies[38, 41], filopodia form the basis for eventual dendritic spines[39, 42, 43]. The maturation of spines is characterized by the assembly of pre- and postsynaptic specializations in physically adjacent neurons stabilized by transsynaptic adhesion molecules[41], with one spine usually containing one synapse[38]. However, spine morphology is tremendously variable, even in mature neurons, and changes in spine shape are correlated with changes in synaptic strength[38, 41]. Long-term *in vivo* imaging also revealed activity-dependent plasticity in spine morphology[2, 44], though to a lesser degree than in cultured neurons.

1.5. Formation and Function of Synapses

The unique morphology of neuronal cells has specifically evolved to facilitate the rapid and reliable transmission of signals between neurons. The actual sites of communication between neurons, though, are synapses, and, molecularly speaking, chemical synapses throughout the brain are remarkably similar[45]. A synapse consists of three major components – the presynapse, which sends signals by releasing neurotransmitter-containing vesicles in response to depolarization, the postsynapse, which receives signals due to the opening of ligand-gated ion channels upon binding of neurotransmitter, and the synaptic cleft, the extracellular space between the pre- and postsynaptic sites (Figure 1.3)[46]. The orderly and reliable assembly, maintenance, and plasticity of synapses is critical to neuronal function, and numerous proteins play important roles in ensuring the fidelity of synaptic transmission.

1.5.1 Synaptic cell adhesion molecules

In addition to their importance in general axon guidance (see above), cell adhesion molecules (CAMs) are crucial mediators of target recognition and synaptic assembly[47], and the abundance and variety of potential CAMs implies that they play key roles in establishing the specificity of synaptic connections[48]. On a molecular level, most CAMs have related structures that allow them a great deal of functional ver-

A

B
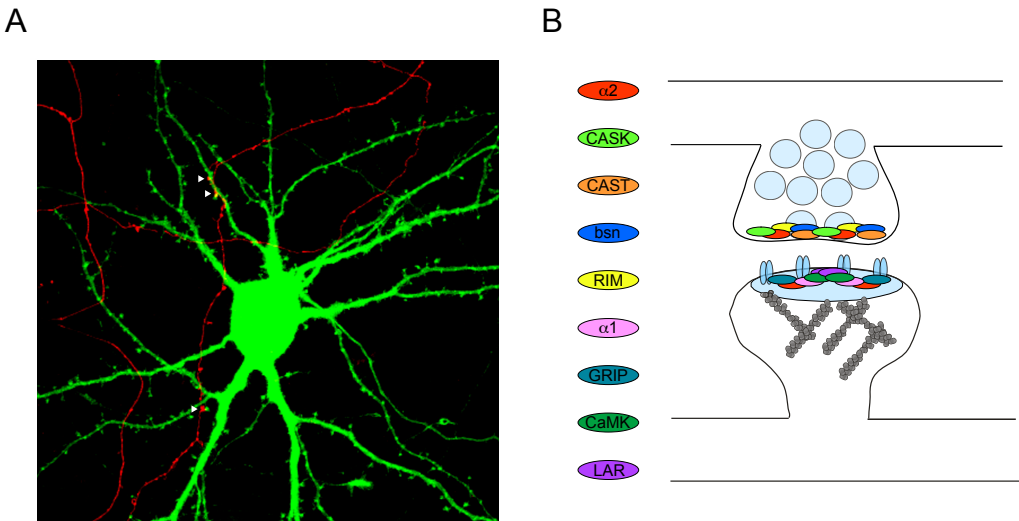
Figure 1.3. *Image and model of synaptic sites in cultured hippocampal neurons.*
(A) Image of synaptic contacts being made between mature (DIV19) hippocampal neurons in culture. Arrows designate sites where a presynaptic site within an axon (red) is juxtaposed with a dendritic spine (green), forming a putative synapse.
(B) Cartoon representing selected components of a typical synapse. The presynapse contains synaptic vesicles (light blue circles) as well as the proteins liprin-α2 (red), CASK (green), CAST1/2 (orange), bassoon (blue), and RIM (yellow). The postsynapse contains glutamate receptors and the postsynaptic density (light blue), actin filaments (grey), and the proteins liprin-α1 (pink), liprin-α2 (red), GRIP (turquoise), CaMKII (dark green), and LAR (purple).

satility. Many are transmembrane proteins whose extracellular region contains Immunoglobulin (Ig) or Ig-like domains that facilitate homo- and heterophilic interactions with other CAMs and extracellular matrix molecules, while their intracellular region acts as a primary signaling molecule, often a kinase or phosphatase, that serves to initiate diverse signaling cascades inside the neuron[47-49]. Adhesion molecules are thought to perform four major tasks with regards to the development and function of a synapse: (1) to provide stability by physically linking pre- and postsynaptic cells, (2) to recognize specific synaptic targets, especially in densely packed networks of neurons, (3) to initiate differentiation of the pre- and postsynaptic membrane, and (4) to regulate synapse structure and function[49]. Two recent papers have again shown key roles for cell adhesion molecules in determining synaptic contacts and inducing synaptic differentiation[50, 51], further emphasizing their importance in synaptogenesis and synaptic function.

1.5.2 Synaptic scaffolding and signaling proteins
Following cell adhesion, the machinery necessary to conduct synaptic transmission

begins to accumulate at nascent synaptic sites[52]. This leads to two electron dense thickenings of the pre- and postsynaptic membranes, called the cytomatrix at the active zone (CAZ) and postsynaptic density (PSD), respectively (Figure 1.3). These two structures are positioned directly across the synaptic cleft from one another[47], and are composed of a tightly packed meshwork of scaffolding and signaling proteins that control presynaptic vesicle release[48, 53, 54] and postsynaptic receptor trafficking[7]. Many molecules, for example CaMKII[55, 56], CASK[57], and liprin-α[58], are major components of both the CAZ and the PSD, while others, like bassoon and piccolo (pre)[53] and PSD-95[59] and homer[60] (post), are only found on one side of the synapse. Proteins in the CAZ and PSD seem to be primarily important in two aspects of synaptic function. First, they provide a stable framework that ensures rapid and reliable synaptic transmission, and second, they act as major signaling molecules to modulate synaptic strength and efficacy in response to the activity of the neuron.

1.5.3 Synaptic vesicles and receptors

Synaptic transmission itself is, however, the release of neurotransmitter from presynaptic vesicles into the synaptic cleft, where it binds and activates postsynaptic receptors (Figure 1.3)[1]. In the hippocampus, glutamate is the major excitatory neurotransmitter[1], and ionotropic glutamate receptors mediate the majority of the postsynaptic response to neurotransmitter release[61]. The synaptic vesicle cycle consists of a stereotyped set of steps that form the basis of presynaptic function. Neurotransmitters are actively loaded into synaptic vesicles which cluster around the active zone. These vesicles are then docked and primed for release. Neurotransmitter release due to the SNARE-mediated fusion of docked vesicles with the plasma membrane is triggered by Ca^{2+} influx stimulated by an action potential, and is immediately followed by endocytosis and recycling of synaptic vesicles back into the total pool of vesicles at a synapse[62]. In addition to SNAREs such as VAMP2 and SNAP-25, active zone and synaptic vesicle-associated proteins such as munc13, munc18, synaptotagmin, and RIM1 play key roles in the regulation of the synaptic vesicle cycle[63]. Active zones in cultured hippocampal neurons contain more than 200 synaptic vesicles[62], on average 4-8 of which are docked[64]. This represents the readily releasable pool of vesicles, or those that are available for immediate release upon high-frequency stimulation[62]. Another ~20 vesicles make up the reserve pool of recycling vesicles[64], while the remainder populate a large resting pool[65].

Once glutamate is released by the presynaptic neuron, it binds to and activates glutamate receptors in the postsynaptic membrane (Figure 1.3). There are two major classes of glutamate receptors found at hippocampal postsynapses, ionotropic and metabotropic glutamate receptors[61]. Ionotropic glutamate receptors open after binding glutamate, while metabotropic receptors respond to glutamate activation by initiating G-protein linked signaling cascades[61]. N-methyl-D-aspartate (NMDA) type receptors are Ca^{2+} permeable cation channels, while α-amino-3-hydroxy-5-methyl-4-isoxazole proprionate (AMPA) type receptors are largely Ca^{2+} impermeable[66]. Though activation of AMPA receptors is the primary means of postsynaptic depolarization at excitatory synapses, NMDA receptors play a critical role in the regulation of AMPA receptors and contribute to neurotransmission as well[61, 66].

1.6. Maintenance and Plasticity of Synapses

Although in fixed light and electron microscopic images, mature synapses appear rather static, they are in fact anything but. Though differentiated neurons are post-mitotic and therefore not replaced over the course of an organism's lifetime, synapses are constantly being created, eliminated, and modified[32]. This occurs on a number of different levels, from basic maintenance of synaptic structure to long-term alterations of synaptic strength in response to activity.

1.6.1 Protein Turnover

In order to understand the molecular dynamics of synaptic transmission, one must understand the dynamics of the proteins that control synapse function, and while the lifetime of neurons and even single synapses can be on the order of days, months, or years, the lifetime of individual proteins is more properly measured in seconds, minutes, or hours. This means that all synapses are in a constant state of molecular flux, wherein the proteins that make up the synapse exchange in both a constitutive and a regulated fashion. Therefore, the work of building a synapse is never complete, as the former ensures proper maintenance of synaptic function, and the latter allows for extensive modification of synaptic efficacy and strength[67, 68]. In addition to the exchange of proteins between neighboring synapses[69], the targeted degradation of proteins by the Ubiquitin Proteasome System (UPS) plays a critical role in both the establishment and maintenance of synaptic contacts[67, 68]. Key components of both the pre- and post-

synaptic compartments are regulated by the UPS, including presynaptic RIM1, UNC-13, and syntaxin-1 and postsynaptic shank, GKAP, and PSD-95[68]. Interestingly, the synaptic localization of numerous postsynaptic proteins[70] and the proteasome itself[71] is dependent on synaptic activity, though the extent to which this is the case presynaptically is still under investigation (see Chs. 4 and 5).

1.6.2 Modification of synapses in response to activity

Synaptic plasticity occurs in two forms, short-term and long-term, both of which are heavily dependent on Ca^{2+} concentration at the synaptic site. Short-term plasticity involves changes in synaptic strength that last on the order of minutes and is primarily a presynaptic phenomenon, whereby the synaptic vesicle release probability at a synapse is altered, albeit not permanently, by the prior activity state of that synapse[72, 73]. Short-term synaptic depression is usually caused by a decrease in the number of docked and primed vesicles available for immediate release, and is therefore heavily influenced by synaptic vesicle recycling[72]. Multiple studies have shown that synapses have the capacity to alter the dynamics of the synaptic vesicle cycle[72], though the ultimate consequences of short-term presynaptic plasticity in terms of overall network activity and behavior are still not clear.

In contrast to short-term plasticity, long-term plasticity refers to changes in synaptic strength that last for hours or even days. Although particular synapses display presynaptic long-term plasticity, the predominant form is expressed postsynaptically[66]. The degree of Ca^{2+} influx through NMDA receptors activates signaling cascades within the dendritic spine, which leads to the regulated insertion or removal of AMPA receptors from the postsynaptic membrane[61, 66, 74]. High frequency stimulation of NMDA receptors over a short period of time, and therefore a rapid increase in the Ca^{2+} concentration in the spine, results in long-term potentiation (LTP), while less intense but prolonged stimuli lead to long-term depression (LTD)[66]. Interestingly, the distinct morphology of dendritic spines allows for the isolation of these Ca^{2+} signals, ensuring that one synapse can be potentiated while its neighbor is depressed, and therefore altering the contribution each individual spine makes to the overall activity of the neuron[75].

1.6.3 Learning and Memory

In particular, long-term plasticity has tremendous implications for behavioral process-

es such as learning and memory. Significant changes in synaptic integration within the dendritic tree result in significant changes in the firing properties of that neuron, and therefore changes in the entire network within which that neuron functions[75]. Intriguingly, genes encoding for proteins that are key in the molecular pathways mediating long-term plasticity have also been shown to be important in determining the performance of mice in learning-dependent behavioral assays[76, 77]. Though our understanding of the fundamental processes underlying learning and memory has increased tremendously, a complete understanding of the molecular function of the synaptic terminal is still elusive.

1.7. Scope of the Thesis

The establishment and maintenance of synaptic transmission is a highly regulated and choreographed process, and innumerable proteins play key roles at each stage of synaptic development and function. In this thesis, we examine the role of liprin-α proteins in neuronal development and synaptic function. Chapter 2 explores the expression patterns of liprins in the brain on anatomical and subcellular levels. Chapter 3 describes the importance of liprin-α2 as a coordinator of LAR-RPTP signaling in axon growth and branching in hippocampal neurons. In Chapter 4 we show evidence of activity dependent regulation of liprin-α1 protein levels due to degradation by active CaMKII and highlight the importance of this mechanism in LAR-RPTP trafficking and dendrite development. Chapter 5 illuminates the differential roles of liprin-α1 and liprin-α2 in the molecular organization and subsequent function of the presynaptic terminal. Chapter 6 provides a comprehensive description of the experimental procedures involved in this thesis. Chapter 7 consists of a general discussion of the role of liprins in the neuronal development and synapse function and highlights future research directions.

Chapter 2

The Liprin-α Family of Proteins

Samantha A. Spangler[1], Dick Jaarsma[1],
and Casper C. Hoogenraad[1]

[1]Department of Neuroscience, Erasmus MC, Rotterdam, The Netherlands

Synapses are specialized communication junctions between neurons whose plasticity provides the structural and functional basis for information processing and storage in the brain. Recent biochemical, genetic, and imaging studies in diverse model systems are beginning to reveal the molecular mechanisms by which synaptic vesicles, ion channels, receptors, and other synaptic components assemble to make a functional synapse. Recent evidence has shown that the formation and function of synapses are critically regulated by the liprin-α family of scaffolding proteins. The liprin-αs have been implicated in pre- and post-synaptic development by recruiting synaptic proteins and regulating synaptic cargo transport. Here, we will summarize the diversity of liprin binding partners, highlight the factors that control the function of liprin-αs at the synapse, and discuss how liprin-α family proteins regulate synapse formation and synaptic transmission.

2.1. The Liprin-α Family of Proteins

The liprin-α family of proteins was first identified by their interaction with the LAR family of receptor protein tyrosine phosphatases (LAR-RPTPs)[78, 79]. In vertebrates four liprin-α genes were found, liprin-α1, α2, α3, and α4, whereas *C. elegans* and *Drosophila* have only a single liprin-α gene, *syd-2* (synapse-defective-2) and *dliprin*-α respectively. Liprin-α2 and liprin-α3 are expressed primarily in mammalian brain, while liprin-α1 and liprin-α4 are also found in non-neuronal tissue[79, 80]. Liprin-αs are well conserved, with ~50% amino acid identity between human liprin-α1 and worm SYD-2. This family of proteins is characterized by an N-terminal coiled-coil region that mediates homo- and heteromultimerization, and three sterile-α-motif (SAM) domains making up the liprin homology (LH) region that binds to LAR-RPTP[78, 79, 81]. In addition to their protein binding capabilities[82], the SAM domains of liprin-α were recently shown to interact with ATP[83], and SAM domains in general are known to bind to RNA[84] and lipid membranes[85]. The diverse range of SAM domain interactions makes liprin proteins attractive candidates for linking a multitude of cellular components into large protein complexes (Figure 2.1 and Table 2.1). To date, the liprin-α family of proteins has been implicated in multiple processes important for proper cellular and synaptic function.

2.2 Liprin-α and Presynaptic Development

In immature neurons, liprin-αs are necessary for presynaptic development. A loss of function mutant of the *C. elegans* homolog of liprin-α, *syd-2*, was isolated in a screen for mislocalized synaptic vesicle proteins[86]. Studies on this mutant indicated that SYD-2 localized at synapses independently of synaptic vesicles, and its absence caused a variety of structural presynaptic defects[86]. Active zones in these mutants were lengthened, and synaptic vesicle proteins were diffusely localized rather than clustered at presynaptic sites[86]. Later studies confirmed that SYD-2 acts to recruit not only synaptic vesicles to presynaptic sites, but other important components of the presynaptic machinery as well. In liprin-α mutants, ELKS-1 (also named CAST/ERC), GIT (G-protein coupled interactor), SAD-1 (Synapses of Amphids Defective-1), UNC-57 (Uncoordinated-57 / Endophilin), and SNN-1 (Synapsin-1) were not synaptically, but

Figure 2.1. *Liprin-α interaction map.* The orthologs of vertebrate, *Drosophila*, and *C.elegans* liprin-α binding proteins are indicated by hexagons. Liprin-α interactions demonstrated by at least yeast-two hybrid assays and/or co-immunoprecipitations are shown by solid lines. The references to papers describing particular interactions are indicated in Table 2.1. The binding partners of liprin interacting proteins are shown by broken lines.
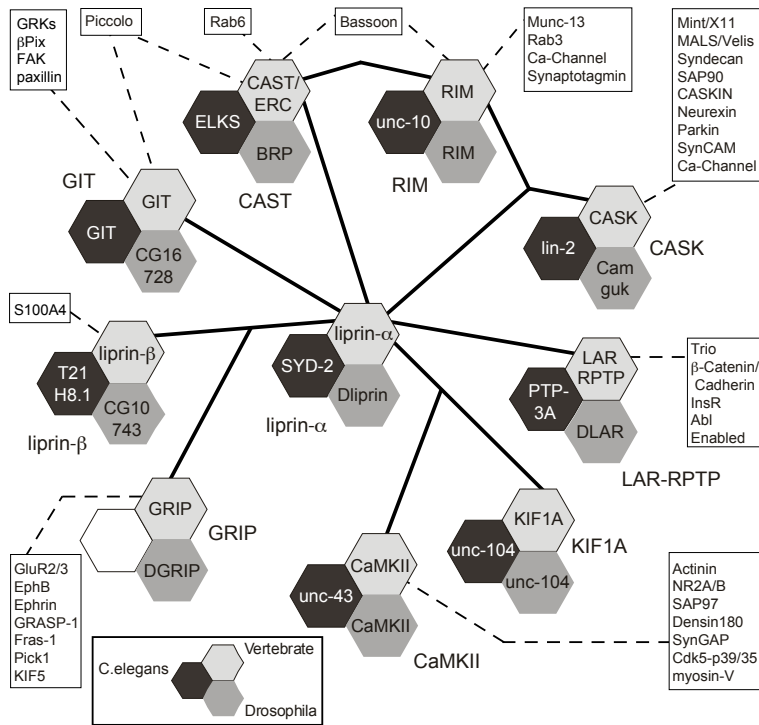
diffusely, expressed[87]. These same studies showed that SYD-2 is very closely linked to the synaptic membrane itself, as only loss of the immunoglobulin domain membrane proteins SYG-1/2 (Synaptogenesis abnormal-1/2) disrupts the synaptic clustering of SYD-2[87]. A *syd-2* gain of function mutant was able to rescue these defects, implying that SYD-2 protein itself is specifically responsible for the recruitment of synaptic proteins, although the presence of ELKS-1 is required to mediate this rescue[88].

In *Drosophila*, liprin-α homolog *dliprin-α* mutants displayed a similar defect in active zone morphology[89]. Endogenous dliprin-α is also located at synapses and colocalizes with dlar[89], the *Drosophila* homolog of LAR-RPTP, which is required for axon guidance[90]. *Dliprin-α* was shown to be important for the formation of new synaptic boutons at the *Drosophila* neuromuscular junction (NMJ) and for dlar action at the synapse[89]. Recently, further evidence of a function of liprin-α in conjunction with LAR was found for R1-R6 photoreceptor axon targeting in *Drosophila*[91]. However, liprin-α functions independently of LAR in the axonal targeting of R7 photoreceptors[92], indicating that liprin-α plays a more complex role than merely a facilitator of LAR. LAR has also been implicated in vertebrate motor axon guidance[93], but the role of its interaction with liprin-α in these processes has not been investigated.

Figure 2.2. *Domain structures of liprin-α and key binding partners.*
Sizes are relative to sizes of the actual proteins. FNIII, Fibronectin III; GK, Guanylate Kinase; Ig, Immunoglobulin; PDZ, PSD-95, DlgA, Zo-1; SAM, Sterile-α-Motif; SH3, Src Homology 3.
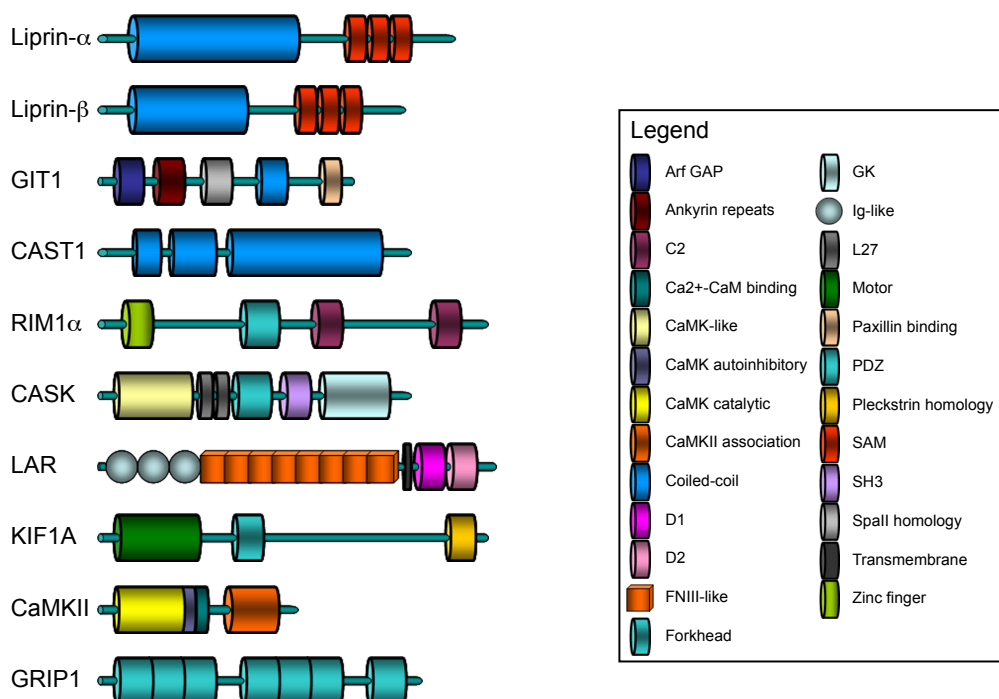
2.3. Liprin-α and Postsynaptic Development

Liprin-αs are also thought to be involved in multiple processes important for postsynaptic development. The C-terminal TVRTYSC motif of liprin-αs interacts with PDZ6 of GRIP1[94], an AMPA receptor (AMPAR) binding protein[95]. The disruption of this interaction causes a decrease in dendritic AMPAR clustering and surface expression, although other postsynaptic markers are normal[94]. Similarly, the interaction between liprin-α and LAR[96] is necessary for proper AMPAR targeting and dendritic spine morphology. Interestingly, LAR phosphatase activity and LAR-liprin-α-GRIP interactions have also been found to regulate dendritic targeting of the cadherin-β-catenin complex and are implicated in the development and maintenance of excitatory synapses[96].

2.4. Liprin-α and Neurotransmitter Release

After establishing a functional synaptic contact, neurotransmission requires a constant organization of synaptic vesicles and neurotransmitter receptors on their respective

A

```
Liprin-α1 MMCEVMPTISEAEGPPGGGGGHGSGSPSQPDADSHFEQLMVSMLEERDRLLDTLRETQETLALTQGKLHEVGHERDSLQRQLNTALPQ------------ 88
Liprin-α2 MMCEVMPTINEDT-PMSQRGSQSSGS----DSDSHFEQLNVNMLDERDRLLDTLRETQESLSLAQQRLQDVIYDRDSLQRQLNSALPQDIESLTGGLAGS 95
Liprin-α3 MMCEVMPTISEDG-RRG----SALGPD---EAGGELERLMVTMLTERERLELTLREAQDGLATAQLRLRELGHEKDSLQRQLSIALPQ------------ 80
Liprin-α4 -MCEVVMPTINEGD-RLG----PPHGA----DADANFEQLMVNMLDEREKLLESLRESQETLAATQSRLQDAIHERDQLQRHLNSALPQ------------ 78
          ********.*   .   .   *. :..::..::*:***.** **::**::***:*: *: :* :*::  :::*.***:*. ****

Liprin-α1 ------EFAALTKELNVCREQLLEREEEIAELKAERNNTRLLLEHLECLVSRHERSLRMTVVKRQAQSPAGVSSEVEVLKALKSLFEHHKALDEKVRERL 182
Liprin-α2 KGADPPEFAALTKELNACREQLLEKEEEISELKAERNNTRLLLEHLECLVSRHERSLRMTVVKRQAQSPGSVSSEVEVLKALKSLFEHHKALDEKVRERL 195
Liprin-α3 ------EFAALTKELNLCREQLLEREEEIAELKAERNNTRLLLEHLECLVSRHERSLRMTVVKRQAQSPGGVSSEVEVLKALKSLFEHHKALDEKVRERL 174
Liprin-α4 ------EFATLTRELSMCREQLLEREEEISELKAERNNTRLLLEHLECLVSRHERSLRMTVVKRQAQSPSGVSSEVEVLKALKSLFEHHKALDEKVRERL 172
                ***:**:**. *******:****:************************************:.***************************

Liprin-α1 RVALERCSLLEEELGATHKELMILKEQN---NQKKTLTDGVLDINHEQENTPSTS--GKRSSDGSLSHEEDLAKVIELQEIISKQSREQSQMKERLASLS 277
Liprin-α2 RVSLERVSALEEELAAANQEIVALRGNVHIQRKMASSEGSTESEHLEGMEPGGKVHEKRLSNGSIDSTDETSQIVELQELLEKQNYEMAQMKERLAALS 295
Liprin-α3 RMALERVAVLEEELELSNQETLNLREQ-------LSRRRSGLEEPGKDGDGQ-------TLANGLGPGGDSNRRTAELEEEALERQRAEVCQLRERLAVLC 260
Liprin-α4 RAALERVTTLEEQLAGAHQQVSALQQG-------AGVRDGAAEEEGTVELGP------KRLWK------EDTGRVEELQELLEKQNFELSQARERLVTLT 253
          * :*** : ***:*  :::: *  *::  . :  :   ::   **:*  ::*  * :*.***.. *

Liprin-α1 SHVTELEEDLDTARKDLIKSEEMNTKLQRDVREAMAQKEDMEERITTLEKRYLAAQREATSVHDLNDKLENEIANKDSMHRQTEDKNRQLQERLELAEQK 377
Liprin-α2 SRVGEVEQEAETARKDLIKTEEMNTKYQRDIREAMAQKEDMEERITTLEKRYLSAQRESTSIHDMNDKLENELANKEAILRQMEEKNRQLQERLELAEQK 395
Liprin-α3 RQMSQLEEELGTAHRELGKAEEANSKLQRDLKEALAQREDMEERITTLEKRYLSAQRESTSLHDANDKLENELASKESLYRQSEEKSRQLAEWLDDAKQK 360
Liprin-α4 TTVTELEEDLGTARRDLIKSEELSSKHQRDLREALAQKEDMEERITTLEKRYLAAQREATSIHDLNDKLENELANKESLHRQCEEKARHLQELLEVAEQK 353
          .: ::*::  **::*:*.*** .:*.***:*:**:**:***************:****:**:**.*******:*.*:::.** *:* *:* *: *:**

Liprin-α1 LQQTLRKAETLPEVEAELAQRVAALSKAEERHGNIEERLRQMEAQLEEKNQELQR----ARQREKMNNEEHNKRLSDTVDKLLSESNERLQLHLKERMAAL 473
Liprin-α2 LQQTMRKAETLPEVEAELAQRIAALTKAEERHGNIEERMRHLEGQLEEKNQELQR----ARQREKMNEEHNKRLSDTVDRLLTESNERLQLHLKERMAAL 491
Liprin-α3 LQQTLQKAETLPEIEAQLAQRVAALNKAEERHGNFEERLRQLEAQLEEKNQELQR----ARQREKMNDDHNKRLSETVDKLLSESNERLQLHLKERMGAL 456
Liprin-α4 LQQTMRKAETLPEVEAELAQRIAALTKAEERHGNIEEHLRQLEGQLEEKNQELARTAVQVRQREKMNEDHNKRLSDTVDKLLSESNERLQLHLKERMAAL 453
          ****:******:**:***.***.*********:***:*.:*.*********** *   .*****:.:*****:***:**:**:*******.**

Liprin-α1 EDKNSLLREVESAKKQLEETQHDKDQLVLNIEALRAELDHMRLRGASLHHG---RPHLGSVPDFRFPMADGHTDS--YSTSAVLRRPQKGRLAALRDEPS 568
Liprin-α2 EEKNVLIQESETFRKNLEESLHDKERLAEEIEKLRSELDQLKMRTGSLIEPTIPRTHLDTSAELRYSVGSLVDSQSDYRTTKVIRRPRRGRMGVRRDE-P 590
Liprin-α3 EEKNSLSEEIANMKKLQDELLLNKEQLLAEMERMQMEIDQLRGRP----PSSYSRSLPGSALELRYSQAPTLPSG-AHLDPYVAGSGRAGKRGR----WS 547
Liprin-α4 EEKNTLIQELESSQRQIEEQHHHKGRLSEEIEKLRQEVDQLKGRGGPFVDGVHSRSHMGSAADVRFSLGTTTHAPPGVHRRYSALREESAKLAL-----P 548
          *:** *. * .:: :* .:*  *  .* :* .:*  *:*::: *.       :   . *.  .: :*: :

Liprin-α1 KVQTLNEQDWERAQQASVLANVAQAFESDADVSDGE-DDRDTLLSSVDLLSPSGQADAHTLAMMLQEQLDAINKEIRLIQEEKENTEQRAEEIESRVGSG 667
Liprin-α2 KVKSLGDHEWNRTQQIGVLS--SHPFESDTEMSDIDDDDRETIFSSMDLLSPSGHSDAQTLAMMLQEQLDAINKEIRLIQEEKESTELRAEEIENRVASV 688
Liprin-α3 GVKEEPSKDWERSAPAGSIP-----PPFGELDGSDEEEAEGMFG-AELLSPSGQADVQTLAIMLQEQLEAINKEIKLIQEEKETTEQRAEELESRVSSS 641
Liprin-α4 LTVTLRSPTWMRMSQG--------------VCCNLEYHSSGTLCGSSGPLPVP-----------------------EMIQEEKESTELRAEEIETRVTSG 611
           .  .   * *  .  .:  .        :.: ..:  :*  *. .:. :.  *  :    ...:.:  .:******.** ****:*.** *

Liprin-α1 SLD--NLGRFRSMSSIPP-YPASSLASSSPPGSGRSTPRRIPHSPAREVDRLGVMTLLP------------PSREEVRDDKTTIKCETSPPSSPRALRLD 752
Liprin-α2 SLEGLNLARVHPGTSITASVTASSLASSSPP-SGHSTPKLTPRSPAREMDRMGVMTLPSDLRKHRRKIA--VVEEDGREDKATIKCETSPPPTPRALRMT 785
Liprin-α3 GLD--SLGRYRSSCSLPPSLTTSTLASPSPPSSGHSTPRLAPPSPAREGTDKANHVPKE-------------EAGAPRGEGPAIPGDT-PPPTPRSARLE 725
Liprin-α4 SMEALNLKQLRKRGSIPTSLTALSLASASPPLSGRSTPKLTSRSAAQDLDRMGVMTLPSDLRKHRRKLLSPVSREENREDKATIKCETSPPSSPRTLRLE 711
          .::  .*  : :   *::. .: :***.*** **:***:  . *.*:. .        . .    :* .*:* :*:**.:**: *:

Liprin-α1 RLHKGALHTVSHEDIRDIRNSTGSQDGPVSNPSSSNSSQDSLHKAPKKKGIKSSIGRLFGKKEKGRPGQTGKEALG-QAGVSETDNSSQDALGLSKLGGQ 851
Liprin-α2 HT-LPSSY---HNDARSSLSVSLEPES--LGLGSANSSQDSLHKAPKKKGIKSSIGRLFGKKEKARLGQLRG--------FMETEAAAQESLGLGKLGTQ 871
Liprin-α3 RMTQALAL----------QAGSLEDGG---PPRGSEGTPDSLHKAPKKKSIKSSIGRLFGKKEKGRMGPPGRDSSS-LAGTPSDETLATDPLGLAKLTGP 811
Liprin-α4 KLGHPALS----QEEGKS----ALEDQG--SNPSSSNSSQDSLHKGAKRKGIKSSIGRLFGKKEKGRLIQLSRDGATGHVLLTDSEFSMQEPMVPAKLGTQ 802
           :      :   : : .. .:  . .:  . . .:: .  .*****. *:*.*****..*****.*  .*         : . .:* .:*:**. .**

Liprin-α1 AEKNRKLQKKHELLEEARRQGLPFAQWDGPTVVVWLELWVGMPAWYVAACRANVKSGAIMSALSDTEIQREIGISNPLHRLKLRLAIQEIMSLTSPSAPP 951
Liprin-α2 AEKDRRLKKKHELLEEARRKGLPFAQWDGPTVVAWLELWLGMPAWYVAACRANVKSGAIMSALSDTEIQREIGISNPLHRLKLRLAIQEMVSLTSPSAPP 971
Liprin-α3 GDKDRRNKRKHELLEEARRQGLPFAAWDGPTVVSWLELWVGMPAWYVAACRANVKSGAIMANLSDTEIQREIGISNPLHRLKLRLAIQEMVSLTSPSAPP 911
Liprin-α4 AEKDRRLKKKHQLLEDARRKGMPFAQWDGPTVVSWLELWLGMPAWYVAACRANVKSGAIMSALSDTEIQREIGISNALHRLKLRLAIQEMVSLTSPSAPP 902
          .:*:*: ::**:***:* *:*:*** ******* ***** *:*************.***:***************.*******.**:*****:*:*****

Liprin-α1 TSRT------------------------------------TLAYGDMNHEWIGNEWLPSLGLPQYRSYFMECLVDARMLDHLTKKDLRGQLKMVDSFHR 1014
Liprin-α2 TSRTPSGNVWVTHEEMENLAAPAKTKESEEGSWAQCPVFLQTLAYGDMNHEWIGNEWLPSLGLPQYRSYFMECLVDARMLDHLTKKDLRVHLKMVDSFHR 1071
Liprin-α3 SSRTSTGNVWMTHEEMESLTATTKP-ETKEISWEQ------ILAYGDMNHEWVGNDWLPSLGLPQYRSYFMESLVDARMLDHLNKKELRGQLKMVDSFHR 1004
Liprin-α4 TSRTSSGNVWVTHEEMETLETSTKT-DSEEGSWAQ------TLAYGDMNHEWIGNEWLPSLGLPQYRSYFMECLVDARMLDHLTKKDLRVHLKMVDSFHR 995
          :***         . .        .          **********:.**:****************:***********.**:** :*******

Liprin-α1 NSFQCGIMCLRRLNYDRKELERKREESQSEIKDVLVWSNDRVIRWILSIGLKEYANNLIESGVHGALLALDETFDFSALALLLQIPTQNTQARAVLEREF 1114
Liprin-α2 TSLQYGIMCLKRLNYDRKELERRREASQHEIKDVLVWSNDRVRWIQAIGLREYANNILESGVHGSLIALDENFDYSSLALLLQIPTQNTQARQILEREY 1171
Liprin-α3 VSLHYGIMCLKRLNYDRKDLERRREESQTQIRDVMVWSNERVMGWVSGLGLGKEFATNLTESGVHGALLALDETFDYSDLALLLQIPTQNAQARQLLEKEF 1104
Liprin-α4 TSLQYGIMCLKRLNYDRKELERKREESQIKDVLVWTNDQVVHWVQSIGLRDYAGNLHEGVHGALLALDENFDHNTLALILQIPTQNTQARQVMEREF 1095
          *:: *****.*******:**:** ** :*:**:**:**:*: *: .:**::**: *.: .***:.*:****.**... *** **:*** :*:*:*

Liprin-α1 NNLLVMGTDRRFDEDDDKSFRRAPSWRKKFRPKDIRGLA---AGSAETLPANFRVTSS--MSSPSMQPKKMQMDGNVSGTQRLDSATVRTYSC 1202
Liprin-α2 NNLLALGTERRLDESDDKNFRRGSTWRRQFPPPREVHGIS-MMPGSSETLPAGFRLTTT------SGQSRKMTTDVASSRLQRLDNSTVRTYSC 1257
Liprin-α3 SNLISLGTDRRLDEDSAKSFSRSPSWRKMFREKDLRGVT---PDSAEMLPPNFRSAAAGALGSPGLPLRKLQPEGQTSGSSRADGVSVRTYSC 1194
Liprin-α4 NNLLALGTDRKLDDGDDKVFRRAPSWRKRFRPREHHGRGGMLSASAETLPAGFRVSTLGTLQPPPAPPKKIMPEAHSHYLYGHMLSAFRD--- 1185
          .**: :**:*:::*:..  * *  *..:**: *  .:: :*   .*:* **..** :.  ..   :*: :        . :.*  :.
```

**Figure 2.3.** *Sequence alignment of liprin-α family proteins.*
(A) Alignment (ClustalW) of full length amino acid sequences of human liprin-α proteins. Under-lined: coiled coil domain; Brackets: Liprin Homology domain/SAM domains; Red: Antigen regions for liprin-α1/α2/α3/α4 antibodies; Blue: Linker region inserted into GFP-liprin-α1L construct (Ch. 5). "." – semi-conserved substitutions; ":" – conserved substitutions; "*" identical.

sides of the synapse in order to regulate the strength of the synaptic connections. In both of the above described invertebrate liprin-α mutants, synaptic transmission was impaired. *Syd-2* mutants displayed abnormal behavior in induced egg laying tasks and sensitivity to aldicarb consistent with a defect in synaptic transmission[86]. *Dliprin-α* mutants showed decreased evoked excitatory junctional potentials and decreased quantal content per synaptic event[89], implying a specific impairment in presynaptic function.

Mammalian liprin-α proteins associate with two major synaptic protein complexes that have been closely linked to presynaptic neurotransmitter release and vesicle cycling (Figure 2.1 and Table 2.1). First is the complex formed by liprin-α, CAST, and RIM. The coiled-coil region of liprin-α binds the coiled-coil domain of CAST (Figure 2.2), and the two proteins colocalize at synapses[97] and growth cones[98] of cultured hippocampal neurons. The same liprin-α region also interacts with the C2B domain of RIM[99] that is thought to link RIM-containing active zones to rab3A-positive synaptic vesicles[100, 101]. Additionally, RIM binds munc13-1[102], a protein involved in the priming of vesicles for exocytosis[103]. RIM1a-knockout mice display a decreased probability of neurotransmitter release which is not explained by defects in rab3A or munc13-1 targeting[99], indicating a potential role of the liprin-α/CAST/RIM complex in synaptic vesicle exocytosis. More recently, a second interaction, between liprin-α and the MALS/CASK/mint1 complex, has also been identified[104]. The first SAM domain of liprin-α binds the L27 and CamK-like domains of CASK (Figure 2.2), and disruption of this interaction causes mislocalization of MALS protein[104]. MALS triple knockout mice have decreased CASK localization at the synapse and decreased excitatory postsynaptic currents (EPSCs)[104]. MiniEPSCs are normal in these mice, and EPSC depression following high frequency stimulation is increased[104], most probably implying an impairment of presynaptic vesicle cycling. Both presynaptic liprin-α complexes may be involved in recruiting components of the synaptic release machinery to the active zone and thereby facilitating neurotransmitter release.

2.5. Neuroanatomical Expression Patterns of Liprin-α Proteins

To date, research on mammalian liprin proteins has failed to consistently distinguish between the individual members of the liprin-α protein family. However, it has provided significant insight into which processes liprins are likely to be involved. Both
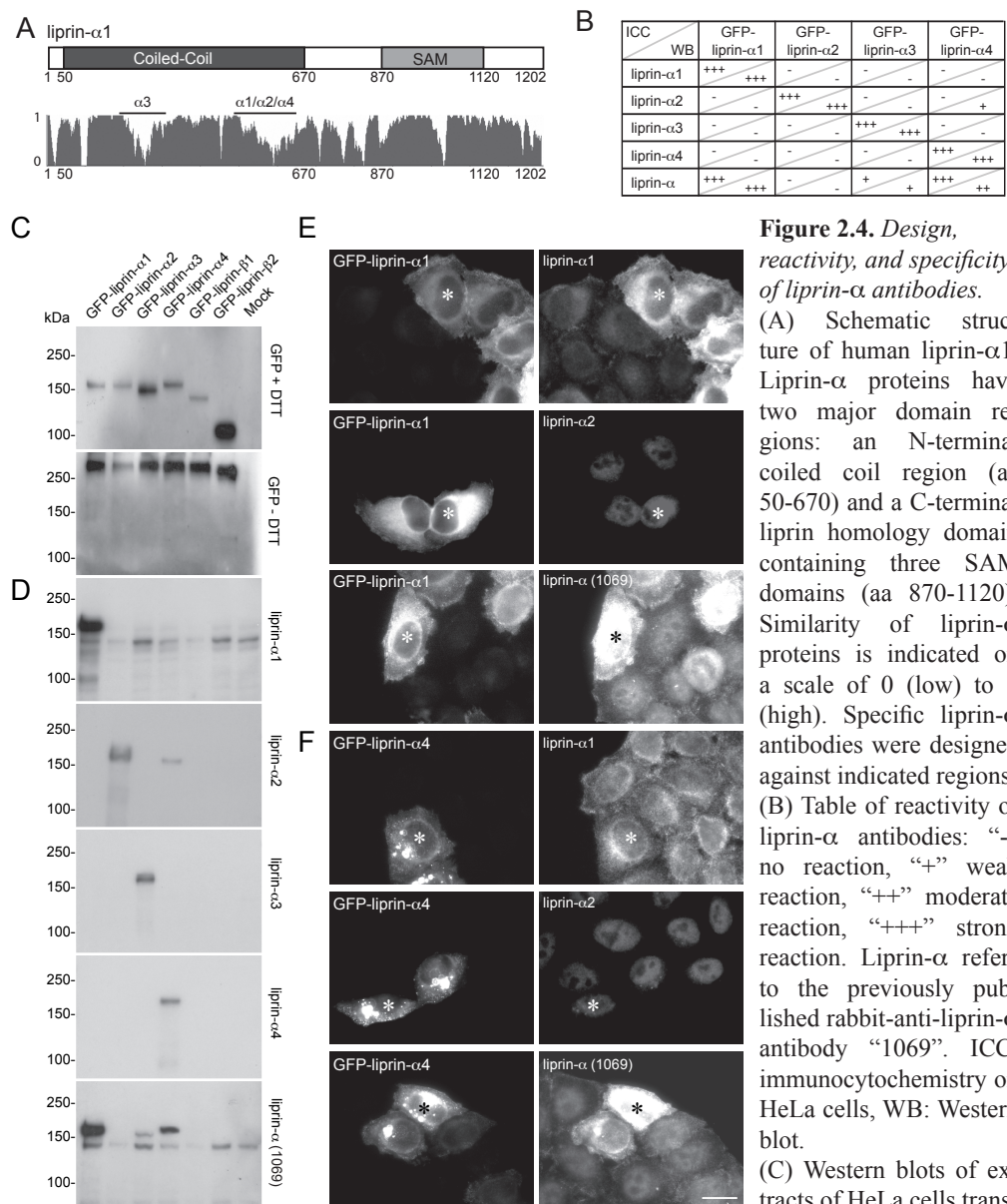
Figure 2.4. *Design, reactivity, and specificity of liprin-α antibodies.*
(A) Schematic structure of human liprin-α1. Liprin-α proteins have two major domain regions: an N-terminal coiled coil region (aa 50-670) and a C-terminal liprin homology domain containing three SAM domains (aa 870-1120). Similarity of liprin-α proteins is indicated on a scale of 0 (low) to 1 (high). Specific liprin-α antibodies were designed against indicated regions.
(B) Table of reactivity of liprin-α antibodies: "-" no reaction, "+" weak reaction, "++" moderate reaction, "+++" strong reaction. Liprin-α refers to the previously published rabbit-anti-liprin-α antibody "1069". ICC: immunocytochemistry on HeLa cells, WB: Western blot.
(C) Western blots of extracts of HeLa cells transfected with GFP-liprin proteins, run with and without DTT, and blotted with GFP antibody.
(D) Western blots of extracts of HeLa cells transfected with GFP-liprin proteins and blotted with new liprin-α antibodies and previously published liprin-α antibody #1069.
(E) Representative images of HeLa cells transfected with GFP-liprin-α1 and stained with new liprin-α1, liprin-α2, and 1069 antibodies.
(F) Representative images of HeLa cells transfected with GFP-liprin-α4 and stained with new liprin-α1, liprin-α2, and 1069 antibodies.
"*" denotes transfected cell. Please note that the exposure time of blots and images vary to show appropriate levels of endogenous protein relative to overexpressed protein. Scale bar, 10 μm.

invertebrate and mammalian liprin-α proteins are enriched in the nervous system, with the exception of vertebrate liprin-α1, which is ubiquitously expressed, though only at low levels in the brain[79, 86, 89]. There is tremendous similarity between the *C.elegans* SYD-2 and human liprin-α protein sequences, particularly in the C-terminal LH region[79], as well as between the mammalian liprin-α proteins (Figures 2.3 and 2.4)[79]. This suggests that their functions may be largely redundant, however, the extent that this is or is not the case has yet to be determined.

2.5.1 Generation and specificity of anti-liprin antibodies

To determine the role of liprin-α family members in the brain, we first generated antibodies to all four liprin-α proteins. The antibodies were raised against regions of at least 100 amino acids within each liprin-α which showed the lowest amount of sequence homology between family members (Figures 2.3 and 2.4). All of the newly generated liprin-α antibodies reacted strongly and specifically with the appropriate protein but did not recognize other liprin-α proteins or control proteins such as members of the liprin-β family, liprin-β1 and liprin-β2 (Figure 2.4). Only the liprin-α2 antibody displayed a slight cross-reaction to high levels of overexpressed liprin-α4 on Western blot (Figure 2.4). The previously published liprin-α antibody #1069[94] was shown in these assays to react strongly to liprin-α1 and to a lesser extent to liprin-α3 and liprin-α4 (Figure 2.4).

2.5.2 Nervous system expression of liprin proteins

Consistent with previous Northern blot[79], *in situ* hybridization[105], and quantitative PCR[106] analyses of liprin-α mRNA expression, Western blotting and immunohistochemistry showed that all four liprin-α family members are expressed throughout the rodent brain with distinct but largely overlapping patterns of expression (Figure 2.5). Western blotting revealed that the four liprin-α proteins are present throughout the brain, though they are enriched in different subregions (Figure 2.5A). In brain sections, all antibodies predominantly stained the grey matter, but distinct immunostaining patterns were obtained with the different liprin antibodies (Figure 2.5B). A low level of liprin-α1 immunoreactivity was observed throughout the brain. Liprin-α2 staining was prominent in neuronal cell bodies throughout the brain, as well as in the proximal dendrites of pyramidal neurons of CA1-CA3 of the hippocampus and the dendritic arbors of Purkinje cells (data not shown). The liprin-α4 antibody, like the
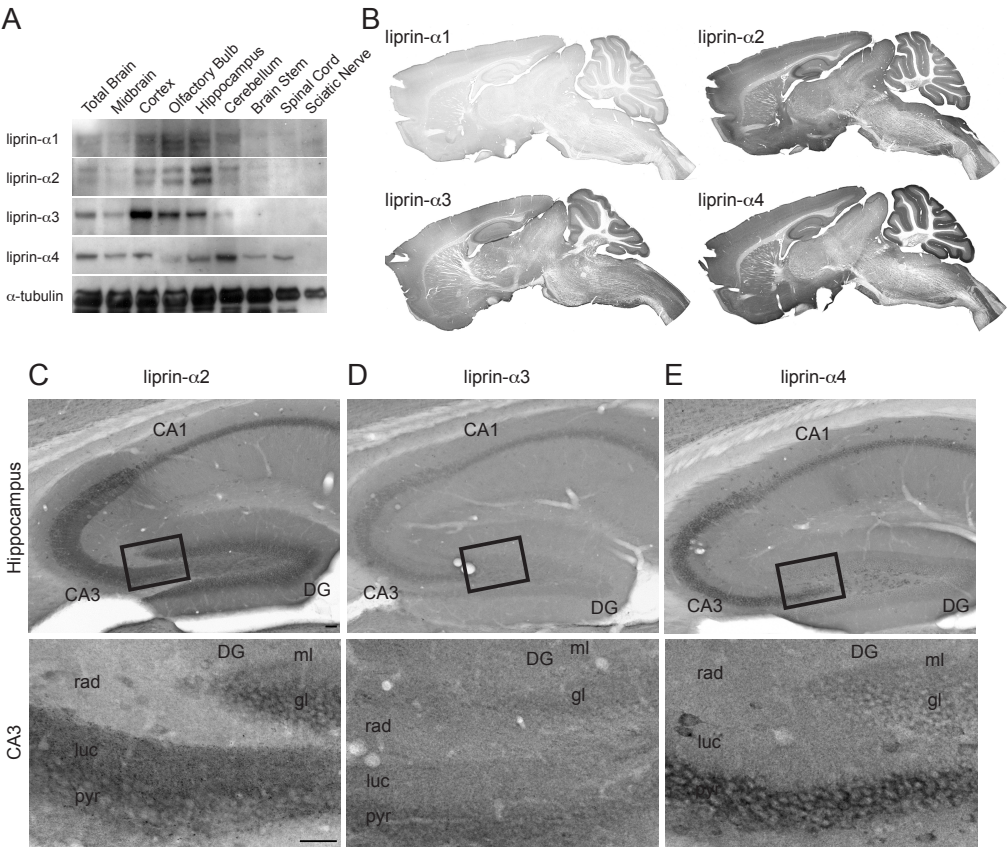
Figure 2.5. *Liprin-α distribution in the brain.*
(A) Western blots of liprin-α protein expression in extracts from isolated regions of rat brain. Equal amounts of protein were loaded for each lane (10 μg for α2/α3/α-tubulin; 100 μg for α1/α4). α-tubulin was used as a loading control.
(B) Immunohistochemistry of liprin-α proteins on adult mouse brain sections.
(C-E) Labeling of liprin-α2(C)/α3(D)/α4(E) in the hippocampus. An enlargement of the CA3/dentate gyrus is shown below. DG, Dentate Gyrus; ml, molecular layer; gl, granule cell layer; rad, stratum radiatum; luc, stratum lucidum; pyr, stratum pyramidale. Scale bars, 50 μm.

α2 antibody, predominantly stained neuronal cell bodies throughout the brain including CA1 pyramidal neurons (data not shown), but particularly strong liprin-α4 immunoreactivity was observed in the molecular layer of the cerebellum (Figure 2.5B), consistent with the enrichment of liprin-α4 protein in that brain region (Figure 2.5A). Additionally, liprin-α3 immunoreactivity was found in neuronal cell bodies throughout the brain and in the neuropil of multiple brain areas including all hippocampal subregions, the neocortex, the olfactory bulb, and cerebellar cortex (Figure 2.5B,D).

Immunoreactivity for all four liprin-α proteins was present in the hippocampus (Figure 2.5B-E), producing moderate to intense staining in pyramidal cell somata and

fine punctate staining in the stratum radiatum and oriens of the CA1-CA3 subfields and the molecular layer of the dentate gyrus (Figure 2.5C-E). Western blotting revealed, however, that only liprin-α2 is enriched (Figure 2.5A). Furthermore, liprin-α2 protein levels were particularly high in the stratum lucidum of the CA3 region (Figure 2.5C), and liprin-α2 staining highly colocalized with the presynaptic markers synaptophysin and vGluT1 in mossy fiber endings (see Chapter 5). In sum, liprin-α family members have specific but overlapping expression patterns in the mammalian brain, and liprin-α2 is likely the prominent liprin-α in the hippocampus.

Binding Partner	Liprin-α Tested	Interaction	Function	Reference
liprin-β	liprin-α1,2,3	Y2H, IF	unknown	79
LAR-RPTP (LAR, PTPδ,σ)	liprin-α1,2,3	Y2H, IP, IF	axon, dendrite, and spine development, AMPAR trafficking	78, 79, 94
GIT1	liprin-α1,2,3,4	Y2H, IP, IF, GST	AMPAR trafficking, axon and spine development	97, 107
GRIP1	liprin-α1, 4	Y2H, IP ,IF	AMPAR trafficking	94
CASK	liprin-α2	Y2H, IP	neurotransmitter release	104
CaMKII	liprin-α1	IP, IF	dendrite and spine development	108
CAST/ERC	liprin-α1,2,3,4	Y2H, IP, IF, GST	presynaptic scaffolding	97
RIM	liprin-α3,4	Y2H	neurotransmitter release	99
KIF1A	liprin-α1,2,4	Y2H, IF, IP	microtubule-based transport	109

Table 2.1. *Liprin-α binding partners.*
IP, immunoprecipitation; Y2H, yeast-two hybrid assay; IF, immunofluorescence; GST, GST-pull down assay.

Chapter 3

LAR Controls Axon Growth and Branching via Interaction with Liprin-α and Cortactin

Samantha A. Spangler[1], Linde Kegel[1],
and Casper C. Hoogenraad[1]

[1]Department of Neuroscience, Erasmus MC, Rotterdam, The Netherlands

In the early stages of nervous system development, neurons form multiple neurites, one of which becomes the axon. Axons then grow and branch rapidly as they seek to establish connections with other cells. This process requires careful control of the speed and direction of axon extension, which is mediated by signaling of cell adhesion molecules based on growth and guidance cues in the neuron's environment. Invertebrate homologs of LAR receptor tyrosine phosphatase and the scaffolding protein liprin-α play key roles in regulating axon pathfinding. Here we show that LAR and liprin-α2 are both necessary molecules in the control of axon growth and branching. LAR signals through liprin-α2 and p140Cap to influence axon growth, likely through regulation of the microtubule cytoskeleton, and interacts with cortactin to control axon branching via actin polymerization. These results suggest that LAR and liprin-α2 act in concert to form a protein complex in the axonal growth cone that is capable of transmitting signals from the extracellular matrix to the neuronal cytoskeleton.

3.1. Introduction

Following the establishment of neuronal fate, the neuron develops numerous neurites, one of which soon differentiates into the axon. The newly formed axon begins to grow rapidly and develop multiple branches as it seeks to innervate the appropriate part of the brain. This occurs starting at around DIV1-2 in cultured neurons and continues until approximately DIV5[13].

Axon outgrowth occurs as a result of rapid changes in the neuronal cytoskeleton, particularly actin and microtubule polymerization and depolymerization. Each branch of the axon has at its end an axonal growth cone which provides the primary means of force necessary for the forward extension of the axon[21]. The peripheral region of the growth cone contains large amounts of actin, while the central region is comprised of microtubules (see Figure 1.2)[24]. The growth cone is characterized by the protrusion of numerous filopodia from the end of the axon as a result of axon polymerization at the distal tip of the filopodia[21]. Actin is simultaneously depolymerized at the opposite end and the whole actin filament is pulled backwards toward the center of the growth cone by myosin motors, resulting in a net retrograde flow of actin in the peripheral region of the growth cone[21]. At the same time, microtubules in the central region of the growth cone rapidly polymerize to explore the growth cone in its entirety[24]. Microtubule polymerization, however, is inhibited by retrograde actin flow in the absence of growth cues[21]. Axon growth and branching occur as cell adhesion molecules (CAMs) in the membrane of the growth cone interact with proteins in the extracellular matrix. Interaction of the growth cone with a CAM or other substrate causes increased connectivity between the CAM and the actin cytoskeleton, resulting in decreased retrograde flow and increased microtubule polymerization toward the substrate either by turning of the growth cone or formation of a new branch of the axon[24].

One such CAM is LAR-RPTP (leukocyte common antigen related – receptor protein tyrosine phosphatase). LAR is a type IIa RPTP which has a large extracellular domain consisting of three immunoglobulin (Ig)-like domains and 4-8 fibronectin type III (FNIII) domains, a transmembrane domain, and two intracellular tyrosine phosphatase domains[81]. Similar to other PTPs, only the first, D1, phosphatase domain has notable catalytic activity; the D2 domain is thought to be involved in regulating D1 activity and determining substrate specificity[110]. Liprins interact with the D2 domain of LAR[81], and the interaction between liprin and LAR is important for AMPA receptor

targeting and dendritic spine morphology in hippocampal neurons[96] as well as R1-R6 photoreceptor targeting[91] and synapse formation[89] in *Drosophila*. Moreover, *Drosophila* LAR (dlar) mutants display significant axon growth and guidance defects[111], and innervation of the dentate gyrus is disrupted in LAR knockout mice[112, 113]. Dlar binds to the actin regulating proteins trio, abl, and ena, suggesting that LAR influences axon growth and guidance via remodeling of the actin cytoskeleton[110]. In mammals, however, the importance of LAR in axon development is less clear. Here, we describe the effects of LAR on axon growth and branching and investigate the downstream signaling pathways that are involved. We propose that LAR is a positive regulator of axon growth through promoting microtubule growth and a negative regulator of axon branching by inhibiting actin polymerization. We identified cortactin as a novel binding partner and potential substrate of LAR and showed that LAR acts through liprin-α2 to facilitate axon growth. These results show that LAR is a critical controller of cytoskeletal dynamics in developing axons and indicate that LAR and liprin function to promote neuronal development prior to synapse formation.

3.2. Results

3.2.1 LAR-RPTP controls axon growth and branching

The LAR receptor protein tyrosine phosphatase is known to be involved in the development and function of excitatory synapses in the hippocampus[96]. Additionally, work done on *Drosophila* dlar mutants indicates that dlar is important for axon growth and guidance. To study mammalian LAR function in axon development we expressed LAR specific shRNA[96] as well as GFP-tagged full length LAR in cultured hippocampal neurons (Figure 3.1A). Neurons were transfected after one day in vitro (DIV1) and fixed after four days at DIV5. Morphological analysis of a 0.45 mm x 0.45 mm field of view revealed that the axons of transfected control neurons (Figure 3.1A, left) are, at this age, on average 4.5 ± 0.2 mm long (Figure 3.1B) and have 77 ± 4 branches (Figure 3.1C). However, the axons of neurons transfected with LAR shRNA (Figure 3.1A, center) are significantly shorter (2.5 ± 0.2 mm long, Figure 3.1B), yet have more total branches (92 ± 7, Figure 3.2C). GFP-LAR overexpressing neurons (Figure 3.1A, right) do not display a significant change in total axon length (3.6 ± 0.4 mm long, Figure 3.1B), but have notably fewer axonal branches (45 ± 7, Figure 3.1C) than control neurons, implying that LAR is both necessary for axonal growth and an inhibitor of
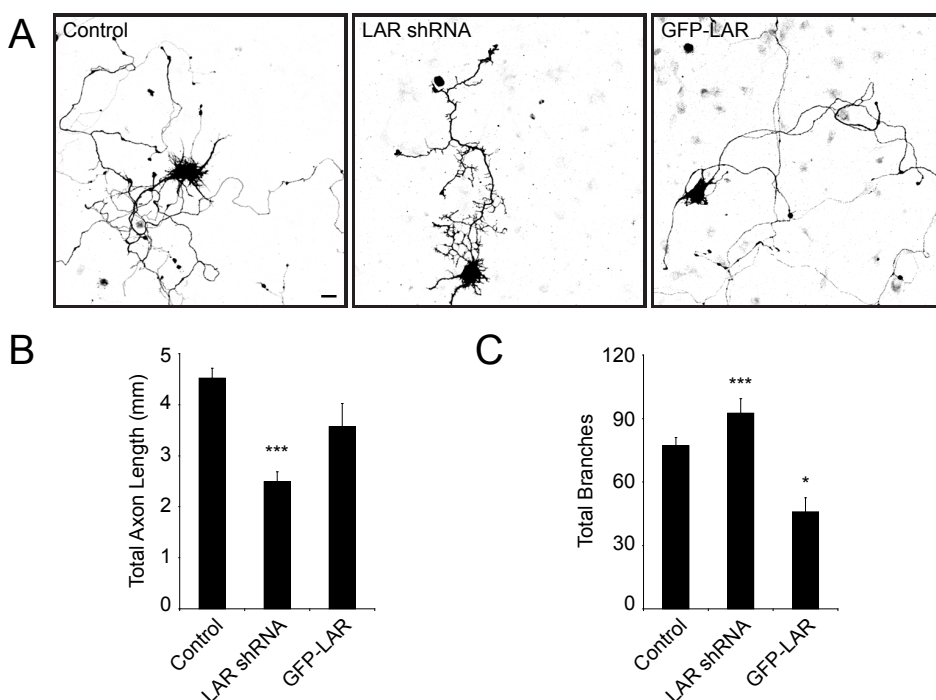
Figure 3.1. *LAR controls axon outgrowth and branching.*
(A) Representative images of DIV1+4 neurons transfected with β-galactosidase and either LAR shRNA or GFP-LAR. Scale bar, 10 μm.
(B) Quantification of the total axon length visible in a single field of view 460.7μm x 460.7μm (n=14-78 neurons from 2-8 experiments).
(C) Quantification of the total axon branching points per neuron (n=14-78 neurons from 2-8 experiments).
T-test: *, p<0.05; **, p<0.005; ***, p<0.0005. All data are expressed as mean ± SEM.

axonal branching.

3.2.2 The LAR intracellular domain is associated with liprin-α, p140Cap, and cortactin

To determine the mechanism by which LAR regulates axonal growth and branching, we searched for potential interaction partners of the LAR intracellular domain. The interaction between LAR and liprin-α is known to be important in axon growth and guidance in the Drosophila nervous system[89] and dendrite growth and spine formation in mammalian neurons (Ch. 4)[96]. By pulling down biotin-tagged liprin-α from HEK293 cells and incubating with P2/DOC extracted brain lysates (see Ch. 6), we identified p140Cap as a potentially novel liprin interacting partner (Table 5.1). p140Cap inter-
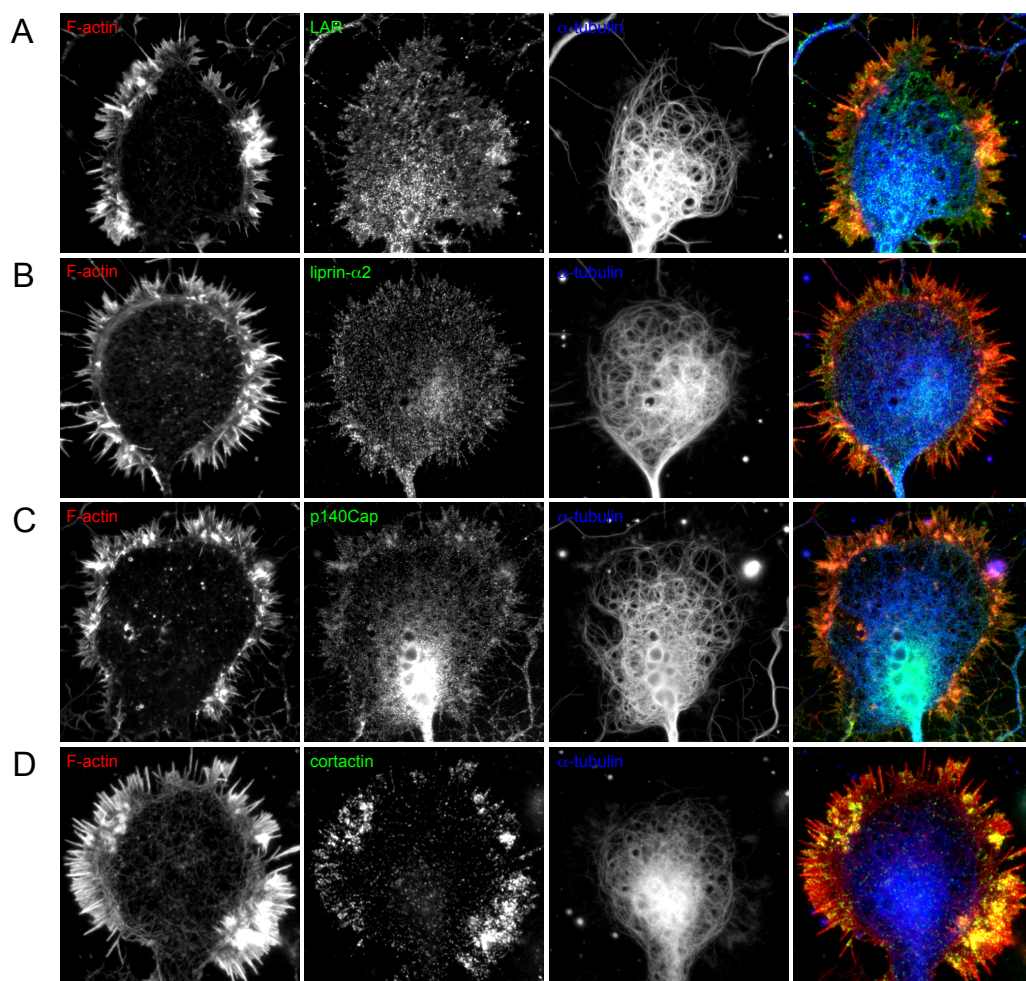
Figure 3.2. *LAR, liprin-α2, p140Cap, and cortactin are present in axonal growth cones.*
(A-D) Images of DIV3 neurons stained for F-actin (Phalloidin, red), α-tubulin (blue), and LAR (A), liprin-α2 (B), p140Cap (C), or cortactin (D, green).

acts with both the microtubule plus-end tracking protein EB3 and the actin regulator cortactin[114] and coimmunoprecipitates with liprin-α1 (data not shown), making it an attractive candidate as a downstream effector of LAR. Immunostaining of endogenous LAR, liprin-α2, p140Cap, and cortactin in DIV3 neurons showed that all four proteins are present in axonal growth cones (Figure 3.2A-D). To determine whether these proteins were capable of forming a complex in cells, we overexpressed them in different combinations in HeLa cells. To enhance LAR clustering at the cell surface, we used a fusion of the extracellular and transmembrane regions of the glycoprotein CD8 to the complete intracellular region of LAR, which contains both the active phos-
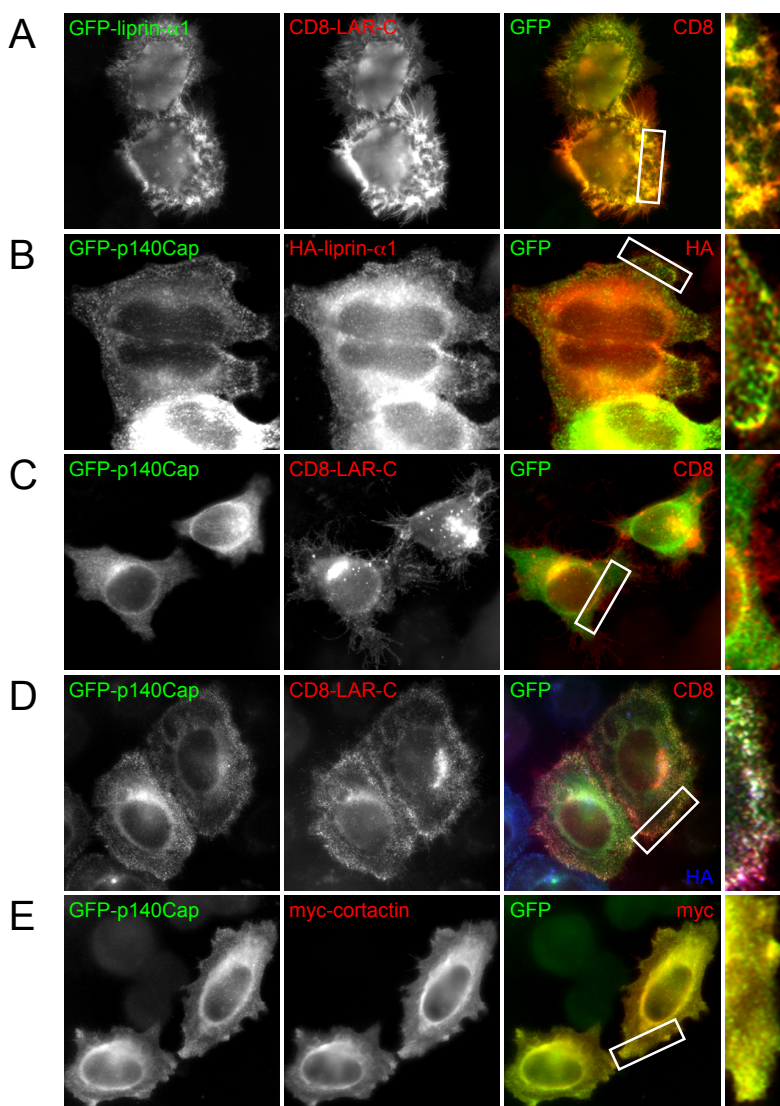
Figure 3.3. *LAR, liprin-α2, p140Cap, and cortactin colocalize in HeLa cells.*

(A) Representative images of HeLa cells transfected with GFP-liprin-α1 and CD8-LAR-C and imaged for GFP (green) and CD8 (red). Box indicates zoomed in region.

(B) Representative images of HeLa cells transfected with GFP-p140Cap and HA-liprin-α1 and imaged for GFP (green) and HA (red). Box indicates zoomed in region.

(C) Representative images of HeLa cells transfected with GFP-p140Cap and CD8-LAR-C and imaged for GFP (green) and CD8 (red). Box indicates zoomed in region.

(D) Representative images of HeLa cells transfected with GFP-p140Cap, CD8-LAR-C, and HA-liprin-α1 and imaged for GFP (green), CD8 (red), and HA (blue). Box indicates zoomed in region.

(E) Representative images of HeLa cells transfected with GFP-p140Cap and myc-cortactin and imaged for GFP (green) and myc (red). Box indicates zoomed in region.
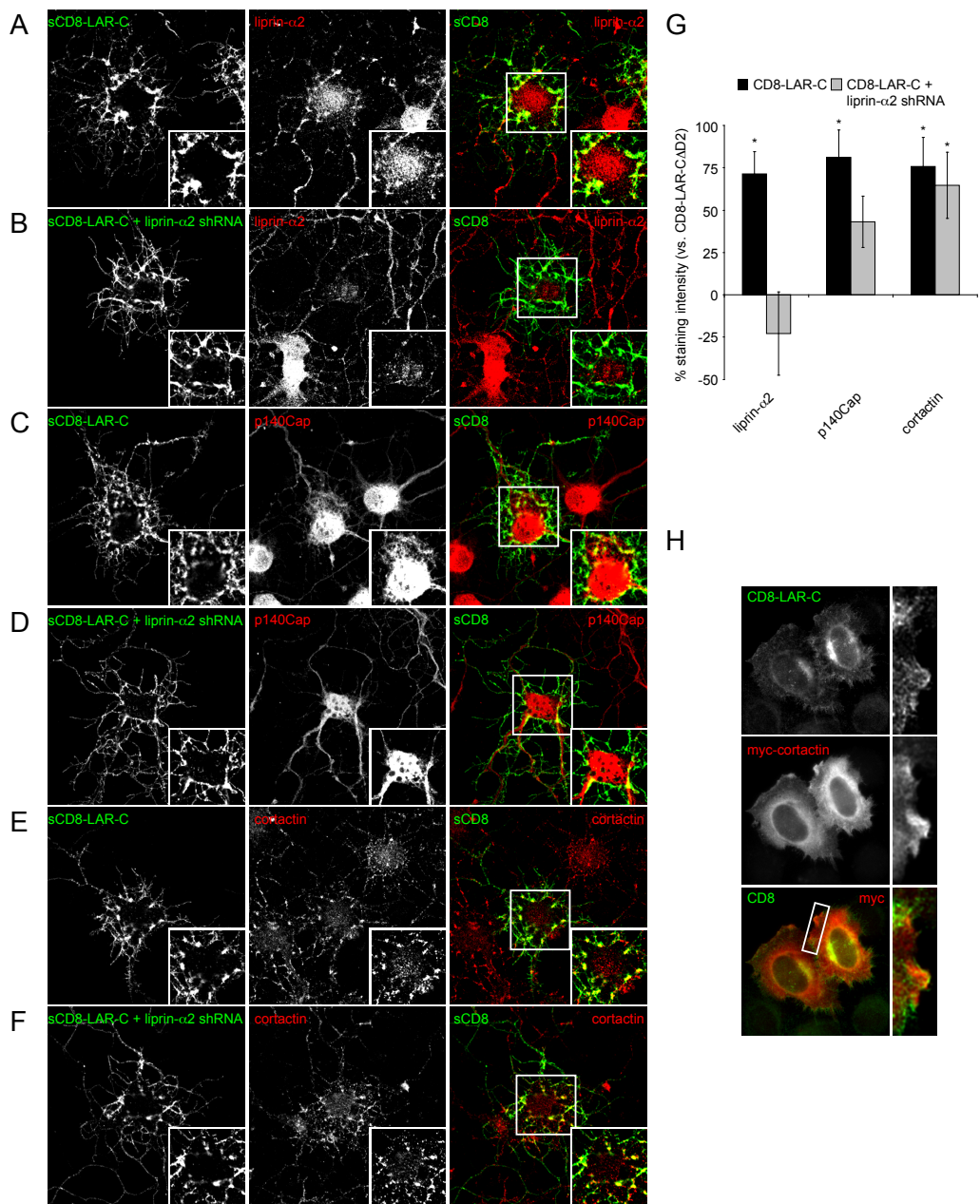
Figure 3.4. *LAR and cortactin co-cluster independently of liprin-α2 in neurons.*
(A,C,E) Representative images of neurons transfected with CD8-LAR-C and imaged for surface CD8 (green) and endogenous liprin-α2 (A), p140Cap (C), or cortactin (E, red). Box indicates zoomed in region.
(B,D,F) Representative images of neurons transfected with CD8-LAR-C and liprin-α2 shRNA and imaged for surface CD8 (green) and endogenous liprin-α2 (B), p140Cap (D), or cortactin (F, red). Box indicates zoomed in region.
(G) Quantification of percentage staining intensity of endogenous liprin-α2, p140Cap, or cortactin in

phatase D1 domain and the inactive phosphatase D2 domain that is critical for the LAR-liprin interaction (see Ch. 4)[78]. Overexpressed CD8-LAR-C formed clusters on the surface of the cell and was also found in significant levels on the Golgi apparatus (Figure 3.3A,C,D). When CD8-LAR-C was overexpressed in conjunction with liprin-α1, LAR surface clustering was enhanced (Figure 3.3A, Ch. 4) and liprin-α1 was associated with those clusters (Figure 3.3A). Overexpressed liprin-α1 targets to focal adhesion-associated patches at the cell cortex[78] in the absence of CD8-LAR-C, and overexpressed p140Cap colocalizes with liprin-α1 in double expressing cells (Figure 3.3B). Additionally, when CD8-LAR-C is expressed in conjunction with liprin-α1 and p140Cap, the three form a triple complex both in surface clusters (data not shown) and cortical patches (Figure 3.3C). No colocalization was seen between CD8-LAR-C and p140Cap in cells when liprin-α1 was not coexpressed (data not shown). As was previously reported[114], overexpressed p140Cap colocalized with overexpressed cortactin in HeLa cells (Figure 3.3D). These colocalization experiments indicate that LAR, liprin-α, p140Cap, and cortactin are capable of forming a complex in cells.

3.2.3 LAR and cortactin co-cluster independently of liprin-α in neurons

Do LAR, liprin-α, p140Cap, and cortactin associate with one another hippocampal neurons? To investigate this, we expressed CD8-LAR-C in DIV1 hippocampal neurons for four days and examined the degree to which endogenous liprin-α2, p140Cap, and cortactin were targeted to overexpressed LAR clusters. Neurons were labeled for surface CD8, then fixed and permeablized and stained for liprin-α2, p140Cap, or cortactin (Figure 3.4A, C, E). The intensity of liprin-α2, p140Cap, and cortactin staining within CD8-LAR-C clusters was normalized to their respective intensities in CD8-LAR-CΔD2 clusters, which are not able to bind liprin-α (see Ch. 4, data not shown). All three proteins showed a significant increase in staining intensity at CD8-LAR-C clusters compared to CD8-LAR-CΔD2 (Figure 3.4G), indicating that LAR can induce co-clustering of liprin-α2, p140Cap, and cortactin in neurons, and that this clustering is dependent on the LAR D2 region. We suspected that this was due to the interaction

CD8-LAR-C clusters with and without liprin-α2 shRNA, compared to intensity in CD8-LAR-CΔD2 clusters.
(H) Representative images of HeLa cells transfected with CD8-LAR-C and myc-cortactin and imaged for CD8 (green) and myc (red). Box indicates zoomed in region.
T-test: *, p<0.05; **, p<0.005; ***, p<0.0005. All data are expressed as mean ± SEM.

of the LAR D2 domain with liprin-α2, so we analyzed the staining intensity of liprin-α2, p140Cap, and cortactin in CD8-LAR-C clusters in neurons expressing CD8-LAR-C and liprin-α2 shRNA (Figure 3.4B, D, F). Surprisingly, endogenous cortactin was enriched in CD8-LAR-C clusters in the absence of liprin-α2 (Figure 3.4F,G), meaning that LAR is capable of inducing cortactin clustering independently of liprin-α2, possibly via a direct interaction. Interestingly, in HeLa cells, we did observe colocalization in cells expressing only CD8-LAR-C and cortactin (Figure 3.4H), further supporting a direct interaction between LAR and cortactin. In liprin-α2 knockdown cells, p140Cap was not significantly enriched in CD8-LAR-C clusters, though some enhancement was seen, likely due to its interaction with cortactin (Figure 3.4D, G). Therefore, LAR directly induces the clustering of endogenous liprin-α2 and cortactin in hippocampal neurons, and p140Cap co-clusters through its interaction with liprin-α2.

3.2.4 Liprin-α2 and p140Cap are necessary for axon growth

How do LAR, liprin-α2, p140Cap, and cortactin regulate axon growth and branching, and can the defects seen in LAR shRNA expressing neurons be explained or rescued by the other members of the protein complex? Upon overexpression of GFP-liprin-α2 in LAR knockdown neurons, we observed a significant rescue of the total axon length of doubly transfected cells (4.1 ± 0.5 mm, Figure 3.5A, B). Moreover, when we knocked down liprin-α2 with liprin-α2 specific shRNA (Ch. 5), total axon length was severely decreased (2.1 ± 0.2 mm, Figure 3.5A, B), indicating that liprin-α2 is necessary for normal axon growth, and suggesting that LAR acts through liprin-α2 to support this.

To further investigate the downstream mechanism of LAR/liprin-α2 mediated axon growth, we tested the influence of p140Cap on total axon length. Similar to LAR and liprin-α2 knockdown, depletion of p140Cap by expressing p140Cap shRNA[114] caused a decrease in total axon length compared to control (2.9 ± 0.4 mm, Figure 3.5A, C). Furthermore, expression of a p140Cap dominant negative construct that interferes with the EB3-p140Cap interaction[114] and does not bind liprin-α2 (data not shown) also resulted in diminished axon growth (2.7 ± 0.3 mm, Figure 3.5A, C). These results show that the loss of axon growth caused by LAR knockdown is dependent on liprin-α2, likely via the disruption of microtubule growth by mislocalization of p140Cap.
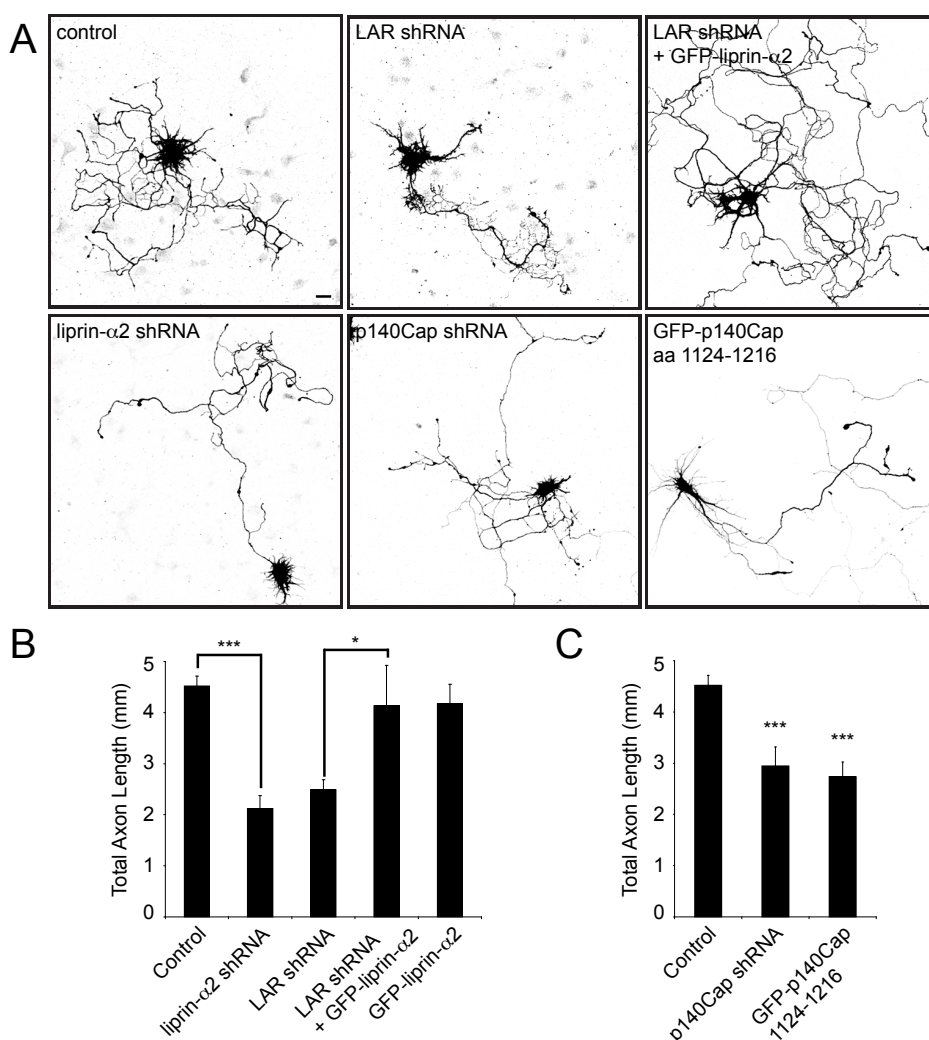
Figure 3.5. *LAR regulates axon growth through liprin-α2 and p140Cap.*
(A) Representative images of DIV1+4 neurons transfected with β-galactosidase and either LAR shR-NA, LAR shRNA with GFP-liprin-α2, liprin-α2 shRNA, p140Cap shRNA, or GFP-p140Cap aa 1124-1216. Scale bar, 10 μm.
(B) Quantification of the total axon length visible in a single field of view 460.7μm x 460.7μm (n=10-78 neurons from 1-8 experiments).
(C) Quantification of the total axon length visible in a single field of view 460.7μm x 460.7μm (n=10-78 neurons from 1-8 experiments).
T-test: *, p<0.05; **, p<0.005; ***, p<0.0005. All data are expressed as mean ± SEM.
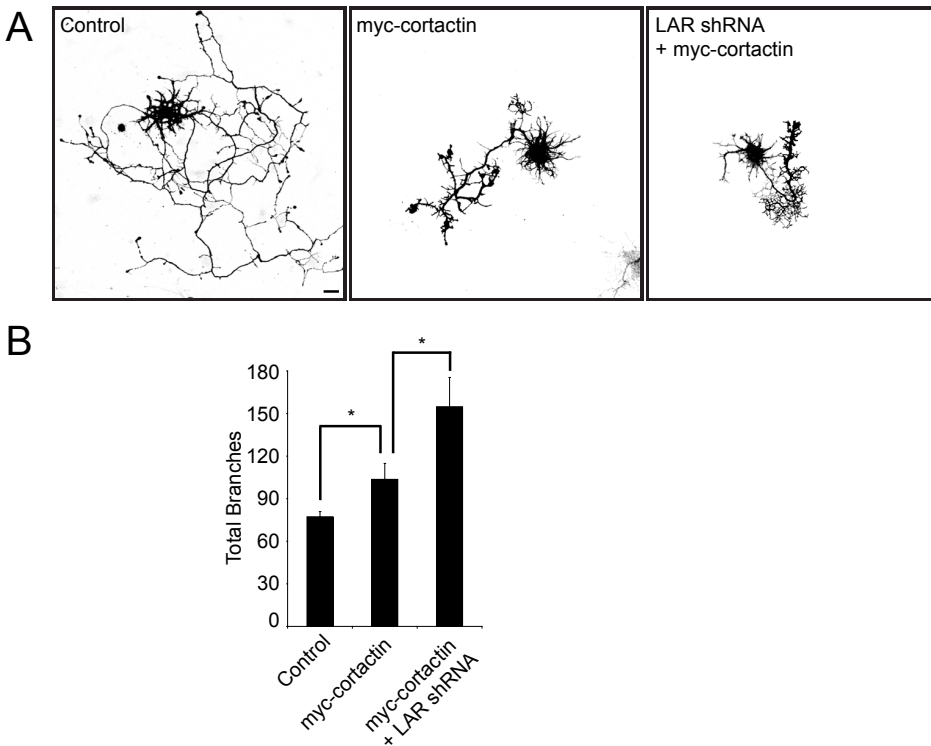
Figure 3.6. *LAR inhibits cortactin-mediated axon branching.*
(A) Representative images of DIV1+4 neurons transfected with β-galactosidase and either myc-cortactin or myc-cortactin with LAR shRNA. Scale bar, 10μm.
(B) Quantification of the total axon branching points per neuron (n=10-78 neurons from 1-8 experiments).
T-test: *, p<0.05; **, p<0.005; ***, p<0.0005. All data are expressed as mean ± SEM.

3.2.5 Cortactin is responsible for promoting axon branching

Though liprin-α2 overexpression returned axon length in LAR deficient neurons to control levels, it did nothing to alter the increase in branches (data not shown), indicating that another molecular pathway is responsible for this phenomenon. Since cortactin is known to cause axon branching by increasing actin polymerization[115], we wondered if LAR was acting through cortactin to control branching. Consistently, overexpression of cortactin caused a marked increase in total branching (104 ± 11 branches, Figure 3.6A,B). In cells coexpressing LAR shRNA and cortactin, this effect was even more pronounced (155 ± 21 branches, Figure 3.6A,B), indicating that in developing neurons, LAR probably functions as an inhibitor of cortactin with regard to actin polymerization and therefore negatively regulates axonal branching.

3.3 Discussion

3.3.1 LAR controls MT and axon growth via liprin-α2, p140Cap, and EB3

The way in which developing axons grow in a rapid and controlled fashion is a multifaceted and highly regulated process. Numerous families of molecules have been identified as key players in axon growth and guidance[22], not the least of which are the protein tyrosine phosphatases[111, 116]. In *Drosophila*, dlar is critical for neuronal development both through its phosphatase activity and independently of it[29], and LAR knockout mice have impaired innervation of the dentate gyrus[112, 113]. Here we show that LAR is a critical regulator of axon development in cultured hippocampal neurons. Depletion of LAR causes a severe decrease in axon length coupled with an increase in total axonal branches. Investigation of the downstream pathway involved in this effect revealed that overexpression of liprin-α2 was capable of restoring LAR shRNA-expressing axons to their normal lengths, though the increase in branches persisted. We identified a novel liprin interacting partner, p140Cap, which, through its interaction with the microtubule plus-end tracking protein (+TIP) EB3[114], promotes axonal extension.

Microtubules make up the main cytoskeletal structure of the axonal shaft and extend into the growth cone, where they splay out and explore the entire surface of the growth cone[24]. Dynamic MTs are crucial for growth cone turning, as many attractive and repulsive axon guidance cues act to stabilize or destabilize microtubules[28]. Additionally, MT polymerization is necessary for axon growth[117], and the structural fidelity of the axon as well as the consolidation of new axonal branches are dependent on MTs[24]. It is thought that much of this behavior is caused by the transient "capture" and subsequent stabilization of MTs due to interactions between MT +TIPs and receptors and signaling proteins at the growth cone membrane[24]. We show that clustering of LAR-RPTP can cause clustering of liprin-α2 and p140Cap at the cell membrane, which can then interact with MTs via EB3[114]. Though the precise relationship between LAR, liprin-α2, p140Cap, and MT polymerization remains unclear, this suggests that LAR promotes axon growth by signaling to MTs via this molecular pathway (Fig. 3.7), the disruption of which results in a severe decrease in axon length.

3.3.2 LAR inhibits axon branching through cortactin

In addition to exhibiting considerably less axonal growth, LAR-deficient neurons displayed a notable increase in axon branching. Moreover, overexpression of LAR in

LAR

liprin-α2   cortactin

p140Cap

EB3

microtubules   actin

axon   axon
growth   branching
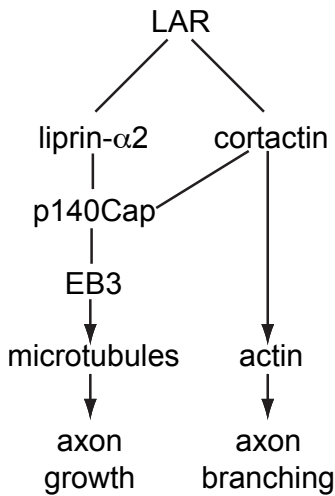
Figure 3.7. *Model of LAR function in axon growth and branching.*
Flow chart of interactions at the axonal growth cone and their consequences for axon growth and branching. Lines indicate proposed interactions and arrows denote the functions of those interactions. LAR binds directly to both liprin-α2 and cortactin. Cortactin regulates the actin cytoskeleton and therefore axon branching. Liprin-α2 binds to p140Cap, which interacts with EB3 and redundantly to cortactin. The interaction between p140Cap and EB3 regulates microtubule polymerization and axon growth.

developing neurons resulted in the neuron having fewer branches, indicating that LAR acts as a negative regulator of axonal branching. These new branches, however, were not consolidated and did not, on average, extend more than a few micrometers, implying that they were caused by excess actin polymerization along the axonal shaft[24]. Axon branching and actin polymerization are known to be highly influenced by local levels of cortactin within the axon[115] and tyrosine-phosphorylation of cortactin by Src kinase stimulates actin assembly[118]. We found that LAR directly influences cortactin localization within neurons and LAR knockdown enhances the super-branching phenotype seen in cortactin overexpressing neurons. Therefore, it appears that LAR inhibits axon branching by negatively regulating cortactin (Figure 3.7), likely as the counterbalancing phosphatase to Src activity. However, the mechanism by which LAR activity is controlled, and whether cortactin is in fact a substrate of LAR phosphatase activity remains to be determined. RPTP catalytic activity is generally thought to be inhibited by dimerization of the intracellular domains, though this has not been shown to be the case for LAR[110]. Intriguingly, it is also possible that actin polymerization and axon branch formation is induced by LAR clustering simply by redistributing cortactin, completely independent of LAR phosphatase activity, as evidenced by the fact that simply increasing global cortactin levels within the neuron is sufficient to induce axon branching (Figure 3.6)[115]

Chapter 4

Liprin-α1 Degradation by Calcium/Calmodulin-Dependent Protein Kinase II Regulates LAR Receptor Tyrosine Phosphatase Distribution and Dendrite Development

Casper C. Hoogenraad[1,2], Monica I. Feliu-Mojer[1], Samantha A. Spangler[2], Aaron D. Milstein[1], Anthone W. Dunah[1], Albert Y. Hung[1], and Morgan Sheng[1]

[1]Picower Institute of Learning and Memory, RIKEN-MIT Neuroscience Research Center, Howard Hughes Medical Institute, Massachusetts Institute of Technology, Cambridge, MA, USA; [2]Department of Neuroscience, Erasmus MC, Rotterdam, The Netherlands

Neural activity regulates dendrite and synapse development but the underlying molecular mechanisms are unclear. Ca^{2+}/calmodulin-dependent protein kinase II (CaMKII) is an important sensor of synaptic activity, and the scaffold protein liprin-α1 is involved in pre- and postsynaptic maturation. Here we show that synaptic activity can suppress liprin-α1 protein level by two pathways: CaMKII-mediated degradation and the ubiquitin-proteasome system (UPS). In hippocampal neurons, liprin-α1 mutants that are immune to CaMKII degradation impair dendrite arborization, reduce spine and synapse number, and inhibit dendritic targeting of receptor tyrosine phosphatase LAR, which is important for dendrite development. Thus regulated degradation of liprin-α1 is important for proper LAR receptor distribution, and could provide a mechanism for localized control of dendrite and synapse morphogenesis by activity and CaMKII.

4.1. Introduction

Activity-dependent calcium entry into neurons induces a variety of changes, ranging from transient post-translational modifications of synaptic proteins to altered gene expression. At excitatory synapses Ca^{2+} influx through voltage-gated Ca^{2+} channels and ionotropic glutamate receptors (particularly NMDA receptors) triggers biochemical cascades that regulate synaptic function[119, 120]. Calcium signaling pathways also control neuronal differentiation, axon pathfinding and dendrite morphogenesis[121].

A major player in all these processes is calcium/calmodulin-dependent protein kinase II (CaMKII), a calcium-activated serine/threonine kinase that is abundant in neurons, especially at postsynaptic sites[121, 122]. The CaMKII holoenzyme, consisting of approximately 12 α and/or β subunits, is the most abundant constituent of the postsynaptic density (PSD)[45]. In mature hippocampal neurons, both CaMKIIα and CaMKIIβ are present at postsynaptic sites but seem to play different roles[123, 124]. Ca^{2+}/calmodulin binding to CaMKII subunits stimulates intersubunit Thr286 autophosphorylation (resulting in an activated kinase) and leads to phosphorylation of many substrates[122].

Several CAMKII substrates, such as the NR2B subunit of NMDA receptors and the *Drosophila* homolog of mammalian CASK, camguk, interact directly with CaMKII[125, 126]. These interactions differ in their dependence on Ca^{2+}/calmodulin binding and autophosphorylation and require different domains of the kinase; some even appear to be specific for either CaMKIIα (densin-180) or CaMKIIβ (F-actin)[125]. The variety of CaMKII interactions with neuronal proteins could target CaMKII to specific subcellular domains and modulate CaMKII activity during synapse formation[124], synaptic plasticity[123], axonal arborization and dendrite morphogenesis[127, 128]. By functioning as a local calcium sensor, CaMKII exerts a critical influence on the architecture of the developing and plastic brain.

The liprin-α family of proteins (liprin-α1, α2, α3, α4) were originally identified by their interaction with the LAR (leukocyte common antigen-related) family of receptor protein tyrosine phosphatases (LAR-RPTPs)[81]. Liprin-α proteins consist of an N-terminal coiled-coil region that mediates homo- and heteromultimerization, followed by three SAM domains making up the liprin homology region (LH) that binds to the D2 (inactive phosphatase) domain of LAR-RPTPs[79]. In cultured cell lines liprin-αs regulate LAR localization and clustering[78, 79]. In *Drosophila* both liprin-α and LAR are required for photoreceptor axon targeting in the visual system[91, 92] and
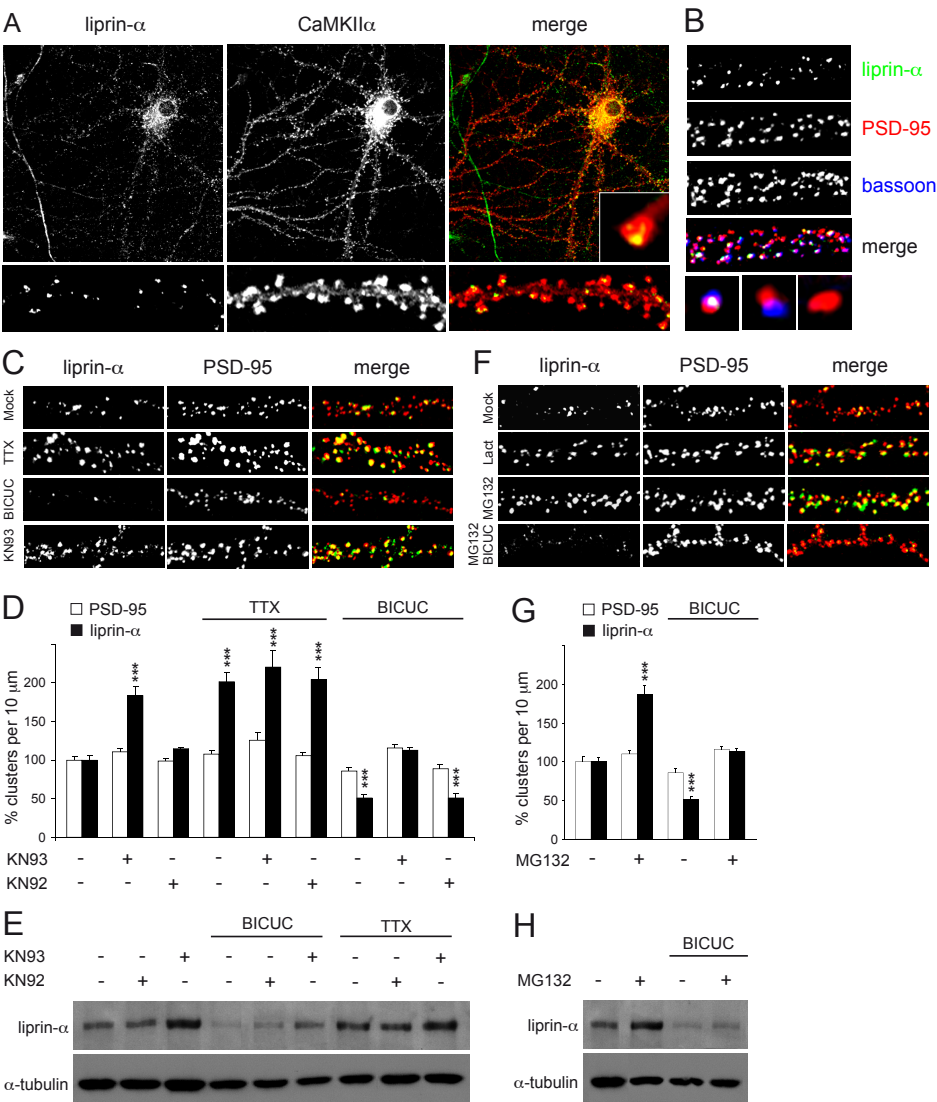
Figure 4.1. *Regulation of liprin-α levels by CaMKII and proteasome in hippocampal neurons.*
(A) Representative images of rat hippocampal neurons (DIV13) double-labeled with rabbit anti-liprin-α antibody (green) and mouse anti-CaMKIIα antibody (red). Only the merge is shown in color. Dendritic segments (lower panels) are enlarged to show colocalization of liprin-α and CaMKIIα in spines. One single spine is enlarged (inset).
(B) Dendrites of hippocampal neurons triple-labeled with rabbit anti-liprin-α antibody (green), guinea pig anti-PSD-95 (red) and mouse anti-bassoon (blue). High magnification panels (bottom) show three examples of synaptic clusters triple stained for liprin-α (green), PSD-95 (red), and bassoon (blue).
(C) Dendrites of hippocampal neurons at DIV17 treated with control vehicle (Mock), KN93 (10μM), TTX (2μM), and bicuculline (BICUC, 40μM) for 24 hours and stained for liprin-α (green) and PSD-95 (red) as indicated.
(D) Quantification of number of liprin-α and PSD-95 clusters per 10 μm dendrite, normalized to control. Hippocampal neurons at DIV17 were treated for 24 hours with control vehicle (-), KN92 or KN93 (+) in combination with TTX and bicuculline (BICUC), as indicated. Histograms indicate mean ± SEM.

normal synaptic morphology at the larval neuromuscular junction[89]. Mutants in the *C. elegans* liprin-α homolog *syd-2* display an abnormally diffuse distribution of presynaptic markers, lengthening of active zones, and impaired synaptic transmission[86].

In mammals, liprin-α proteins bind to several proteins present at presynaptic sites[53]. Together with data showing altered synaptic vesicle movement in *Drosophila* liprin-α mutants[129], it is believed that in axons liprin-α has a role both in synaptic vesicle trafficking and active zone organization. However, liprin-α is also localized in dendrites and postsynaptic sites, suggesting additional roles[94, 107, 109]. A postsynaptic function for liprin-α has been described in hippocampal neurons, where liprin-α binds to glutamate receptor interacting protein (GRIP) and regulates synaptic targeting of AMPA receptors[94]. In addition, liprin-α associates with cadherin-β-catenin and, in conjunction with LAR-RPTPs, regulates its trafficking; in this way, liprin-α is implicated in the development and/or maintenance of dendritic spines and excitatory synapses[96].

Here we describe a novel activity-dependent regulation of liprin-α by CaMKII, in which liprin-α1 is degraded in response to CaMKII phosphorylation. Liprin-α1 levels in hippocampal neurons are additionally regulated by the UPS via the E3 ubiquitin ligase APC (Anaphase Promoting Complex). Expression of liprin-α1 mutants insensitive to CaMKII degradation specifically inhibits the dendritic targeting of LAR receptors and leads to reduced dendrite arborization and synapse number. These findings provide a molecular basis for activity-dependent regulation of dendrite and synapse development by CaMKII, liprin-α1 and LAR-RPTPs.
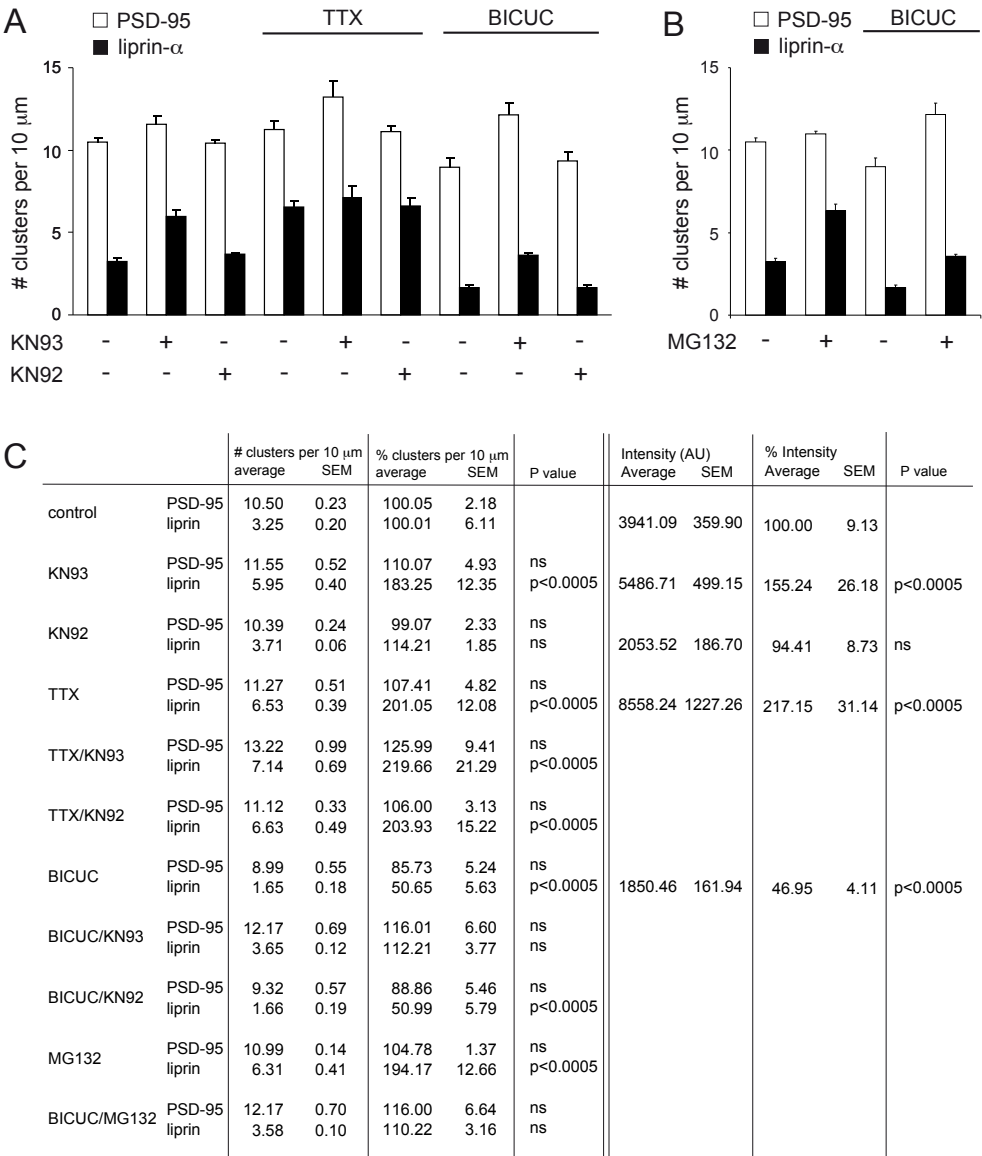

(E) Hippocampal cultures (DIV17) were treated for 24 hours with control vehicle (-), KN92 or KN93 (+) in combination with TTX or BICUC, as indicated. Total lysates were immunoblotted for liprin-α and α-tubulin as a loading control.

(F) Dendrites of hippocampal neurons at DIV17 treated with control vehicle (Mock), lactacystin (5µM), MG132 (20µM), or a combination of BICUC and MG132 for 24 hours and double stained for liprin-α (green) and PSD-95 (red).

(G) Number of liprin-α and PSD-95 clusters per 10 µm dendrite (mean ± SEM). Hippocampal neurons at DIV17 were treated for 24 hours with control vehicle (-) or MG132 (+), with or without BICUC, as indicated. The number of clusters is normalized to unstimulated conditions.

(H) Hippocampal cultures (DIV17) were treated for 24 hours with control vehicle (-) or MG132 (+), with or without BICUC, as indicated. Total lysates were immunoblotted for liprin-α and α-tubulin as a loading control. * p<0.05, ** p<0.005, *** p<0.0005.

Figure 4.2. *Quantification of endogenous liprin-α and PSD-95 cluster density.*
(A) Number of liprin-α and PSD-95 clusters per 10 μm dendrite length. Hippocampal neurons at DIV17 were treated for 24 hours with control vehicle (-), KN92 or KN93 (+), with TTX or bicuculline (BICUC), as indicated. Histograms indicate mean ± SEM.
(B) Number of liprin-α and PSD-95 clusters per 10 μm dendrite. Hippocampal neurons at DIV17 were treated for 24 hours with control vehicle (-) or MG132 (+), with or without BICUC, as indicated.
(C) Table of data values for the absolute number of liprin-α and PSD-95 clusters per 10 μm; percentage of liprin-α and PSD-95 clusters normalized to control; and the p-values for all treatments used in Figure 1. Right part of table shows the liprin-α immunostaining intensities (in arbitrary units (AU)).

4.2. Results

4.2.1 Downregulation of liprin-α in hippocampal neurons by CaMKII and proteasome-mediated degradation

In screening for synaptic proteins whose abundance is regulated by synaptic activity, we discovered that liprin-α levels fluctuate greatly in response to altered activity in cultured neurons. Liprin-α proteins are present at both presynaptic and postsynaptic sites in the brain[94, 96]. In cultured hippocampal neurons (17 days in vitro (DIV17)) fixed with ice cold methanol, immunostaining with antibody made against liprin-α1 shows a punctate pattern as previously described[94, 107, 109], colocalizing with CaMKIIα in dendritic spines (Figure 4.1A). Liprin-α puncta also showed extensive overlap with PSD-95, a postsynaptic density (PSD) protein, and with bassoon, a presynaptic active zone protein (Figure 4.1B), indicating the presence of liprin-α at synapses. The intensity of liprin-α staining was generally weaker and more variable than the staining of these synaptic markers, such that some synapses had robust liprin-α staining while other synapses showed undetectable signal (Figure 4.1A,B). Quantification revealed that ~90% of liprin-α puncta overlapped with PSD-95 and bassoon clusters, but only ~30% of the PSD-95 and bassoon coclusters contained liprin-α staining (Figures 4.1B and 4.2C).

Suppressing activity with tetrodotoxin (TTX, 2 μM, 24 h) strongly increased liprin-α expression, whereas increasing synaptic activity with the $GABA_A$ receptor antagonist bicuculline (40 μM, 24 h) reduced liprin-α expression in cultured hippocampal neurons (DIV17) (Figure 4.1C). The density of liprin-α clusters doubled in TTX-treated cells, associated with increased immunofluorescence intensity of the clusters (Figures 4.1C,D and 4.2A,C). Bicuculline profoundly reduced liprin-α puncta density and brightness of staining. PSD-95 immunostaining showed similar bidirectional trends with altered activity, but the magnitude of fluctuation was much lower than that of liprin-α (Figures 4.1C,D and 4.2A,C). Western blotting confirmed that liprin-α protein levels fell with increased activity (bicuculline) and rose with inactivity (TTX) (Figure 4.1E).

We tested whether CaMKII might play a role in the activity-dependent loss of liprin-α, because this protein kinase is activated by synaptic excitation. Bath application of KN93, an inhibitor of CaMKII, strongly enhanced liprin-α protein levels (Figure 4.1E) and increased the brightness and density of liprin-α clusters (Figure

4.1C,D). KN92, an inactive analogue of KN93, had no effect on liprin-α levels by Western blot or by immunocytochemistry (Figure 4.1D,E). Again, PSD-95 showed a similar trend with KN93, but the degree of increase was much smaller than that of liprin-α (Figure 4.1C,D). Thus KN93 mimicks the effect of TTX on liprin-α expression. More importantly, KN93 prevented the effect of bicuculline and "rescued" liprin-α back to control levels (Figure 4.1D, E); however, liprin-α expression in neurons treated with both KN93 and bicuculline did not reach the high level seen with KN93 alone (Figure 4.1D,E). These data indicate that CaMKII plays an important role in activity-dependent loss of liprin-α, but suggest that additional independent mechanisms might be involved.

Since the UPS plays an important role in synaptic protein turnover[70], we tested whether proteasome inhibitors affected liprin-α expression in hippocampal neurons. MG132 (20 μM, 24 h) or lactacystin (5 μM, 24 h) caused a robust increase in liprin-α protein levels and in liprin-α cluster density (Figures 4.1F-H and 4.2B,C). MG132 also blocked the reduction of liprin-α by bicuculline (Figures 4.1F,G and 4.2B,C); however, liprin-α level or cluster number did not reach the high values seen with MG132 alone (Figure 4.1F-H). These data indicate that proteasome-mediated degradation keeps the "basal" level of liprin-α low and contributes substantially to activity-induced loss of liprin-α; however, additional mechanisms seem to be involved, as noted above for CaMKII. Another possibility is that CaMKII- and proteasome-mediated down-regulation of liprin-α1 activity only partially depend on synaptic activity, as induced by bicuculline. Together, our results suggest that downregulation of liprin-α in hippocampal neurons is mediated by CaMKII activity as well as proteasome degradation.

4.2.2 RNAi knockdown of APC increases liprin-α

In *Drosophila* neurons liprin-α may be regulated by APC, which acts as an E3 ubiquitin ligase[130]. APC consists of >11 core subunits, including catalytic subunits APC2 and APC11, and is activated by regulatory subunits such as Cdh1[131]. We tested whether APC might regulate liprin-α1 in mammalian neurons by using small hairpin RNA (shRNA) expressed from the pSuper vector to knock down endogenous APC2 and Cdh1. Hippocampal neurons were transfected at DIV13 for 4 days with two independent APC2-shRNA (APC2-shRNA#1 or APC2-shRNA#2) or Cdh1-shRNA constructs, together with β-galactosidase to mark transfected neurons. To better preserve

the β-gal staining, these cultures were fixed with formaldehyde, which results in a more diffuse staining of liprin-α in dendrites in addition to the punctate synaptic pattern seen predominantly under methanol fixation conditions (Figure 4.3A,D). In neurons transfected with APC2-shRNA or Cdh1-shRNA constructs[131], the intensity of liprin-α immunostaining in dendrites was drastically increased (~100-150% increase compared to control neurons) (Figure 4.3A,B). The intensity of PSD-95, revealed by double staining, was unchanged in the same neuron (Figure 4.3C). Together with the MG132 and lactacystin results, these findings indicate that the UPS, particularly that
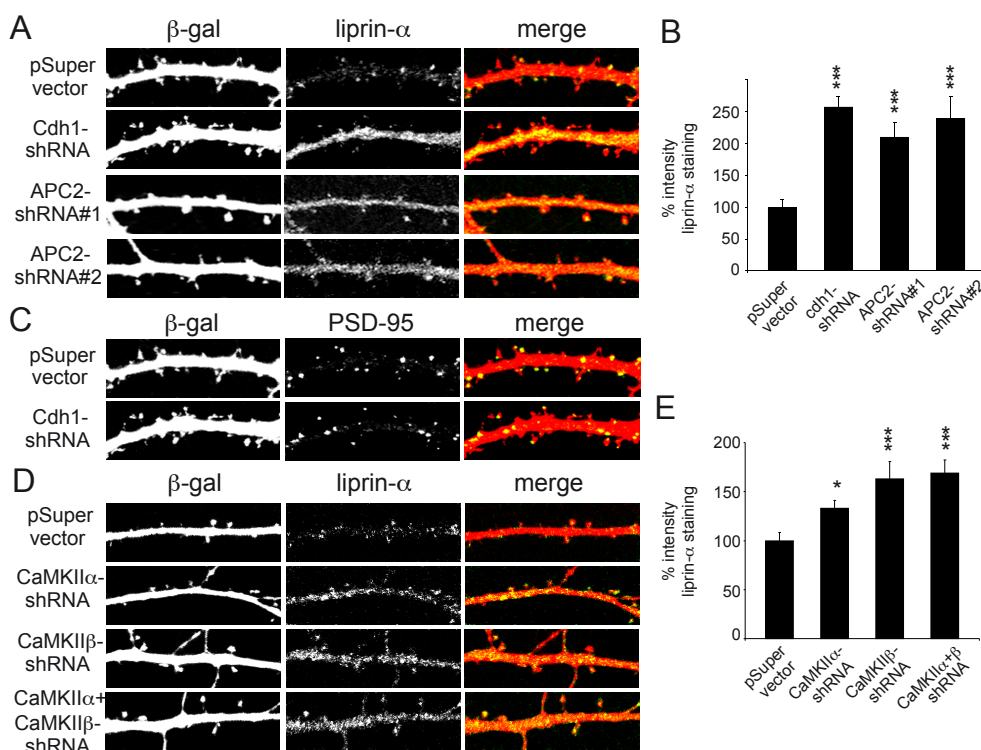
Figure 4.3. *APC and CaMKIIα/β knock down by RNAi alters liprin-α levels in hippocampal neurons.*
(A) Dendrites of hippocampal neurons transfected at DIV13 for 4 days with control pSuper vector, Cdh1-shRNA, APC2-shRNA#1 or APC2-shRNA#2 and labeled with rabbit anti-liprin-α antibody (green) and for cotransfected β-galactosidase (β-gal; red).
(B) Quantification of liprin-α immunostaining intensity (mean ± SEM; normalized to control) in dendrites of hippocampal neurons transfected as in A.
(C) Dendrites of hippocampal neurons transfected at DIV13 for 4 days with control pSuper vector or Cdh1-shRNA and labeled for PSD-95 (green) and cotransfected β-gal (red).
(D) Dendrites of hippocampal neurons transfected at DIV13 for 4 days with empty pSuper vector, CaMKIIα-shRNA, CaMKIIβ-shRNA, or a combination of CaMKIIα-shRNA and CaMKIIβ-shRNA, and double-labeled for liprin-α and cotransfected β-gal (red).
(E) Quantification of liprin-α immunostaining intensity (mean ± SEM; normalized to control) in dendrites of hippocampal neurons transfected as in D. * $p<0.05$, ** $p<0.005$, *** $p<0.0005$.

mediated by APC, downregulates expression of liprin-α in hippocampal neurons.

4.2.3 CaMKIIα/β knockdown by RNAi increases liprin-α in hippocampal neurons

To test which CaMKII isoform regulates liprin-α levels in hippocampal neurons, we knocked down expression of endogenous CaMKIIα or CaMKIIβ by transfection of shRNA expressing constructs. When tested in COS-7 cells, CaMKIIα-shRNA construct specifically inhibited protein expression of CaMKIIα, and CaMKIIβ-shRNA specifically suppressed CaMKIIβ (Figure 4.4E). These RNAi constructs were co-transfected in hippocampal neurons (DIV13) with green fluorescent protein (GFP) to visualize morphology. Cells transfected with CaMKIIα-shRNA showed ~70% reduction in immunostaining for CaMKIIα in dendrites and cell body, with no change in CaMKIIβ staining intensity (Figure 4.4A-D). CaMKIIβ-shRNA-transfected neurons showed diminished staining for both CaMKIIβ (~80% reduction) and CaMKIIα (~60% reduction) (Figure 4.4A-D). Since CaMKIIβ-shRNA did not affect CaMKIIα expression in COS-7 cells, we believe that the loss of neuronal CaMKIIα induced by CaMKIIβ-shRNA is likely a secondary consequence of CaMKIIβ knockdown than due to non-specicitiy of CaMKIIβ-shRNA (for instance, CaMKIIβ might be required for formation of stable CaMKIIα/β hetero-oligomeric holoenzymes).

We measured liprin-α by immunostaining in hippocampal neurons transfected at DIV13 with CaMKIIα-shRNA, CAMKIIβ-shRNA, or both. β–Galactosidase (β-gal) was cotransfected to mark and outline the transfected cell. These cultures were fixed with formaldehyde. Four days after transfection of CaMKII-shRNA (DIV13+4), the integrated intensity per area (diffuse plus punctuate staining) of liprin-α immunostaining in the dendrite shaft was increased compared to control (~30% increase for CaMKIIα-shRNA, ~50% increase for CaMKIIβ-shRNA or CaMKIIα + CaMKIIβ-shRNA) (Figure 4.3D,E). Intensity of PSD-95 staining was unchanged (data not shown). These RNAi data extend the KN93 pharmacological results, confirming that CaMKII inhibits liprin-α protein expression in hippocampal neurons. At least the CaMKIIα isoform is involved; however, because CaMKIIβ-shRNA reduces expression of both CaMKIIα and CaMKIIβ, we cannot be certain if CaMKIIβ directly regulates liprin-α levels.
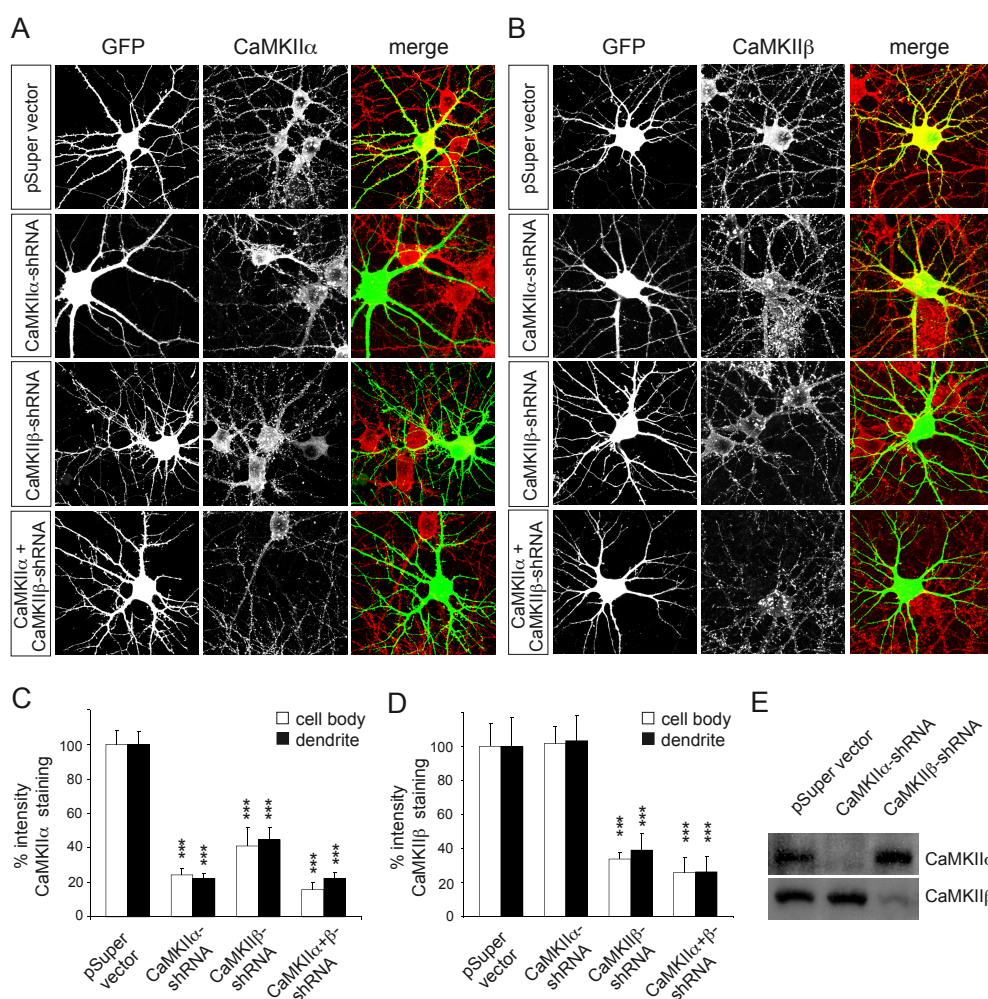
Figure 4.4. *CaMKIIα-shRNA and CaMKIIβ-shRNA suppress the expression of CaMKIIα and CaMKIIβ.*
(A-B) Representative images of hippocampal neurons transfected at DIV13 with control pSuper vector, CaMKIIα-shRNA, CaMKIIβ-shRNA, or a combination of CaMKIIα-shRNA and CaMKIIβ-shRNA and double-labeled with anti-CaMKIIα (A) or anti-CaMKIIβ (B) antibody (red) and for cotransfected GFP (green).
(C-D) Quantification of CaMKIIα (C) and CaMKIIβ (D) immunostaining intensities (mean ± SEM, normalized to pSuper control) in cell body and dendrites of hippocampal neurons transfected at DIV13 for 4 days with control pSuper vector, CaMKIIα-shRNA, CaMKIIβ-shRNA, or a combination of CaMKIIα-shRNA and CaMKIIβ-shRNA.
(E) COS-7 cells were cotransfected with pSuper-based shRNA constructs targeting CaMKIIα or CaMKIIβ or empty vector, together with cDNAs expressing CaMKIIα or CaMKIIβ, and immunoblotted for the transfected protein (indicated at right). * $p<0.05$, ** $p<0.005$, *** $p<0.0005$.
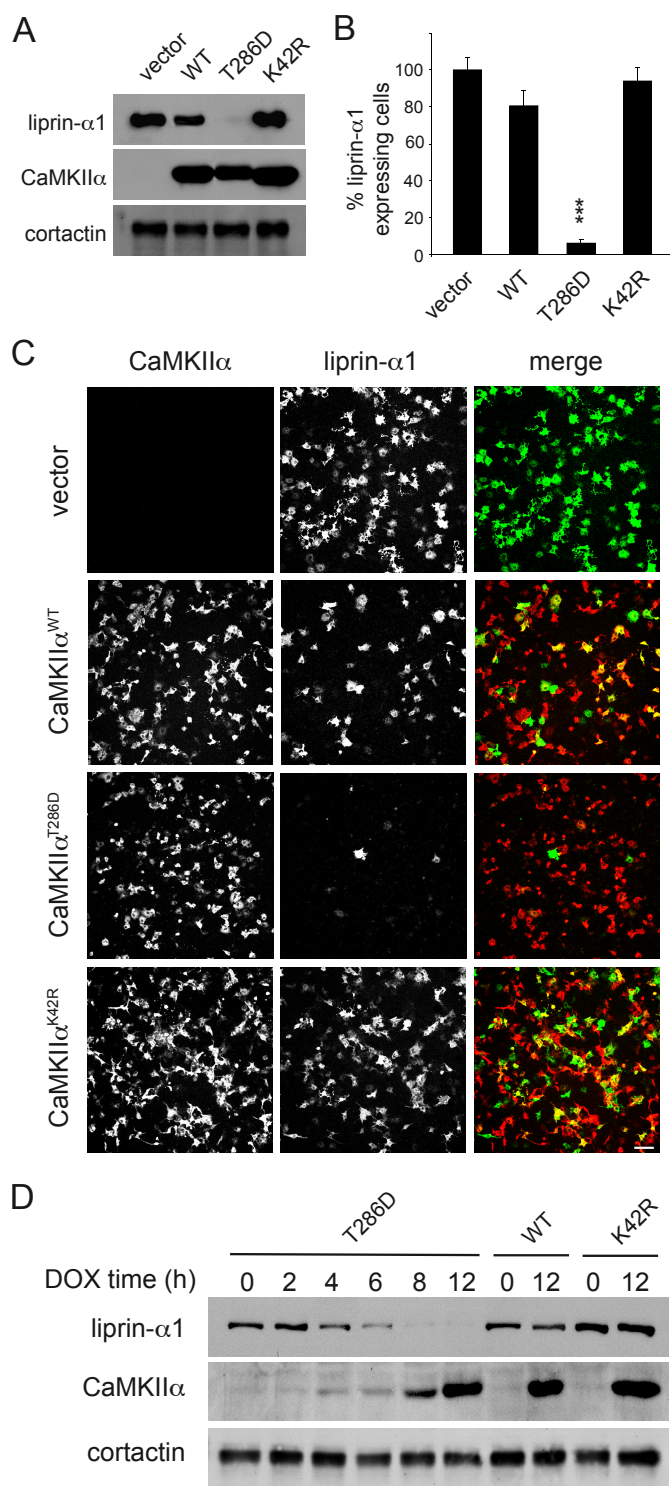
Figure 4.5. *Induction of active CaMKIIα suppresses liprin-α1 protein levels.*

(A) COS-7 cells were double transfected for 2 days with myc-liprin-α1 plus empty vector control, wildtype (WT) CaMKIIα, constitutively active CaMKIIα(T286D), or kinase dead CaMKIIα(K42R), as indicated. Whole cell lysates from transfected COS-7 cells were immunoblotted for liprin-α1 and CaMKIIα to detect the transfected constructs, and for endogenous cortactin as a loading control.

(B) Number of liprin-α1-immunopositive cells (mean ± SEM; normalized to control) in COS-7 cultures transfected with GFP-liprin-α1 and CaMKII constructs as in C.

(C) Representative images of COS-7 cells cotransfected with GFP-liprin-α1 (green) plus control vector, CaMKIIα(WT), CaMKIIα(T286D), or CaMKIIα(K42R) (red), as indicated. The merge is shown in color at right. Scale bar, 100 μm. * p<0.05, ** p<0.005, *** p<0.0005.
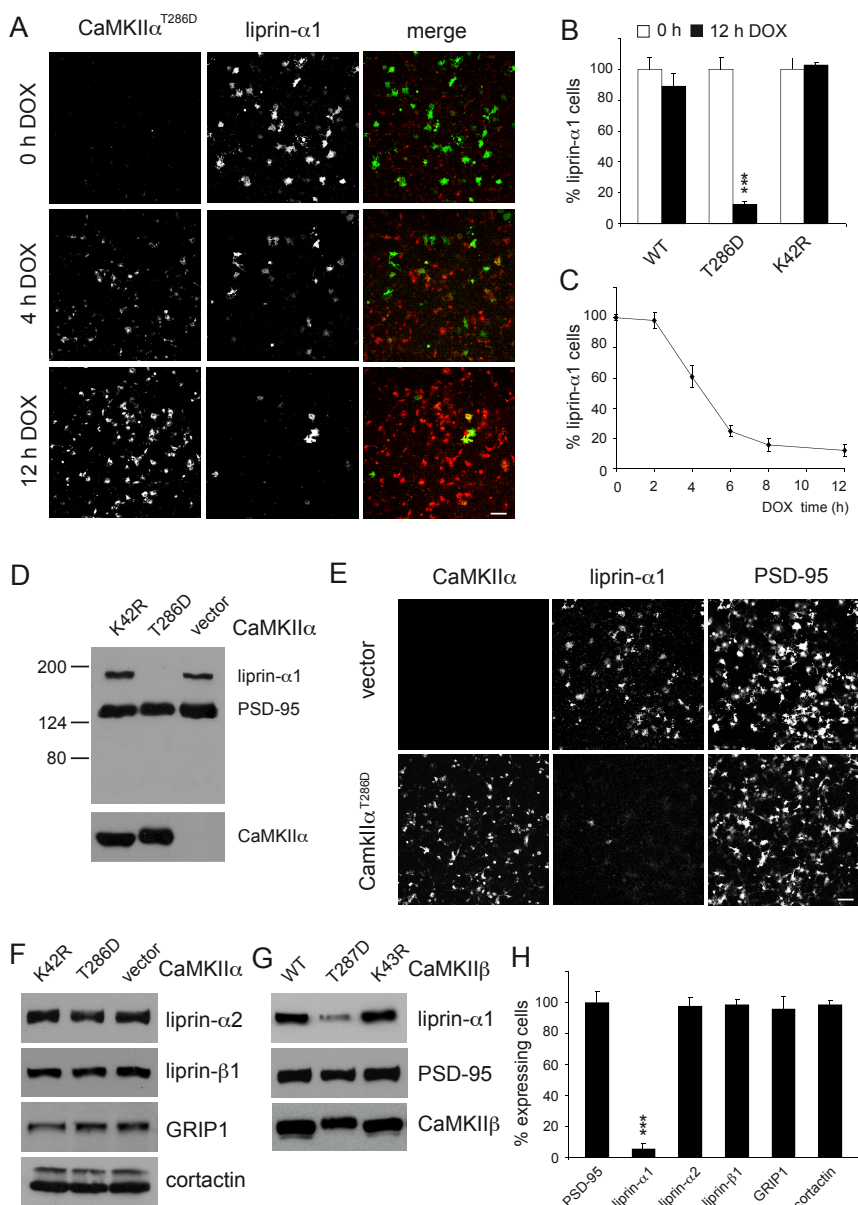
(D) COS-7 cells were cotransfected with myc-liprin-α1, pTRE-CaMKIIα (WT, T286D, or K42R) and rtTA expression construct. Two days after transfection, cells were treated with doxycycline (DOX) for various times as indicated (0-12 hours), and were immunoblotted for liprin-α1 and CaMKIIα to detect the transfected constructs and for endogenous cortactin as loading control.

4.2.4 Active CaMKII decreases liprin-α1 protein level in COS-7 cells

To investigate the mechanism by which liprin-α1 expression is suppressed by CaM-KII, we first turned to heterologous cells. In COS-7 cells, exogenous myc-tagged liprin-α1 was expressed as a band of ~160 kD (Figure 4.5A). Remarkably, when constitutively active CaMKIIα (T286D) was cotransfected, myc-liprin-α1 levels became virtually undetectable (Figure 4.5A). Cotransfection of wild-type CaMKIIα (WT) or kinase-dead CaMKIIα (K42R) mutant did not affect liprin-α1 protein levels (Figure 4.5A). A similar degree of suppression by cotransfected CaMKIIα(T286D) was seen for untagged liprin-α1, liprin-α1 tagged with GFP or HA, and liprin-α1 expressed from different promoters (CMV, SV40, chicken βactin), with or without the 3' and 5' untranslated regions of liprin-α1 (data not shown). These results argue that CaMKII is not acting on the transcription or mRNA stability of liprin-α1.

We also analyzed the effect of CaMKII on liprin-α1 by an immunocytochemical assay. Liprin-α1 cotransfected into COS-7 cells with empty vector control showed on average ~94 liprin-α1-immunoreactive cells per 1.7 mm^2 in a 50-70% confluent cell layer (Figure 4.5B,C). When liprin-α1 was cotransfected with constitutively active CaMKIIα(T286D), however, only very few cells (~6 per 1.7 mm^2) expressed liprin-α1 by immunostaining (Figure 4.5B,C). Cotransfection with wild-type (WT) or kinase dead (K42R) CaMKIIα did not reduce the number of liprin-α1-immunoreactive cells (Figure 4.5B,C).

To confirm that the loss of liprin-α1 protein is due to the expression of CaMKIIα protein, we used a doxycycline (DOX)-inducible expression system (TETon) and followed over time the level of liprin-α1 protein following the induction of active CaMKIIα. COS-7 cells were triply transfected with GFP-liprin-α1, CaMKIIα(T286D) under the control of a tetracycline-responsive element (pTRE-CaMKIIα(T286D)), and a tetracycline transcriptional activator (rtTA) expression construct. At time 0 (no DOX added), liprin-α1 protein was robustly detected by immunoblot in the absence of CaMKIIα signal (Figure 4.5D). From 4-12 hours after adding DOX, liprin-α1 expression declined steadily, inversely correlated with a progressively rising CaMKIIα (Figure 4.5D). At 12 hours after DOX addition, liprin-α1 was almost undetectable. No effect on liprin-α1 protein expression was seen 12 hours after induction of CaMKIIα(K42R) or CaMKIIα(wt) using the same TETon system (Figure 4.5D). Similar results were obtained with these constructs using an immunocytochemical assay (Figure 4.6A-C). Induction of CaMKIIα(T286D), but not CaMKIIα(K42R) or CaMKIIα(wt), caused a

Figure 4.6. *CaMKIIα(T286D) causes loss of liprin-α1.*
(A) COS-7 cells cotransfected with GFP-liprin-α1 and pTRE-CaMKIIα(T286D) at 0, 4, and 12 hours post-DOX treatment.
(B) Number of liprin-α1 immunopositive cells (mean ± SEM; normalized to 0 h) transfected with CaMKIIα(WT), CaMKIIα(T286D), or CaMKIIα(K42R) at 0h (untreated) and 12 hours after DOX treatment.
(C) Time course of number of liprin-α1 immunopositive cells (mean ± SEM; normalized to 0 h) trans-fected with CaMKIIα(T286D) as in A at various times (hours) following DOX treatment.
(D) COS-7 cells triple-transfected with myc-liprin-α1 and myc-PSD-95, plus control vector, CaMKIIα(T286D), or CaMKIIα(K42R), and immunoblotted for myc and CaMKIIα.

dramatic reduction in the number of liprin-α1-positive cells over time (Figure 4.6A-C and data not shown). These data provide compelling evidence that active CaMKIIα suppresses liprin-α1 protein levels, with a time course suggesting active degradation of liprin-α1 stimulated by CaMKIIα.

In COS-7 cells triply transfected with liprin-α1, PSD-95 and CaMKIIα, PSD-95 protein level was unaffected by CaMKIIα(T286D), even while liprin-α1 disappeared (Figure 4.6D). Immunocytochemistry analysis showed similar results: the percentage of PSD-95-immunoreactive COS cells was unaltered by cotransfection with CaMKIIα(T286D) (Figure 4.6E). CaMKIIα(T286D) also had no effect on GRIP1 (a multi-PDZ protein that binds to liprin-α1 and AMPA receptors), cortactin, liprin-α2 or liprin-β1 (proteins closely related to liprin-α1) (Figure 4.6F,H). Thus the effect of CaMKIIα(T286D) appears relatively specific for liprin-α1.

Liprin-α1 protein expression in COS-7 cells was also strongly inhibited by cotransfection of active CaMKIIβ (T286D), but not by wild-type or inactive CaMKIIβ (K43R) (Figure 4.6G). Polo-like kinase-2 (Plk-2, also known as serum-inducible kinase (SNK)) did not affect liprin-α1 levels in COS-7 cells (data not shown), even though it strongly suppressed expression of SPAR, a Rap guanosine triphosphatase activating protein[132]. Thus both CaMKIIα and CaMKIIβ can specifically suppress liprin-α1 expression in heterologous cells, consistent with RNAi results obtained in neurons (see Figure 4.3). The data are most simply explained by active CaMKII stimulating the degradation of liprin-α1.

4.2.5 C-terminus and PEST motif are essential for CaMKII dependent liprin-α1 degradation

As a first step toward the molecular mechanism behind this effect, we investigated the domains of liprin-α1 required for CaMKII-mediated suppression (Figure 4.7A). GFP-tagged wildtype and deletion mutants of liprin-α1 were cotransfected with

(E) COS-7 cells triple-transfected with GFP-liprin-α1 and myc-PSD-95 plus control vector or CaMKIIα(T286D).

(F) COS-7 cells cotransfected with control vector, CaMKIIα(T286D), or CaMKIIα(K42R) with myc-liprin-α2, HA-liprin-β1, GRIP1-HA, or myc-cortactin, and immunoblotted for HA and myc.

(G) COS-7 cells cotransfected with myc-liprin-α1 or myc-PSD-95 plus CaMKIIβ(WT), CaMKIIβ(T287D), or CaMKIIβ(K42R), and immunoblotted for myc and CaMKIIβ.

(H) Number of PSD-95, liprin, GRIP, or cortactin immunopositive cells (mean ± SEM; normalized to PSD-95 co-expressing cells) in COS-7 cultures transfected with indicated protein plus active CaMKIIα(T286D). * $p<0.05$, ** $p<0.005$, *** $p<0.0005$. Scale bar, 100 μm.

CaMKIIα(T286D), CaMKIIα(K42R) or empty vector in COS-7 cells. Expression of liprin-α1 constructs was quantified by immunocytochemistry and Western blotting assays (Figure 4.7B-D). The C-terminal region of liprin-α1 contains four potential CaMKII phosphorylation sites (RXXS/T) which are conserved in human, rat, mouse and chicken liprin-α1 proteins. The liprin-α1 splice variant lacking the last 18 amino acids (liprin-α1a)[94], which deletes two of the putative phosphorylation sites, and a C-terminal deletion mutant lacking the last 88 residues (liprin-α1ΔC (1-1112)), which is missing all four phosphorylation sites, were still efficiently suppressed by CaMKIIα(T286D) and unaffected by CaMKIIα(K42R) (Figure 4.7D).

A mutant with a larger C-terminal truncation, liprin-α1ΔCM (containing residues 1-712), was not degraded by CaMKIIα(T286D), implying that the C-terminal half of liprin-α1 contains determinants for CaMKII-induced degradation (Figure 4.7B-D). In this region there is a PEST (proline, glutamate, serine, threonine rich) sequence (amino acids 771 to 795), which is conserved among mammalian liprin-α1 proteins, and which has a PEST score of +8.83 based on the PEST-FIND program[133]. A PEST score of more than 5 denotes a very strong proteolytic degradation signal. Deleting the PEST sequence (liprin-α1ΔPEST) resulted in somewhat reduced susceptibility of liprin-α1 to CaMKII suppression, compared with wildtype or ΔN (Figure 4.7B-D). Combining the PEST deletion with the C-terminal deletion left a liprin-α1 mutant (liprin-α1ΔPESTΔC) that was completely insensitive to suppression by CaMKIIα(T286D) (Figure 4.7B-D). We also mutated the serine residues of the putative C-terminal CaMKIIα phosphorylation sites to alanine (S1139A, S1168A, S1194A, S1201A) in a ΔPEST background, giving rise to liprin-α1ΔPEST/S-A. The liprin-α1ΔPEST/S-A mutant also was insensitive to CaMKIIα(T286D) (Figure 4.7B,D). Thus both the central PEST sequence and the C-terminal putative CaMKII phosphorylation sites are important for liprin-α1 degradation by active CaMKII.
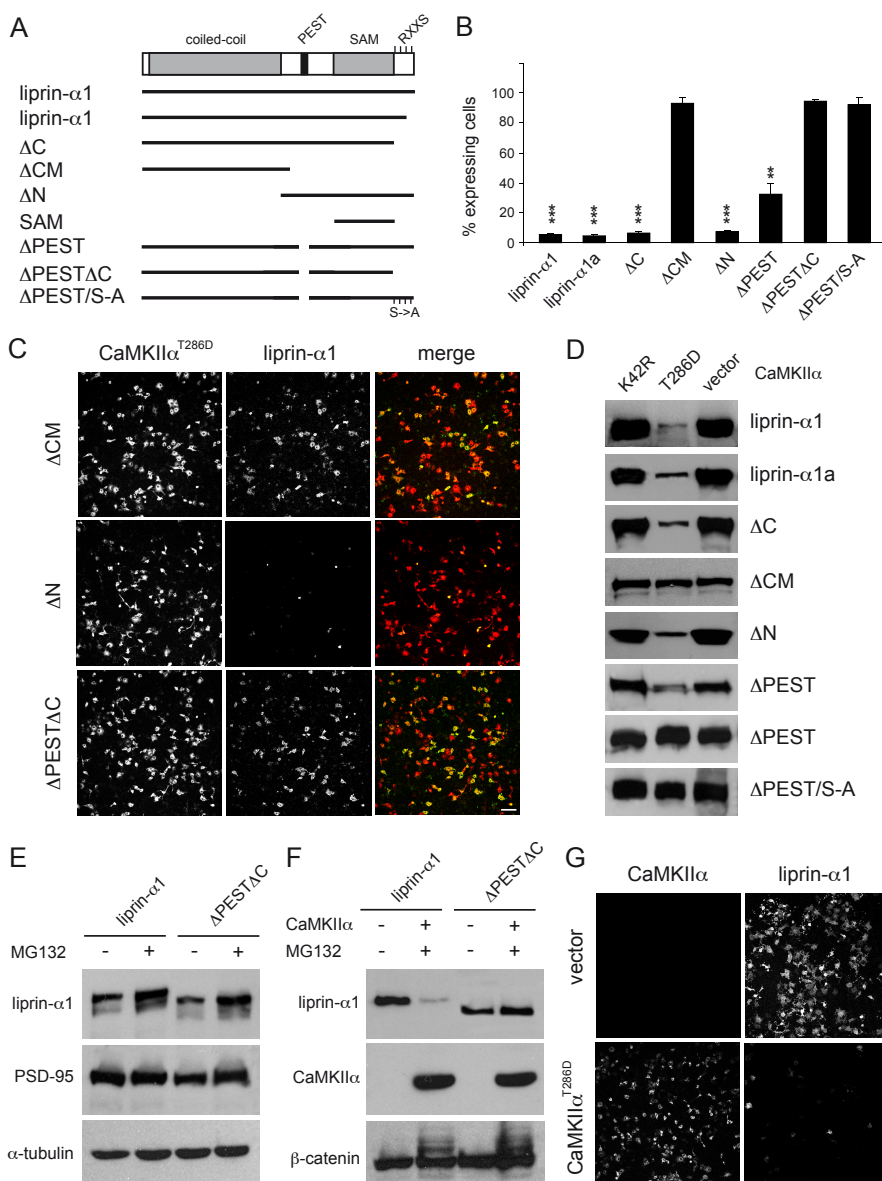
Figure 4.7. *C-terminus and PEST motif but not the proteasome are required for CaMKII-mediated liprin-α1 degradation in COS-7 cells.*
(A) Diagram of liprin-α1 mutant constructs (GFP or HA tag was placed at N-terminus).
(B) Number of cells immunopositive for indicated liprin-α1 mutant construct (mean ± SEM; normalized to control vector (not shown)) when cotransfected with CaMKIIα(T286D). * p<0.05, ** p<0.005, *** p<0.0005.
(C) Representative images of COS-7 cells cotransfected with CaMKIIα(T286D) (red) and GFP-liprin-α1 mutant constructs (green), as indicated. Color merge is shown at right. Scale bar, 100 μm.
(D) COS-7 cells cotransfected with indicated GFP-liprin-α1 mutant constructs plus control vector, CaMKIIα(T286D) or CaMKIIα(K42R), and immunoblotted for the transfected liprin-α1 construct us-

ing HA or GFP antibodies.

(E) COS-7 cells cotransfected with myc-PSD-95 plus GFP-liprin-α1 or GFP-liprin-α1ΔPESTΔC were treated (+) or not treated (-) with 5 μg/ml MG132 for 4 hours and immunoblotted for myc and GFP. Endogenous α-tubulin was used as loading control.

(F) COS-7 cells transfected with GFP-liprin-α1 or GFP-liprin-α1ΔPESTΔC plus control vector (-) or CaMKIIα(T286D) (+) were treated (+) or not treated (-) with 5 μg/ml MG132 for 4 hours as indicated, and immunoblotted for GFP or CaMKIIα. Endogenous β-catenin was used as a positive control for MG132 treatment.

(G) Representative images of COS-7 cells cotransfected with GFP-liprin-α1 (green) and control vector or CaMKIIα(T286D) (red), and treated with 5 μg/ml MG132 for 4 hours.
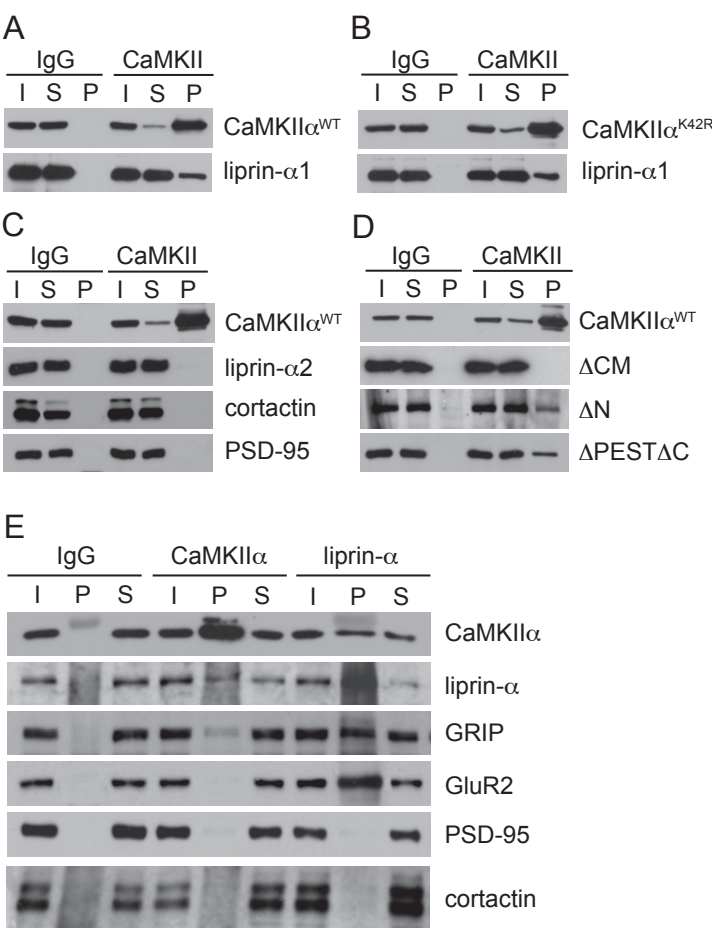
Figure 4.8. *CaMKII interaction with liprin-α1 in vitro and in vivo.*
(A-B) COS-7 cells cotransfected with wildtype (WT) GFP-CaMKIIα and myc-liprin-α1 (A), or GFP-CaMKIIα(K42R) and myc-liprin-α1 (B), were immunoprecipitated with non-immune rabbit IgG or CaMKII antibodies. Each IP reaction is shown in three lanes: I: input to IP reaction; S: supernatant remaining after IP; P: precipitated pellet. The I, S, and P samples were immunoblotted for the indicated proteins.
(C-D) COS-7 cells cotransfected with GFP-CaMKIIα(WT) and indicated proteins (C) or liprin-α1 mutant constructs (D) were immunoprecipated and immunoblotted as in A, B.
(E) Coimmunoprecipitation of CaMKII and liprin-α from rat cortex. DOC extracts were immunoprecipitated with non-immune rabbit IgG or CaMKIIα or liprin-α antibodies, and immunoblotted for the proteins indicated at right.

Figure 4.9. *Impairment of dendrite morphogenesis by liprin-α1 mutants insensitive to CaMKII degradation, LAR-liprin interfering constructs and LAR-shRNA.*
(A) Morphology of hippocampal neurons (visualized in the RFP channel) cotransfected at DIV13 for 4 days with control vector, GFP-liprin-α1 or GFP-liprin-α1ΔPESTΔC, plus mRFP as transfection marker. "+ KN93" indicates treatment for 24 hours with 10 μM KN93 to inhibit CaMKII. GFP-liprin-α1 signals are shown in insets. Scale bar, 20 μm.
(B) Representative images (RFP channel) of hippocampal neurons cotransfected at DIV13 for 4 days with control vector, LAR-liprin interfering constructs or LAR-shRNA, plus mRFP to visualize the transfected cell. Scale bar, 20 μm.
(C) Sholl analysis of hippocampal neurons transfected at DIV13 for 4 days with liprin-α1, LAR and shRNA constructs.
(D-F) Quantification of total dendritic length (D), number of dendritic tips (E) and number of primary dendrites (F) in hippocampal neurons transfected at DIV13 for 4 days with indicated constructs (mean ± SEM). * p<0.05, ** p<0.005, *** p<0.0005
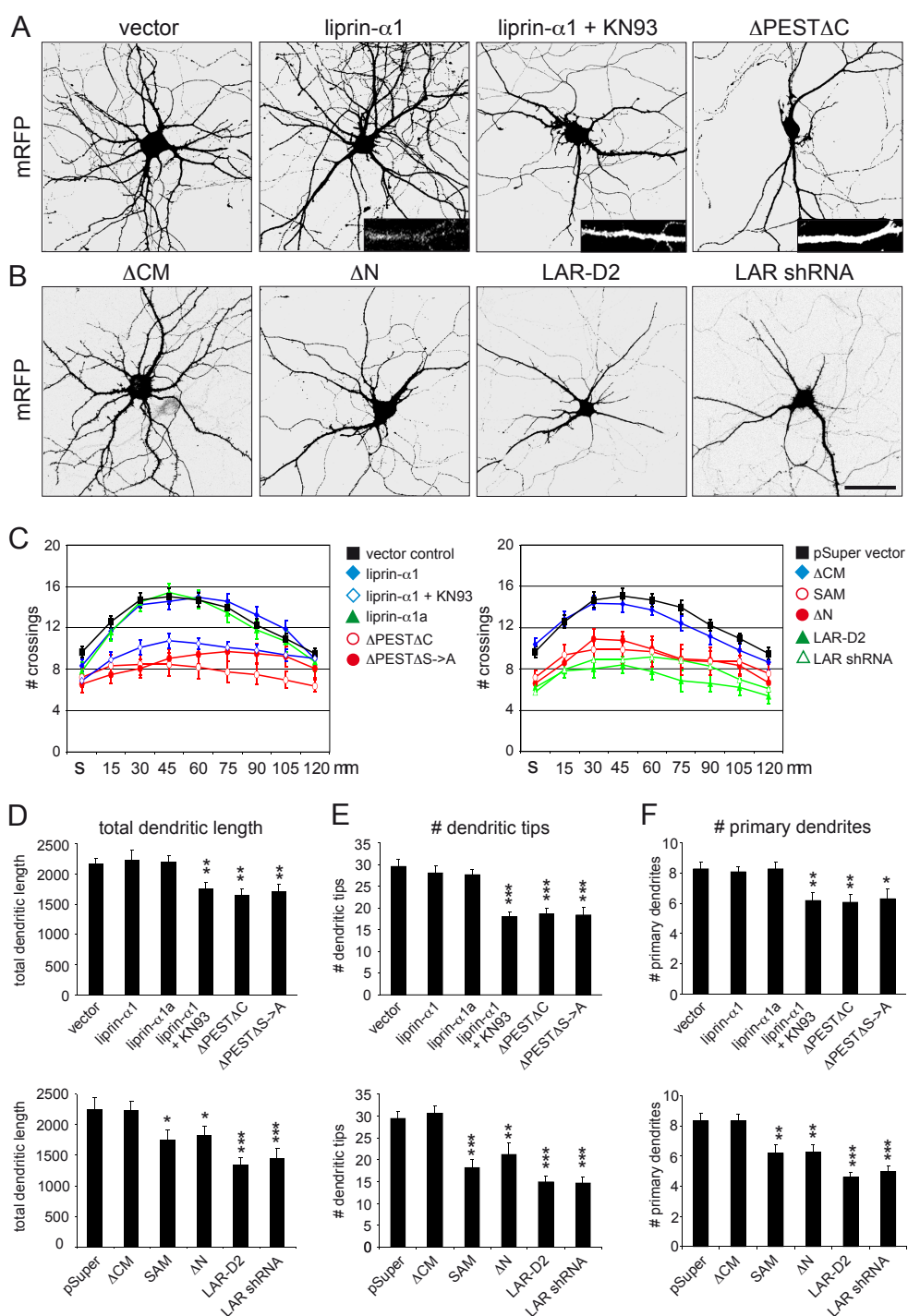
4.2.6 Proteasome is not involved in CaMKIIα dependent liprin-α1 degradation in COS-7 cells

The PEST motif is known to promote rapid protein turnover, however the pathways responsible for degrading PEST proteins are not always clear. Several PEST proteins have been reported to be degraded by calpain or proteasome, but degradation of other PEST-containing proteins seems independent of these mechanisms[133]. Two distinct proteasome inhibitors, MG132 and lactacystin, increased the basal level of both liprin-α1 and liprin-α1ΔPESTΔC expressed in COS-7 cells (Figure 4.7E and data not shown), implying that the proteasome is involved in downregulating basal liprin-α1 levels. In contrast, expression of cotransfected PSD-95 was unaffected (Figure 4.7E). Importantly, however, 4, 8 and 12 hour MG132 treatment did not prevent the loss of liprin-α1 induced by cotransfection of CaMKIIα(T286D) (Figure 4.7F,G and data not shown), indicating that proteasome function is not required for elimination of liprin-α1 by active CaMKII. In addition, liprin-α1 degradation by active CaMKII was not blocked by calpain inhibitors (ALLN, ALLM) or inhibitors of lysosomal degradation (chloroquine, leupeptin, ammonium sulfate) (data not shown). Overall these data indicate that although it contributes to basal lowering of liprin-α1, proteasomal activity is not essential for CaMKII-mediated degradation of liprin-α1 in heterologous cells.

4.2.7 Interaction of CaMKII and liprin-α1 *in vitro* and *in vivo*

Our mutational analysis suggests that liprin-α1 is a target of CaMKII phosphorylation; therefore, we tested if liprin-α1 and CaMKII interact biochemically. From cotransfected COS-7 cells, liprin-α1 was readily coimmunoprecipitated with CaMKIIα wildtype and K42R (Figure 4.8A,B). For this experiment we could not use the CaMKIIα(T286D) construct since active CaMKII causes a drastic reduction in the amount of liprin-α1. Non-immune rabbit IgG immunoprecipitated neither liprin-α1 nor CaMKII, and liprin-α2, cortactin and PSD-95 could not be coprecipitated with wildtype CaMKIIα (Figure 4.8A-C), indicating a specific interaction between liprin-α1 and CaMKIIα. The association with CaMKIIα was lost in the liprin-α1 mutant ΔCM but retained in ΔN, indicating that CaMKII interacts with the C-terminal half of liprin-α1 (Figure 4.8D). Interestingly, the mutant ΔPESTΔC, although insensitive to CaMKII-mediated degradation, could be coimmunoprecipitated with CaMKII (Figure 4.8D), implying that the SAM domains are responsible for interaction with CaMKII (see Figure 4.7A for diagram). Notable in this respect is the recent discovery that

Figure 4.10. *Liprin-α1 mutants insensitive to CaMKII degradation and LAR-liprin interfering constructs impair dendritic spine density.*
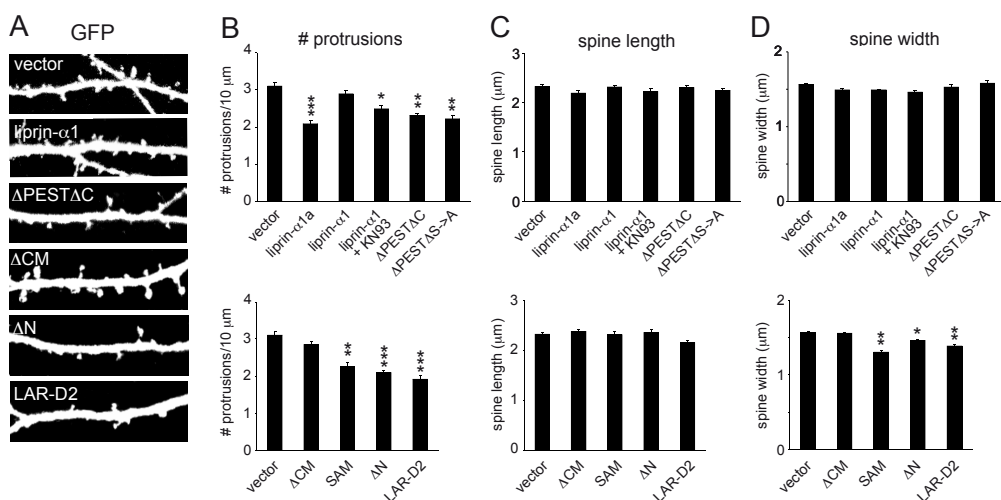(A) Representative high magnification images (GFP channel) of dendrites of hippocampal neurons cotransfected at DIV13 for 4 days with control vector, HA-liprin-α1 or HA-liprin-α1ΔPESTΔC, HA-liprin-α1ΔCM, HA-liprin-α1ΔN, HA-LAR-D2 plus GFP to visualize the transfected cell.
(B-D) Quantification of number of dendritic spines/protrusions per 10 μm (B), spine length (C) and spine width (D) in hippocampal neurons transfected at DIV13 for 4 days with indicated liprin-α1 and LAR constructs. Histograms show mean ± SEM.* $p < 0.05$, ** $p < 0.005$, *** $p < 0.0005$.

the CaMKII-like domain of scaffold protein CASK interacts with the SAM region of liprin-α1[104].

To test for an in vivo interaction, we performed coimmunoprecipitations from deoxycholate (DOC) extracts of rat cerebral cortex. Consistent with earlier studies[94, 96], GRIP and GluR2/3 were robustly coprecipitated with the liprin-α antibody (Figure 4.8E). Liprin-α antibodies also precipitated significant amounts of CaMKIIα. In the inverse reaction, CaMKIIα antibodies brought down a small amount of liprin-α and GRIP in addition to precipitating CaMKIIα, but no detectable GluR2/3 (Figure 4.8E). As a negative control, PSD-95 and cortactin were not coprecipitated by liprin-α or CaMKIIα antibodies and none of the analyzed proteins was pelleted by non-immune rabbit IgG (Figure 4.8E). These biochemical data suggest that a subset of CaMKIIα is present in some fraction of the liprin-α protein complex *in vivo* as well as *in vitro*, which is consistent with the colocalization of liprin-α and CaMKII clusters at synaptic sites (Figure 4.1A,B).
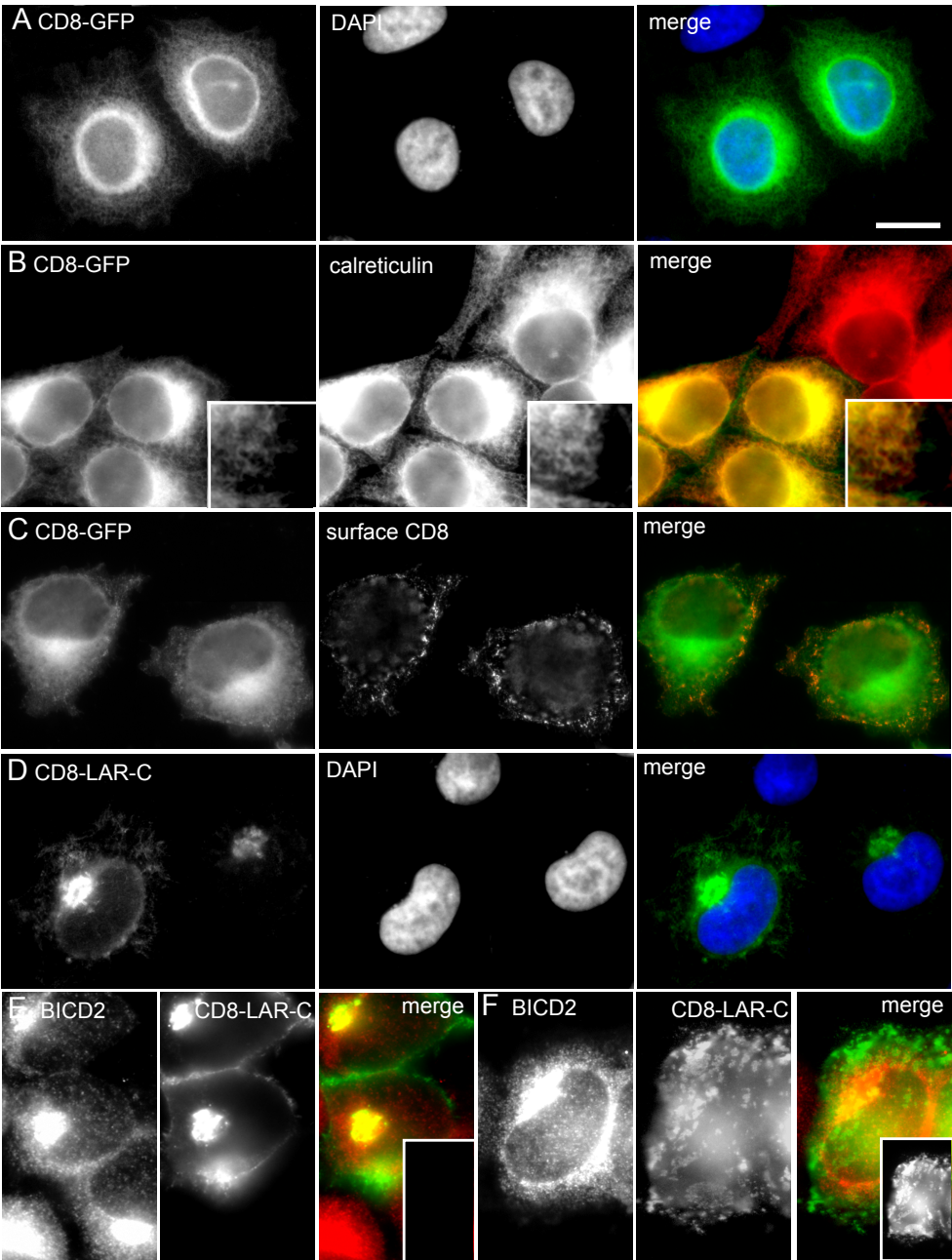
Figure 4.11. *CD8-LAR-C accumulates at the Golgi in HeLa cells.*
(A-C) HeLa cells transfected with CD8-GFP (green) and stained with DAPI (blue) to visualize the nucleus (A), anti-calreticulin antibody (red) to mark the endoplasmic reticulum (B), or anti-CD8 antibody under non-permeabilizing conditions to visualize surface expression (C). Inset in B shows colocalization of calreticulin and CD8-GFP.
(D-E) HeLa cells transfected with CD8-LAR-C (green) and stained with DAPI (blue) to visualize the nucleus (D) or anti-BICD2 antibody (red) to visualize the Golgi-region (E). CD8-GFP localizes at the

4.2.8 Liprin-α1ΔPESTΔC and liprin-α1ΔPEST/S-A inhibit dendrite morphogenesis and reduce synapse density

What is the functional significance in neurons of liprin-α1 degradation by CaMKII? To address this question we transfected hippocampal neurons (DIV13) with liprin-α1 wildtype versus liprin-α1ΔPESTΔC or liprin-α1ΔPEST/S-A mutants that can no longer be degraded by CaMKII. Note however that these mutants are sensitive to proteasome downregulation, insofar as their basal levels are increased by MG132 (Figure 4.7E). Neuronal morphology was visualized by cotransfected monomeric red fluorescent protein (mRFP). Four days after transfection, neurons transfected with liprin-α1ΔPESTΔC or liprin-α1ΔPEST/S-A showed stunted dendritic arbors relative to neurons transfected with liprin-α1 (Figure 4.9A and data not shown). Compared with vector control, overexpression of wildtype liprin-α1 had no effect on any dendrite parameter measured (total dendrite length, number of primary dendrites or dendrite tips, and density or size of dendritic protrusions) (Figure 4.9A,D-F). Total dendrite length decreased by ~30% in liprin-α1ΔPESTΔC and liprin-α1ΔPEST/S-A-transfected neurons (Figure 4.9A,D). Dendrite branching was also reduced, as quantified by total number of dendrite tips (~40% decrease; Figure 4.9E) or by Sholl analysis (which measures the number of dendrites crossing circles at various radial distances from the cell soma; Figure 4.9C). Liprin-α1ΔPESTΔC and liprin-α1ΔPEST/S-A also decreased (by ~25%) the number of primary dendrites (defined as dendrites longer than 21 μm emanating directly from the soma) (Figure 4.9F). Although overexpression of WT liprin-α1 had no effect on dendrite morphology, KN93 treatment of WT liprin-α1-transfected cells mimicked the effects of overexpression of CaMKII-nondegradable mutants on dendrite morphology (Figure 4.9A,C-F). As expected, levels of WT liprin-α1 protein were increased in cells treated with KN93. In summary, the expression of "stable" liprin-α1 caused a decrease in the number of primary, secondary and higher order dendrites and a reduction in the dendritic arbor complexity in cultured hippocampal neurons. We conclude that CaMKII-mediated degradation of liprin-α1 is essential for normal growth and maturation of the dendritic tree.

---

endoplasmic reticulum and CD8-LAR-C accumulates in the perinuclear Golgi region. No liprin-α1 constructs is cotransfected (inset in E).

(F) HeLa cells transfected with CD8-LAR-C (green) and GFP-liprin-α1ΔPEST/S-A (blue, inset) and immunostained with anti-BICD2 antibody (red) to visualize the Golgi-region. The constructs were pseudo-colored for consistency. Coexpression of liprin-α1ΔPEST/S-A causes CD8-LAR-C to redistribute from Golgi to cell surface, where CD8-LAR-C forms clusters. Scale bar, 10 μm.

The density of dendritic protrusions and spines (defined as protrusions of 1−4 µm in length that showed a clear 'head') at DIV17 was reduced by liprin-α1ΔPESTΔC and liprin-α1ΔPEST/S-A, but unaffected by wildtype liprin-α1 (Figure 4.10A,B). The mean length and width of remaining spines were not substantially different in neurons overexpressing any of the liprin-α1 constructs (Figure 4.10A,C,D). In accord with a reduction in the number of spines, we observed a ~40% fall in the density of bassoon puncta on neurons transfected with liprin-α1ΔPEST/S-A (liprin-α1: 4.89 ± 0.21 per 10 µm length of dendrite versus liprin-α1ΔPEST/S-A: 2.74 ± 0.28 per 10 µm length of dendrite), an indication that neurons expressing CaMKII-insensitive liprin-α1 harbor fewer presynaptic contacts. Thus in addition to reduced dendrite branching, CaMKII-non-degradable liprin-α1 mutants impair the development and/or maintenance of spines and synapses.

4.2.9 LAR-liprin interfering constructs and LAR shRNA inhibit dendrite morphogenesis

We investigated which domain of liprin-α1 is important for dendrite morphology by overexpressing liprin-α1 deletion constructs liprin-α1ΔN, liprin-α1SAM and liprin-α1ΔCM (see Figure 4.7A), assuming that the mutants work as dominant negatives. Four days after transfection, neurons expressing liprin-α1ΔN and liprin-α1SAM showed shorter dendritic arbors relative to neurons transfected with control vector or liprin-α1ΔCM (Figure 4.9B,D), similar to liprin-α1ΔPESTΔC and liprin-α1ΔPEST/S-A transfected cells. Dendrite branching was also reduced, as quantified by dendrite tips (~30% decrease; Figure 4.9E), primary dendrites (~25% decrease, Figure 4.9F) and Sholl analysis (Figure 4.9C). The density of dendritic protrusions and spines at DIV17 was reduced by liprin-α1ΔN and liprin-α1SAM, but unaffected by liprin-α1Δ−CM (Figure 4.10A-D). These data argue that the SAM domain of liprin-α1 is impor-

Figure 4.12. *Liprin-α1 and liprin-α1 mutants insensitive to CaMKII degradation promote CD8-LAR-C exit from Golgi and surface expression in HeLa cells.*
(A-D) HeLa cells were double-transfected with CD8-LAR-C plus HA-liprin-α1 (A), HA-liprin-α1ΔPESTΔC (B), HA-liprin-α1ΔCM (C), or with CD8-LAR-CΔD2 plus HA-liprin-α1ΔPESTΔC (D); then fixed and stained with anti-HA (red) and anti-CD8 (green) antibodies. The merge is shown in color at right. Arrowheads indicate CD8-LAR-C localization in the perinuclear Golgi region (A,C,D). Coexpression of liprin-α1 (A) or liprin-α1 mutants insensitive to CaMKII degradation (B) enhance surface expression of CD8-LAR-C. Scale bars, 10 µm.
(E-F) Hela cells transfected with CD8-LAR-C and control GFP (E), or GFP-liprin-α1ΔPESTΔC (F) and immunostained for surface CD8 expression under non-permeabilizing conditions. Liprin-α1 mutants insensitive to CaMKII degradation enhance surface expression of CD8-LAR-C. Scale bar, 10 µm.

A CD8-LAR-C | liprin-α1 | merge

B CD8-LAR-C | ΔPESTΔC | merge

C CD8-LAR-C | liprin-α1ΔCM | merge

D CD8-LAR-CΔD2 | ΔPESTΔC | merge

E GFP | surface CD8 | merge — CD8-LAR-C + GFP

F GFP | surface CD8 | merge — CD8-LAR-C + GFP-ΔPESTΔC
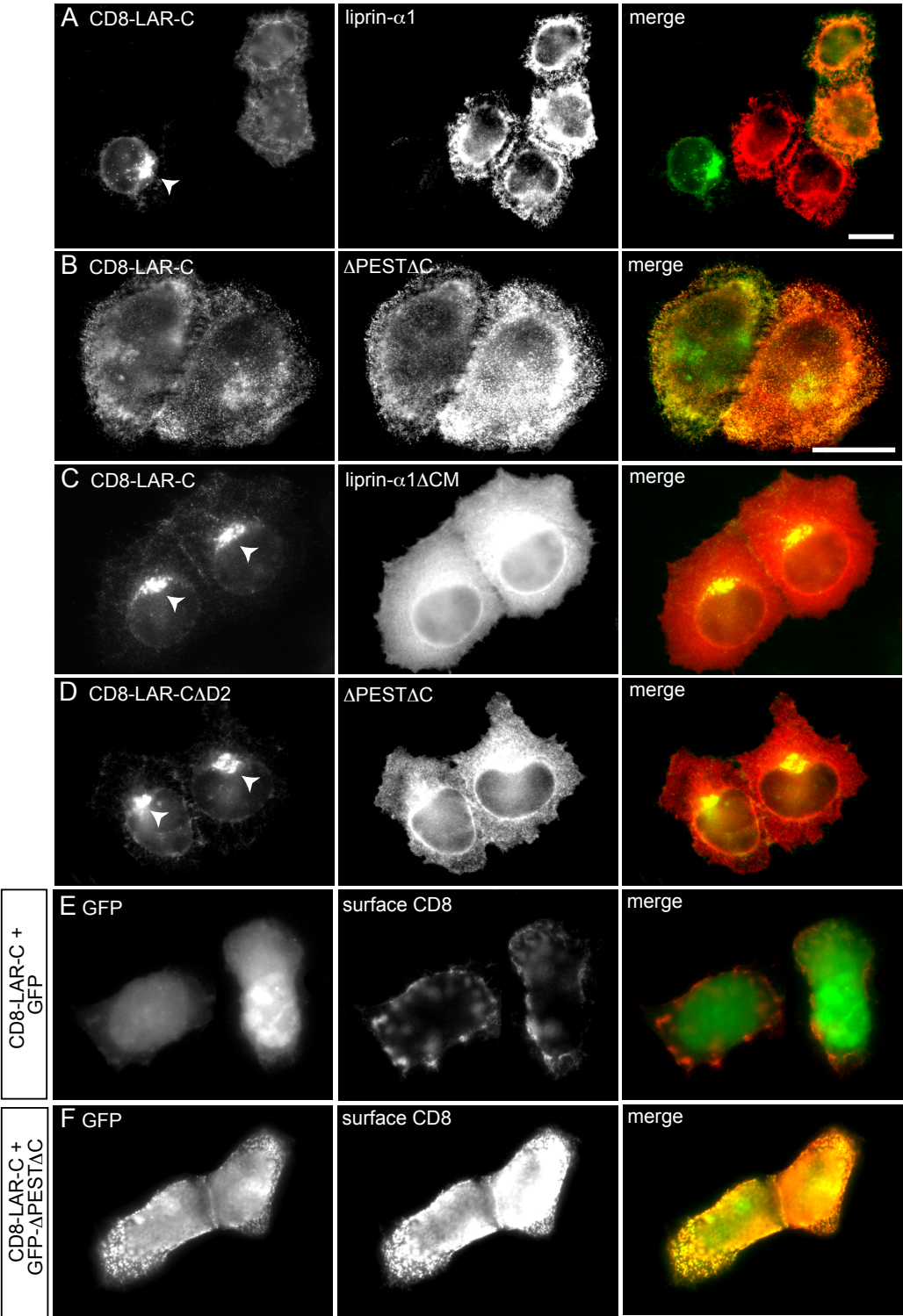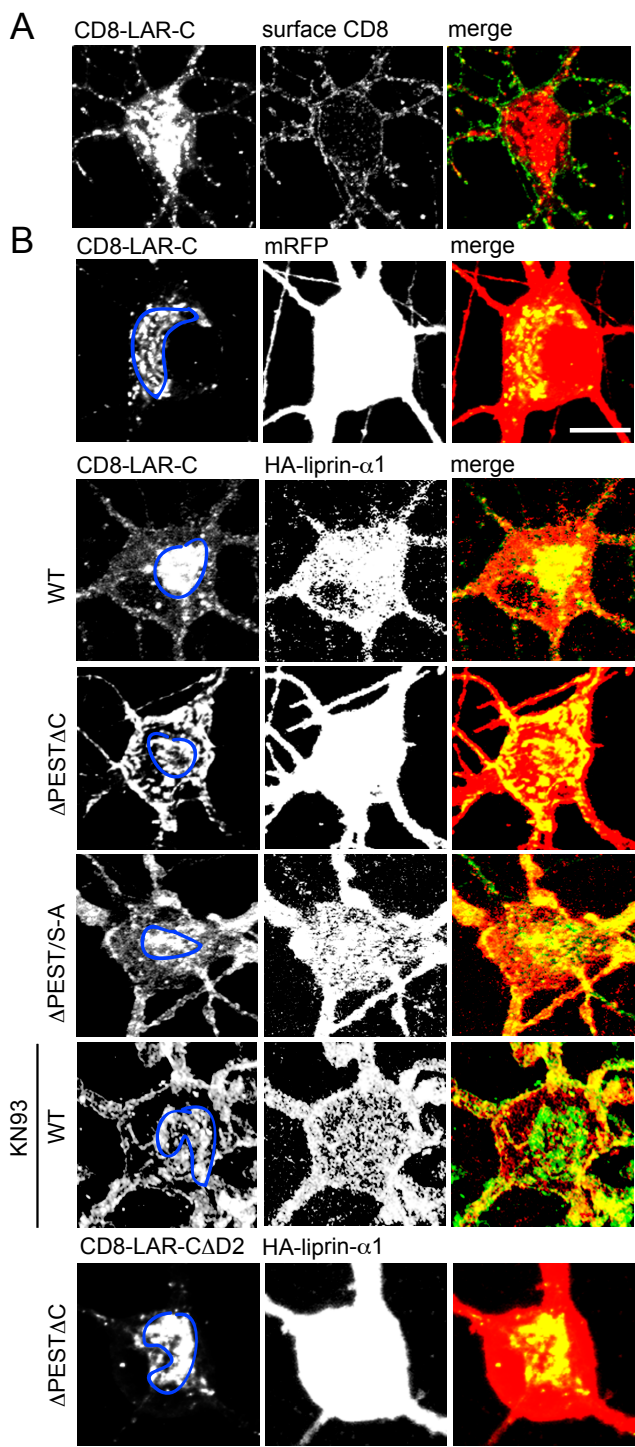
Figure 4.13. *Liprin-α1 mutants insensitive to CaMKII degradation cause accumulation of CD8-LAR-C in cell bodies of hippocampal neurons.*

(A) Representative image of a hippocampal neuron cell body transfected at DIV13 with CD8-LAR-C and stained with anti-CD8 antibody under permeabilizing conditions to visualize total expression (red) and non-permeabilizing conditions to visualize surface expression (green). Note the characteristic labeling of surface CD8-LAR-C around the neuronal cell body.

(B) Representative images of hippocampal neuron cell bodies transfected at DIV13 with CD8-LAR-C or CD8-LAR-CΔD2 plus indicated HA-liprin-α1 construct, and stained with anti-CD8 (green) and anti-HA (red) antibody. CD8-LAR-C is localized in the perinuclear Golgi region in the absence of cotransfected liprin-α1, or when cotransfected with WT liprin-α1. Co-expression of liprin-α1ΔPESTΔC, liprin-α1ΔPEST/S-A caused redistribution of CD8-LAR-C from the Golgi region to clusters at the surface of the cell body. A similar effect was obtained in cells cotransfected with WT liprin-α1 and treated with KN93. The CD8-LAR-C immunostaining intensity in the cell body (soma minus Golgi region) and in the Golgi region (outlined in blue, as revealed by Golgi marker GM130 co-staining) were quantified using MetaMorph (shown in Figure 4.14). Scale bar, 10 μm.
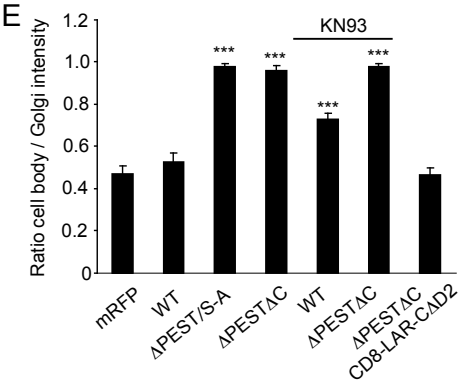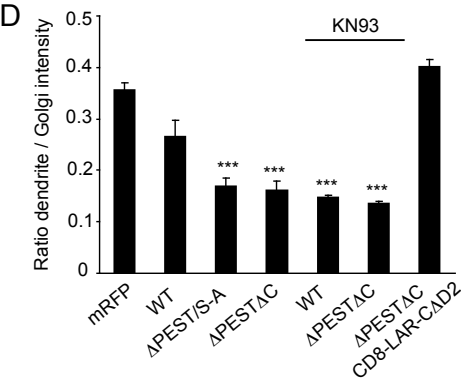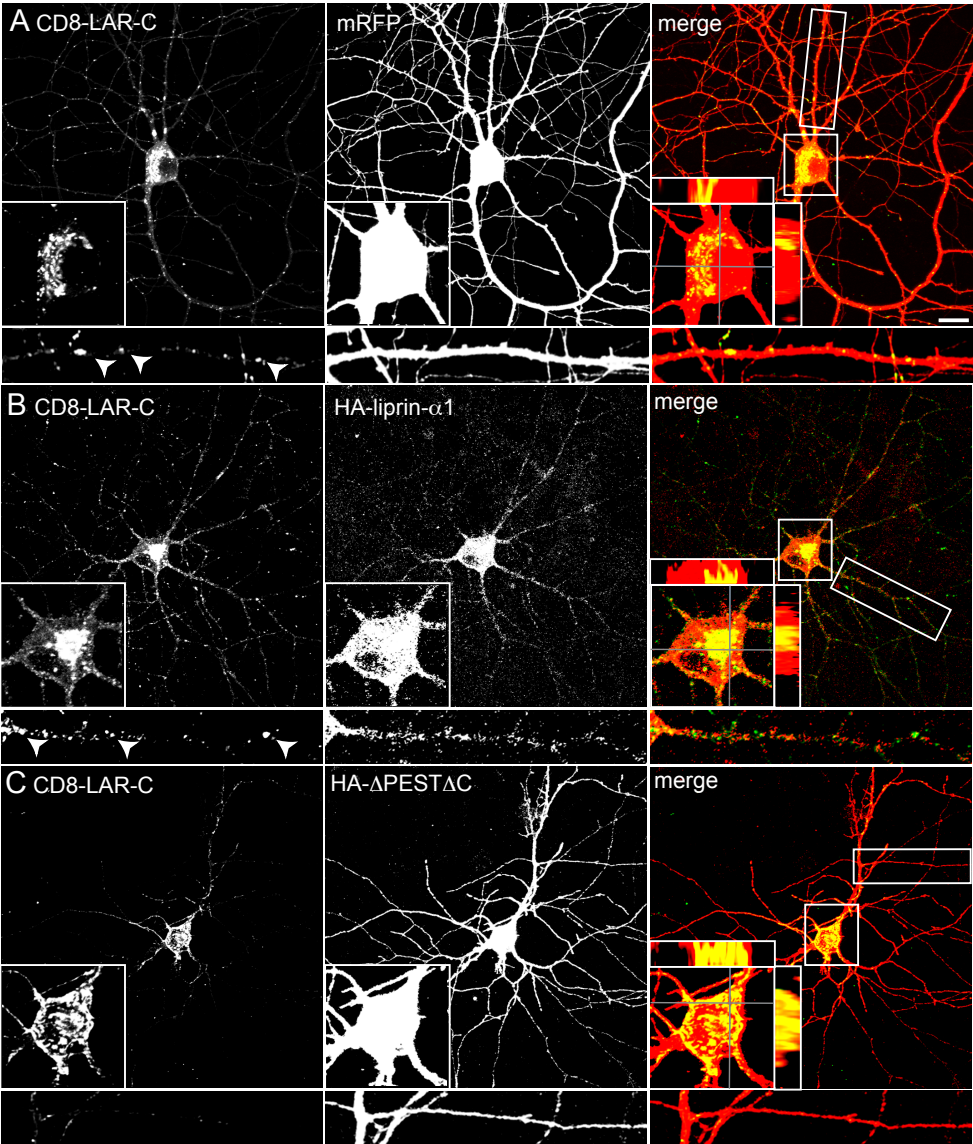
tant for supporting dendrite morphogenesis and normal spine number.

The LAR-RPTPs bind to the SAM domains in liprin-α1[78]. Therefore we investigated the effect on dendrite morphogenesis of overexpression of the isolated liprin-α binding domain of LAR (LAR-D2, fused to a myristoylation motif for membrane targeting), or knock down of LAR by LAR-shRNA[96]. Expression of either LAR-D2 or LAR-shRNA caused marked pruning of the dendritic arbor (Figure 4.9B-F) and loss of dendritic protrusions and spines (Figure 4.10A-D). In summary, the expression of constructs that disrupt the liprin-α1-LAR interaction or that suppress endogenous LAR expression caused a reduction in dendrite arborization and spine density in hippocampal neurons, similar to the effects seen with neurons expressing CaMKII-non-degradable liprin-α1 constructs.

4.2.10 Liprin-α1 increases surface expression and clustering of LAR receptors

Liprin-α has been suggested to regulate LAR localization and clustering in mammalian cell lines[78, 79]. It is difficult to study the regulation of endogenous LAR trafficking in neurons because LAR protein is not highly expressed and our LAR antibodies work insufficiently in immunostaining. We developed a simplified way to investigate LAR receptor trafficking, which makes use of the CD8 glycoprotein as a reporter in protein trafficking[134]. A GFP-tagged CD8 construct containing only the extracellular and transmembrane domain of CD8 accumulated in the endoplasmic reticulum of HeLa cells, colocalizing with calreticulin (Figure 4.11A-B); expression on the cell surface was weak (Figure 4.11C). Fusing the entire cytoplasmic domain of LAR (LAR-C) to the CD8 construct allowed the chimeric construct (CD8-LAR-C) to leave the endoplasmic reticulum and accumulate in the perinuclear Golgi region (Figure 4.11D), where it colocalized with the trans-Golgi marker BICD2 (Figure 4.11E).

In the absence of coexpressed liprin-α1, very little CD8-LAR-C was associated with the cell surface (Figure 4.12E). Cotransfection with liprin-α1, liprin-α1ΔPEST-ΔC, or liprin-α1ΔPEST/S-A resulted in greatly increased expression of CD8-LAR-C at the surface in a patchy pattern in almost all cells (Figure 4.12A, B, F and data not shown). Coexpression of liprin-α1ΔCM, lacking the LAR binding domain, did not change the distribution of CD8-LAR-C, which remained in a Golgi-pattern (Figure 4.12C). Similarly, the CD8-LAR-CΔD2 construct lacking the liprin binding site was unaffected by cotransfection of liprin-α1ΔPESTΔC (Figure 4.12D). These data in heterologous cells suggest that one function of liprin-α1 (both wildtype and CaMKII-

non-degradable mutants) is to drive LAR receptors out of the Golgi and deliver them to the cell surface.

4.2.11 CaMKII-non-degradable liprin-α1 mutants impair dendritic targeting of LAR

We next investigated LAR trafficking in hippocampal neurons. When overexpressed in neurons, CD8-LAR-C was found, in addition to the perinuclear Golgi region (Figure 4.13B), in a punctate pattern in dendrites (Figure 4.14A left, inset, arrowheads) and at low levels on the cell surface (Figure 4.13A). Overexpression of wild type liprin-α1 has no effect on the CD8-LAR-C distribution (Figure 4.14B). However, co-transfection of liprin-α1ΔPESTΔC and liprin-α1ΔPEST/S-A mutants caused redistribution of CD8-LAR-C from Golgi and accumulation of CD8-LAR-C in neuronal cell bodies (Figures 4.13B and 4.14C-E). In these neurons, CD8-LAR-C was predominantly found in a patchy pattern along the periphery of the cell body, suggesting an increased surface expression on the soma (Figures 4.13B and 4.14C). The ratio of cell body (soma without the Golgi)/Golgi immunostaining for CD8-LAR-C increased two-fold in liprin-α1ΔPESTΔC and liprin-α1ΔPEST/S-A expressing neurons compared to control (Figure 4.14E), indicating improved exit from Golgi towards the somatic surface, similar to the findings in HeLa cells. Despite the increased expression on neuronal somata, the punctate staining of CD8-LAR-C in the dendrites was greatly reduced (Figure 4.14C). The ratio of dendrite/Golgi immunostaining for CD8-LAR-C decreased two-fold in neurons expressing liprin-α1ΔPESTΔC or liprin-α1ΔPEST/S-A (Figure 4.14D), signifying that CaMKII-non-degradable liprin-α1 mutants impair dendritic targeting of LAR, despite improving Golgi-to-somatic surface transport. The distribution of CD8-LAR-CΔD2, lacking the liprin-α binding site, was unaffected by CaMKII-non-degradable liprin-α1 constructs (Figure 4.14D, E). In neurons transfected with HA-liprin-α1 and treated with KN93 (10 μM, 24 h), the ratio of cell body/

Figure 4.14. *Liprin-α1 mutants insensitive to CaMKII degradation impair dendritic targeting of CD8-LAR-C in hippocampal neurons.*

(A-C) Representative images of hippocampal neurons cotransfected at DIV13 with CD8-LAR-C and mRFP (A), HA-liprin-α1 (B) or HA-liprin-α1ΔPESTΔC (C), and double-labeled with anti-CD8 (green) and anti-HA (red) antibody. Dendritic segments (bottom) and cell body (inset, including confocal z-scans) are enlarged to show the distribution of CD8-LAR-C.

(D-E) Quantification of the ratio of immunostaining intensity in the dendrites (D) or cell body (E) versus the immunostaining intensity in the Golgi for CD8-LAR-C in neurons transfected with indicated constructs. "KN93" indicates overnight treatment with KN93. Histograms show mean ± SEM. * p<0.05, ** p<0.005, ***p<0.0005. Scale bar, 10 μm.

Golgi intensity of CD8-LAR-C immunostaining increased two-fold and the dendrite/ Golgi ratio decreased two-fold compared to untreated liprin-α1-transfected cells (Figure 4.14D,E), mimicking the effect of overexpressed CaMKII-non-degradable liprin-α1 mutants. Thus prevention of liprin-α1 degradation by CaMKII, either by mutation of liprin-α1 or by drug inhibition of CaMKII, reduces the trafficking of CD8-LAR-C to dendrites. Together these data indicate that liprin-α1 degradation by CaMKII is needed specifically for the dendritic targeting of LAR, thereby promoting normal development of dendrites and synapses.

4.3. Discussion

4.3.1 Activity-dependent regulation of liprin-α1 by two mechanisms: CaMKII and proteasome

Activity regulates the expression and degradation of many neuronal proteins, including several scaffolds of the PSD[70]. One of the major cellular mechanisms controlling protein turnover is the UPS[135, 136]. Ubiquitin-processing enzymes play an essential role in neural development, including synapse growth and development, growth cone guidance and dendritic remodeling[135, 137]. In most cases, the importance of the UPS for neural development is inferred from pharmacological inhibitor or genetic loss-of-function studies, and the specific proteins whose level is controlled by ubiquitination and proteasomal proteolysis are unknown. Here we found liprin-α1 levels to be particularly susceptible to activity-dependent regulation. The suppression of liprin-α1 protein by neural activity depends at least partially on CaMKII and proteasome function. Because inhibitors of either CaMKII or proteasome countered the effect of activity but did not elevate liprin-α1 to the high levels seen with the inhibitors alone, we hypothesize that synaptic activity stimulates at least two pathways for liprin-α1 degradation: one depending on CaMKII phosphorylation, and another depending on the UPS. This idea is supported by the fact that proteasome inhibitors do not prevent the degradation of liprin-α1 by CaMKII in COS-7 cells. In addition, the data in neurons can be explained if CaMKII- and proteasome-mediated turnover of liprin-α1 depend only partially on synaptic activity. Cotreatment of neurons with KN93 and MG132 did not significantly increase liprin-α1 levels compared to either drug alone (data not shown), which does not support the idea that CaMKII and proteasomes lie in independent pathways for liprin-α1 degradation. Thus our findings in heterologous cells do

not rule out that CaMKII degradation of liprin-α1 occurs via the UPS in neurons, or that crosstalk occurs between these pathways.

Our findings indicate that CaMKII affects liprin-α1 levels via protein degradation as opposed to a reduction in transcription or translation. To our knowledge this is the first example of CaMKII signaling in which CaMKII activity stimulates degradation of a specific protein. The degradation of liprin-α1 by CaMKII involves a central PEST sequence and C-terminal phosphorylation sites in liprin-α1. At least 12 CaMKII consensus phosphorylation sites are present in liprin-α1. Phosphorylation of the C-terminal tail and CaMKII sites close to the PEST sequence may recruit degradation factors necessary for proteolysis[138]. Alternatively, CaMKII phosphorylation may induce conformation changes in liprin-α1 which open up additional regions involved in rapid protein degradation. Although mutation analysis in liprin-α1 suggests a direct role for CaMKII phosphorylation in liprin-α1 degradation, we cannot rule out that another factor is activated by CaMKII which subsequently causes liprin-α1 degradation. A PEST motif is absent in liprin-α2, which is not degraded by active CaMKII, but present in the middle part of liprin-α4, which additionally contains two CaMKII phosphorylation sites in its C-terminus. Thus liprin-α4 might also be degraded by active CaMKII.

Given that liprin-α1 exists on both sides of mammalian excitatory synapses[94, 96, 107, 109], does activity regulate the level of liprin-α at pre- or postsynaptic sites? CaMKII is extremely abundant in the postsynaptic density[45, 122], but also exists in axon terminals[139]. Moreover, activity results in Ca^{2+} elevation in both pre- and postsynaptic compartments. Light microscopy cannot definitely distinguish between pre- or postsynaptic accumulation of liprin-α1. However, we believe that the regulation of liprin-α1 levels by CaMKII occurs substantially in the postsynaptic compartment because RNAi knockdown of CaMKII in neurons resulted in increased inmunostaining of dendritic liprin-α1 in a cell-autonomous fashion (Figure 4.3). Regulation of liprin-α1 by APC must also occur at least in part on the postsynaptic side, because Cdh1 RNAi boosted liprin-α1 signal in dendrites of transfected neurons. Finally, CaMKII-insensitive liprin-α1 caused robust changes in dendrite morphology in transfected neurons, implying that this mutant can have a postsynaptic (or dendritic) locus of action. Nevertheless, our study does not rule

out an effect of CaMKII or APC on liprin-α1 in presynaptic compartments.

4.3.2 Importance of CaMKII degradation of liprin-α1 for dendrite morphogenesis

CaMKII has been implicated in neuronal morphogenesis and synapse maturation[121, 122]. CaMKII signaling can regulate dendrite development by local processes or by inducing transcriptional programs in the nucleus[128]. CaMKII activity promotes growth and stabilization of dendrites in *Xenopus* optic tectal neurons[127] and of dendritic spines in hippocampal neurons[124]. The precise mechanisms by which CaMKII influences dendrite and synapse development remain poorly understood. Based on our findings, we propose that CaMKII-mediated phosphorylation and degradation of liprin-α1 is one molecular mechanism for coupling activity to dendrite and synapse morphogenesis. Liprin-α1 mutants resistant to CaMKII degradation impair dendrite arborization and synapse density; thus the ability of liprin-α1 protein to be degraded in response to CaMKII activation is essential for normal dendrite and synapse development. Because CaMKII can be stimulated locally by synaptic activity, suppression of liprin-α1 by CaMKII might be used to promote dendrite growth or stability locally in regions of high synaptic activity. Our data correlate well with previous studies showing that activity -- specifically stimulation of glutamate receptors in mature neurons -- stabilizes dendritic arbors[140], and that inhibition of CaMKII with RNAi or peptide inhibitors reduces dendritic arborization and synapse formation[124].

How does liprin-α1 regulate dendrite morphology? Two obvious candidates are the known liprin-α1 binding proteins: GRIP1[94] and LAR-RPTP[79, 83]. GRIP1 has already been implicated in dendrite development[134]; however, CaMKII non-degradable mutants of liprin-α1 had no effect on the distribution of GRIP1 in hippocampal neurons (data not shown). Here we show that RNAi knockdown of LAR and disruption of the LAR-liprin-α interaction reduces dendritic arbor complexity in cultured hippocampal neurons very similarly to that seen with CaMKII-non-degradable liprin-α1 mutants. Previous work has suggested that liprin-α is involved in the localization and distribution of LAR in mammalian cells[78, 79]. Our experiments indicate that liprin-α1 drives LAR receptors out of the Golgi and

enhances LAR expression and clustering on the neuronal cell body, likely associated with an increased surface expression. This function was independent of liprin-α1 degradation by CaMKII in that ΔPESTΔC and ΔPEST/S-A mutants of liprin-α1 were fully active in this respect. However, specifically the targeting of LAR to dendrites was abrogated by liprin-α1 mutants that are immune to CaMKII degradation, as well as by KN93 block of CaMKII activity, even though both manipulations greatly increase liprin-α1 levels in neurons. Since postsynaptic LAR is critical for dendrite development and synapse/spine maturation (this study and [96]), the loss of dendritic targeting of LAR can largely explain the phenotype of CaMKII-non-degradable liprin-α1 overexpression.

So why is the *degradation* of liprin-α1, rather than just its expression, important for LAR distribution and dendrite and synapse development? Although we can only manipulate CaMKII activity or liprin-α1 expression at a global level within individual neurons, the physiological role of CaMKII regulation of liprin-α-LAR occurs most likely at the local level. We hypothesize that the local regulation of liprin-α1 levels by CaMKII controls the trafficking of LAR to specific regions within dendrites and/or to specific synapses. The CaMKII-mediated degradation of liprin-α1 provides an attractive mechanism for targeting liprin-α1-LAR complexes to active synapses where the kinase is switched "on". We suggest that at such sites the LAR cargo bound to liprin-α1 would be "unloaded" due to CaMKII-mediated degradation of liprin-α1 to promote local growth and stabilization of dendritic structures. However, it is possible that the mutations that block CaMKII-mediated degradation interfere in some other way with liprin-α1's trafficking function in dendrites.

In yeast a specific myosin motor, Myo2p, moves vacuoles to the yeast bud by binding to the vacuole-specific Myo2p receptor Vac17p[141]. The transport complex is disrupted specifically in the bud by degradation of Vac17p, depositing the vacuole in the bud. Vac17p contains a PEST sequence that is required for its degradation, and loss of this PEST sequence causes mis-targeting of vacuoles[141]. By analogy to Vac17p, liprin-α1 also interacts with motor proteins (kinesin-1 and kinesin-3 (KIF1A))[109, 129]. Liprin-α1 also contains a PEST sequence important for rapid degradation, and causes a cargo targeting phenotype when it is rendered

non-degradable. An attractive idea is that PEST protein degradation in yeast and hippocampal neurons represent different aspects of a general molecular mechanism for directed motor trafficking.

Chapter 5

Regulation of Presynaptic Composition and Function by Distinct Liprin-α Family Proteins

Samantha A. Spangler[1], Sabine K. Schmitz[4], Ilya Grigoriev[2], Dick Jaarsma[1], Esther de Graaff[1], Jeroen Demmers[3], Anna Akhmanova[2], Morgan Sheng[5], Ruud F. Toonen[4], and Casper C. Hoogenraad[1]

[1]Department of Neuroscience, [2]Department of Cell Biology and Genetics, [3]Proteomics Center, Erasmus MC, Rotterdam, The Netherlands; [4]Department of Functional Genomics, Center for Neurogenomics and Cognitive Research, Vrije Universiteit, Amsterdam, The Netherlands; [5]Picower Institute of Learning and Memory, RIKEN-MIT Neuroscience Research Center, Howard Hughes Medical Institute, Massachusetts Institute of Technology, Cambridge, MA, USA.

The presynaptic terminal functions to regulate neurotransmitter release through the fusion of synaptic vesicles at the active zone. In order to establish and maintain presynaptic sites along an axon and control presynaptic function, the assembly of synaptic vesicles, ion channels and other presynaptic components must be strictly regulated. Here, we show that liprin-α family proteins are key components of the machinery that coordinates presynaptic protein composition at mature synapses. The liprin-α family proteins are differentially distributed in the mammalian brain, their abundance varies from synapse to synapse, and they selectively interact with other presynaptic proteins. In hippocampal neurons, liprin-α2 is required for CASK and RIM recruitment to presynaptic terminals and facilitates synaptic vesicle exocytosis. In contrast, liprin-α1 interacts with CAST/ERC and reduces presynaptic bassoon and piccolo by competitive binding and interferes with efficient synaptic vesicle release. Consistently, fluorescence recovery after photobleaching revealed that liprin-α1 prevents bassoon targeting to CAST/ERC-containing membrane structures. We propose that liprin-α family proteins differentially regulate presynaptic protein composition, providing a molecular basis for the observed physiological and functional diversity of presynaptic structures.

5.1. Introduction

Synapses are specialized sites of cell contact that mediate information flow between neurons and their targets. The predominant function of the presynaptic site is the regulation of the release of neurotransmitter-filled synaptic vesicles (SVs) in response to action potentials entering the bouton[62]. The SV cycle is tightly controlled, both temporally and spatially, and its performance is modified in response to activity[142]. The cellular and molecular processes underlying regulated neurotransmitter release are important for fine-tuning synaptic connectivity at a single synapse level.

The active zone (AZ) is the specialized region of the presynaptic plasma membrane that is almost exclusively designated for SV exocytosis and neurotransmitter release[143, 144]. Electron tomography of hippocampal presynaptic terminals reveals that long cytoskeletal filaments containing docked SVs assemble at the AZ[145]. It is believed that the architecture and molecular organization of the AZ may play an important role in guiding SVs to their docking and fusion sites and is optimized for rapid and regulated neurotransmitter release[146]. Several families of structural and scaffolding proteins have been identified within AZs[53, 58, 144]. The large structural proteins bassoon and piccolo regulate SV exocytosis and neurotransmitter release[147, 148], CASK, mint, MALS/veli, and RIM influence priming of SVs[99, 104, 149, 150], and the scaffolding proteins CAST1,2/ERC2,1/ELKS (henceforth referred to as CAST) and liprin-α are thought to be essential elements of AZ core complex[87, 88, 97]. Most AZ scaffolding proteins are conserved across evolution[58] and have been shown to interact directly with other AZ components[53]. However, a global understanding of the molecules essential for presynaptic assembly is still lacking, and the molecular mechanisms leading to structurally and functionally distinct presynaptic terminals remain unclear.

Liprin-α family proteins are highly conserved throughout evolution, however *C. elegans* and *Drosophila* contain one gene, SYD-2 and dliprin-α, respectively, while vertebrates have four liprin-α genes (liprin-α1, α2, α3, α4). All liprin-α family proteins consist of multiple N-terminal coiled-coil domains that mediate multimerization and bind to CAST[97] and RIM[99] proteins, followed by three sterile alpha motif (SAM) domains that interact with CASK[104]. The high degree of sequence conservation within the liprin-α protein family (~70% amino acid identity)[79] suggests that their functions may be largely redundant in the vertebrate nervous system; however, whether this is indeed the case has not been determined.

Liprin-α proteins were originally discovered due to their interaction with the LAR (leukocyte common antigen-related) family of receptor protein tyrosine phosphatases (LAR-RPTPs)[81, 96] and shown to be involved in multiple processes at the postsynaptic membrane[58]. Liprin-α is present in the postsynaptic density (PSD), binds directly to calcium/calmodulin-dependent protein kinase II (CaMKII) and GRIP, and is involved in dendrite morphology, dendritic spine development, and AMPA receptor trafficking[94, 108]. To date, the strongest evidence of the role of liprin-α in presynaptic functioning comes from studies at the neuromuscular synapse in invertebrates. *Drosophila* dliprin-α mutants displayed impaired synaptic transmission and abnormal AZ morphology at neuromuscular junctions[89]. In *C. elegans*, the liprin-α homolog SYD-2 is critical for the structural integrity of the AZ[86] and is essential for the presynaptic assembly of numerous AZ components during development[87, 88], suggesting that liprin-α/SYD-2 is a key organizer of the presynaptic terminal that is capable of forming a multimeric interaction network by direct binding to multiple AZ proteins. In vertebrates, liprin-α is known to be present in presynaptic boutons[94], and is implicated in regulating presynaptic CASK localization[104, 151], however the functional role of liprin-α family proteins in mature presynapses is unclear.

Here, we study the role of the liprin-α protein family at presynaptic boutons in hippocampal neurons. We show that the four liprin-α proteins are differentially expressed in the brain and interact with common and specific presynaptic proteins. Liprin-α2 is predominately present in the majority of presynapses in cultured hippocampal neurons and required for the efficient release of SVs. In contrast, liprin-α1 is maintained at low levels at presynapses and its upregulation leads to decreased SV exocytosis. Both of these effects occur as a result of differential or competitive binding of liprin-α proteins with other major AZ components. These results uncover a new mechanism for locally regulating specificity and strength of synaptic connections.

5.2. Results

5.2.1 Liprin-α2 is abundant at synapses in the hippocampus

To determine the role of liprin-α family members at presynaptic terminals, we first generated specific antibodies to all four liprin-α proteins (see Ch. 6, Figures 2.3 and 2.4) and examined their localization in cultured hippocampal neurons and brain sections (Figures 2.5, 5.1, and 5.2). Liprin-α2 protein levels were particularly high in the

A
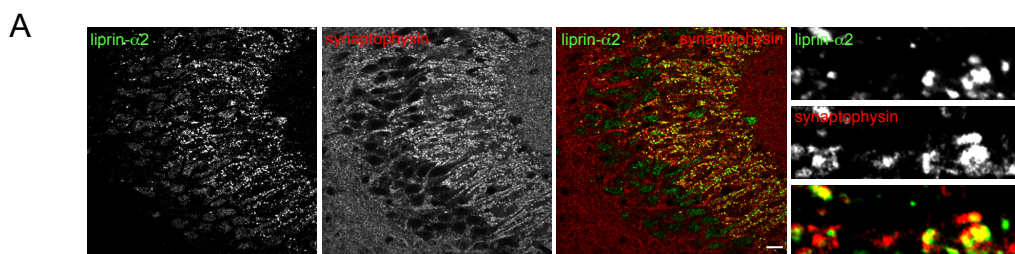
Figure 5.1. *Liprin-α2 is predominately present at synapses in the hippocampus.*
(A) Images of liprin-α2 (green) with synaptophysin (red) in mossy fiber endings in the stratum lucidum of the hippocampus of adult mouse brain sections. Scale bar, 10 μm.

stratum lucidum of the CA3 region of the hippocampus (Figures 2.5 and 5.1). Double labeling confocal immunofluorescence in this region showed liprin-α2 immunoreactivity colocalized with presynaptic markers synaptophysin and vGluT1 (Figure 5.1A and data not shown), indicating that liprin-α2 is present in mossy fiber endings.

To further determine the synaptic localization of liprin-α proteins, we examined their distribution in mature cultured hippocampal neurons (19 days in vitro (DIV19)). In addition to being enriched in PSDs (Figure 5.2D), liprin-α2 is most concentrated at synapses and strongly overlaps with the postsynaptic density protein PSD-95 (data not shown) and the presynaptic AZ protein bassoon (Figures 5.2A). Quantification revealed that liprin-α2 is enriched 2.2-fold at synapses and found in ~68% of bassoon clusters (Figure 5.2B,C). In contrast, the intensity of liprin-α1 staining at synapses is weak and highly variable and only detectable in ~38% of bassoon clusters (Figure 5.2A-C. Therefore, these data indicate that liprin-α2 is the prominent synaptic liprin-α protein in the hippocampus.

5.2.2 Presynaptic localization of liprin-α2 does not depend on other scaffold proteins

The *C. elegans* liprin-α/SYD-2 protein is a central organizer of presynaptic architecture and amongst the most upstream players in assembling presynaptic components at early stages of synaptogenesis[87, 88]. We sought to investigate whether the removal of important presynaptic proteins affects the synaptic localization of liprin-α2 in mature hippocampal neurons. First, we established an unbiased method of quantifying presynaptic protein distributions in hippocampal neuron cultures (see Ch. 6). We identified presynaptic boutons as swellings along GFP-positive axon segments, which colocalize with presynaptic markers such as VAMP2, CASK, CAST1/2, bassoon, piccolo,
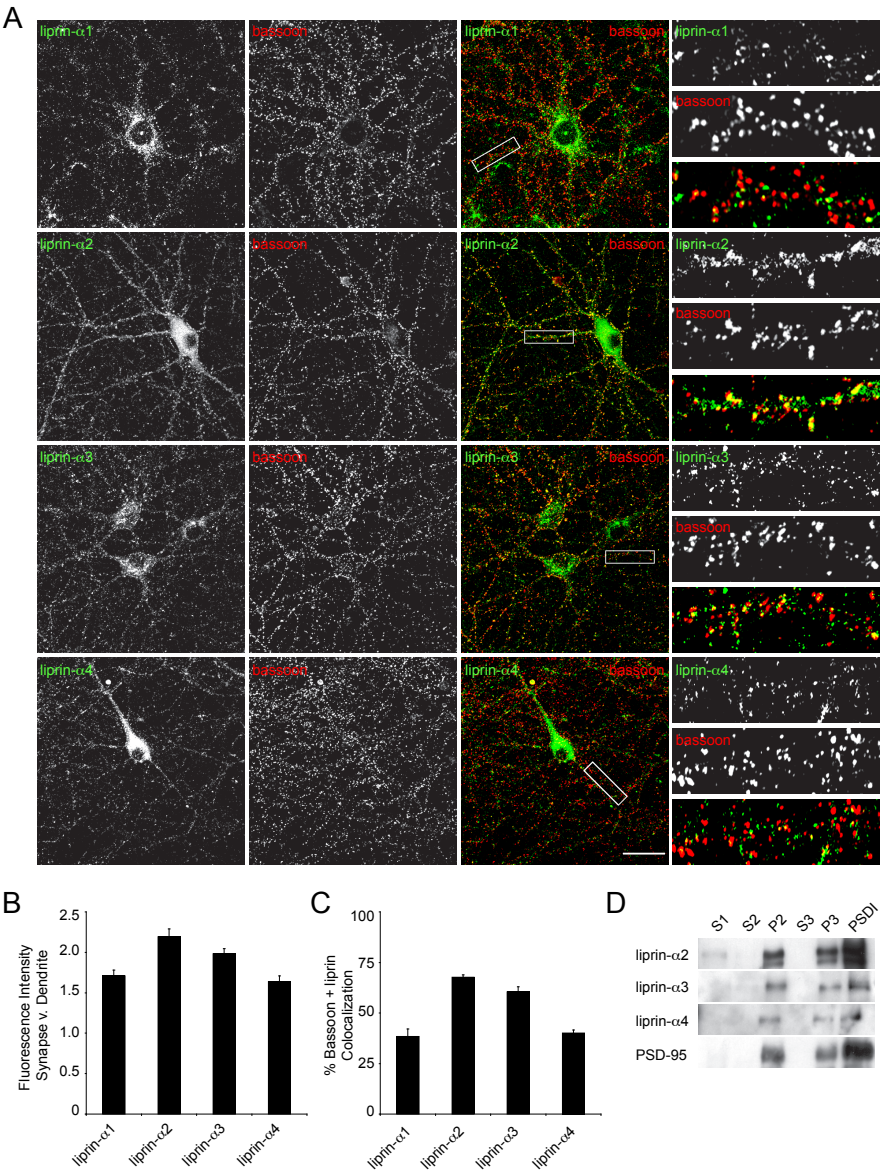
Figure 5.2. *Liprin-α2 is enriched at synapses in hippocampal neuron cultures.*
(A) Images of liprin-α1/α2/α3/α4 (green) and bassoon (red) in DIV19 hippocampal neuron cultures. Box indicates zoomed in region. Scale bar, 10 μm.
(B) Quantification of liprin-α fluorescence intensity at synaptic sites versus dendrites in DIV19 hippocampal neuron cultures (n=5 sets of >100 synapses per group).
(C) Quantification of percentage of colocalization of liprin-α and the presynaptic marker bassoon in DIV19 hippocampal neuron cultures (n=5 sets of >100 synapses per group).
(D) Enrichment of liprin-α2 in the PSD fraction. DIV21 hippocampal neurons were homogenized, fractionated by differential centrifugation, and analyzed by immunoblotting using anti-liprin-α and anti-PSD-95 antibodies.
All data are expressed as mean ± SEM.

and RIM (Figures 5.3A, 5.4, 5.7G, 5.8C, and data not shown) and FM4-64 (Figure 5.5D,G). Quantification showed that ~80% of axonal swellings stained positive for the tested presynaptic markers under basal conditions (Figures 5.3B,C and 5.5D,G), while ~20% of labeling can be considered background due to non-transfected axons in the same culture (Figure 5.3B). We then examined whether the synaptic targeting of liprin-α2 is affected by depleting the expression of several prominent presynaptic proteins in cultured hippocampal neurons by RNA interference. After testing several plasmid (pSuper)-based shRNA constructs for CASK, CAST1/2, bassoon, piccolo, and RIM1, we found specific shRNA sequences which effectively reduced the pro-
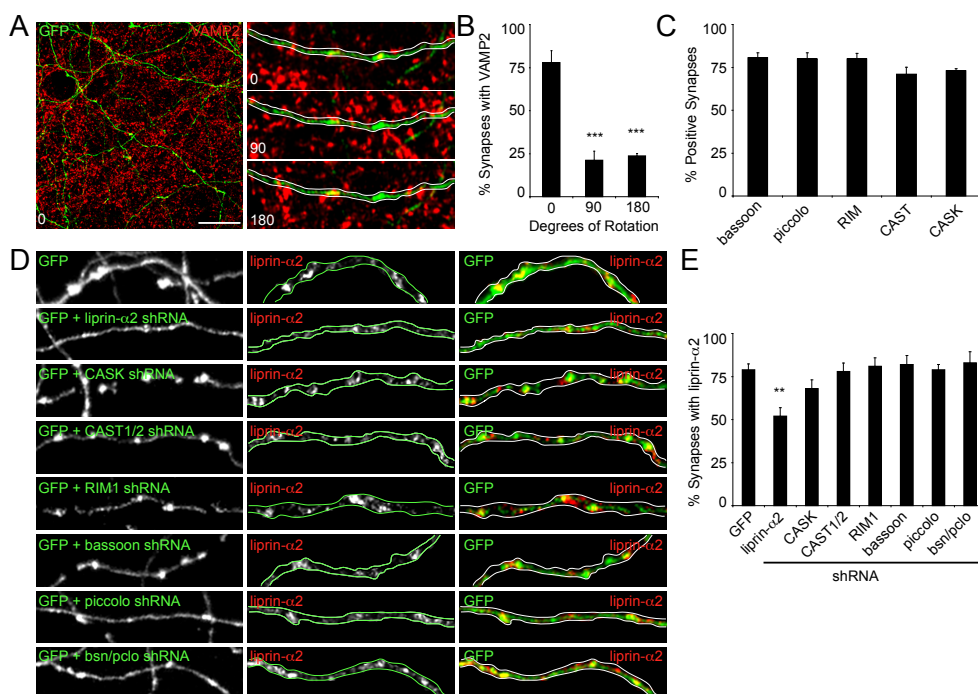
Figure 5.3. *Presynaptic localization of liprin-α2 does not depend on other scaffold proteins.*
(A) Method of quantifying localization of various proteins at presynaptic sites. Synapses are highlighted by GFP transfection and identified as varicosities along the length of the axon. Synapses that contain any staining for the protein being analyzed are counted as positive. Scale bar, 10 μm.
(B) Quantification of number of positive synapses due to labeling in non-specific axons as determined by rotation of endogenous staining (n=4 sets of 20 synapses per group).
(C) Quantification of localization of known presynaptic proteins at synaptic sites identified by GFP (n=5-15 sets of 20 synapses per group).
(D) Representative images of cells transfected with indicated shRNA and imaged for GFP (green) and endogenous liprin-α2 (red).
(E) Quantification of endogenous liprin-α2 at presynaptic sites transfected with shRNA of presynaptic proteins (n=5-15 sets of 20 synapses per group).
T-test: *, p<0.05; **, p<0.005; ***, p<0.0005. All data are expressed as mean ± SEM.

posed presynaptic protein (Figure 5.4 and Table 6.1). Next, the shRNA constructs were cotransfected in hippocampal neurons at DIV15 with GFP to highlight the transfected neurons, expressed for 4 days, and immunostained for liprin-α2 (Figure 5.3D). Under all conditions, no significant change in liprin-α2 localization at synapses was observed, including when both bassoon and piccolo were simultaneously depleted (Figure 5.3D,E). These data suggest that synaptic targeting of liprin-α2 is not dependent on the presence of other key scaffolding proteins.

5.2.3 Liprin-α1 and liprin-α2 differentially regulate presynaptic function

How important are liprin-α proteins for normal presynaptic function, and does it matter which liprin-α is present? We developed and tested several liprin-α2 shRNA constructs in cotransfected HeLa cells and determined that liprin-α2 shRNA#3 was most effective in reducing liprin-α2 levels, but did not affect expression of other liprin-α proteins (Figure 5.5C and Table 5.1). Control shRNA constructs such as liprin-α1- and CASK shRNA did not affect liprin-α2 expression (Figure 5.5C). This liprin-α2 shRNA construct was cotransfected with GFP into hippocampal neurons at DIV15, and, 4 days later, immunostaining for liprin-α2 showed a ~62% reduction of liprin-α2 in the cell body indicating an effective knockdown of endogenous liprin-α2 (Figure 5.5A,B), while no gross changes in endogenous liprin-α1, α3, or α4 were observed (data not shown). Additionally, after transfection with liprin-α2 shRNA, the number of presynaptic boutons positive for liprin-α2 labeling was significantly reduced (Figure 5.3D,E), although overlapping liprin-α2 staining at postsynaptic sites likely obscured the full magnitude of the reduction.

We next investigated the functional importance of liprin-α proteins at the presynapse by monitoring SV recycling using fluorescent membrane FM dyes[152]. We labeled the total recycling pool of vesicles within presynaptic boutons of hippocampal neuron cultures transfected with GFP-tagged liprin-α overexpression constructs or GFP along with liprin-α knockdown constructs by stimulation with 70 mM KCl for 90 seconds in the presence of 10 μM FM4-64 dye[148, 153]. There were no significant differences in the percentage of axonal varicosities that contained FM4-64 puncta (GFP: $84 \pm 4.3\%$, liprin-α1 shRNA: $83 \pm 5.1\%$, liprin-α2 shRNA: $83 \pm 7.3\%$, GFP-liprin-α1: $81 \pm 3.3\%$, GFP-liprin-α2: $90 \pm 2.2\%$; Figure 5.5D,G), and the numbers of FM4-64 positive boutons were consistent with previous immunostaining experiments (Figure 5.3C). However, synapses deficient in liprin-α2 displayed a small but significant re-
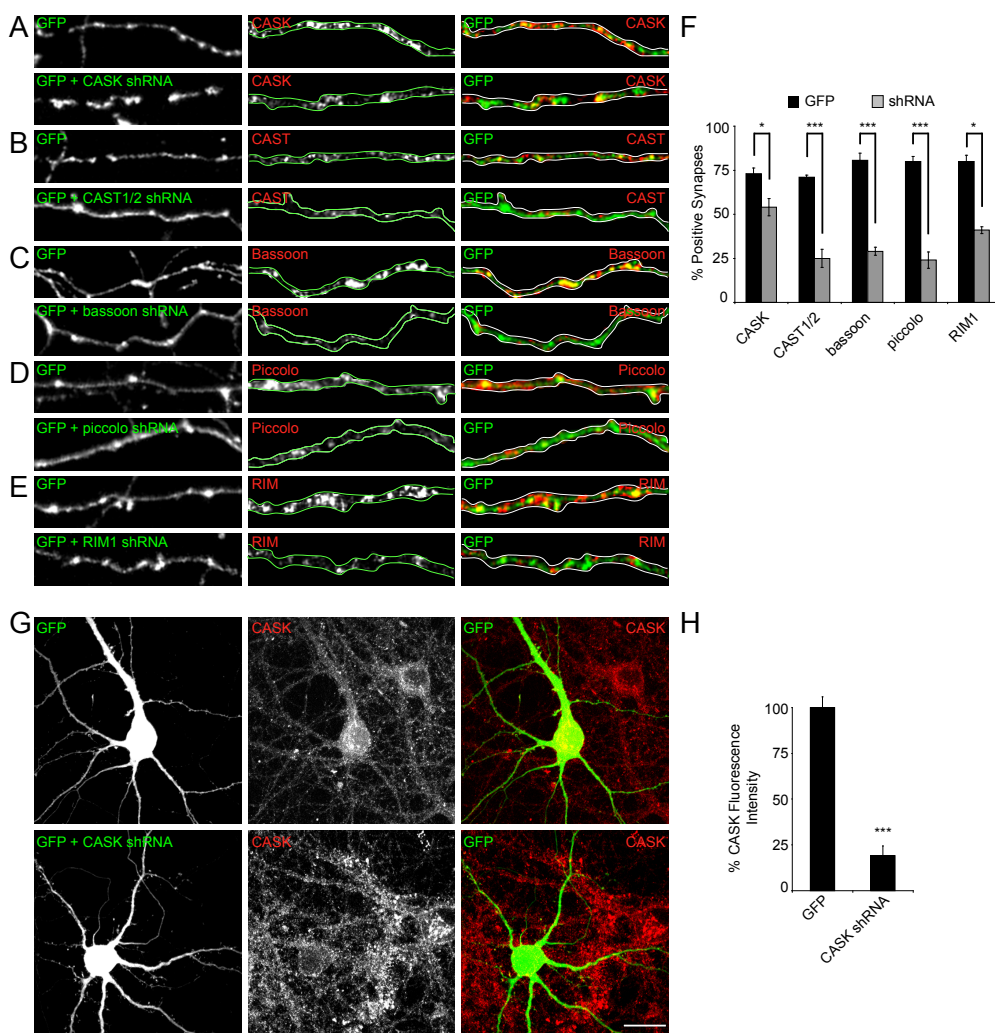
Figure 5.4. *shRNA constructs effectively deplete target proteins.*
(A-E) Representative images of cells transfected with shRNA and imaged for GFP (green) and the targeted protein (red): CASK (A); CAST1/2 (B); bassoon (C); piccolo (D); RIM (E).
(F) Quantification of shRNA knockdown at presynapses (n=5 sets of 20 synapses per group).
(G) Representative images of neurons transfected with GFP or GFP plus CASK shRNA and imaged for GFP (green) and endogenous CASK (red).
(H) Quantification of knockdown of endogenous CASK staining in neuronal cell bodies by liprin-α2-shRNA#3. Fluorescence intensity of CASK staining in GFP transfected cells was set to 100% (n=5 images per group). Scale bars, 10 μm.
T-test: *, p<0.05; **, p<0.005; ***, p<0.0005. All data are expressed as mean ± SEM.
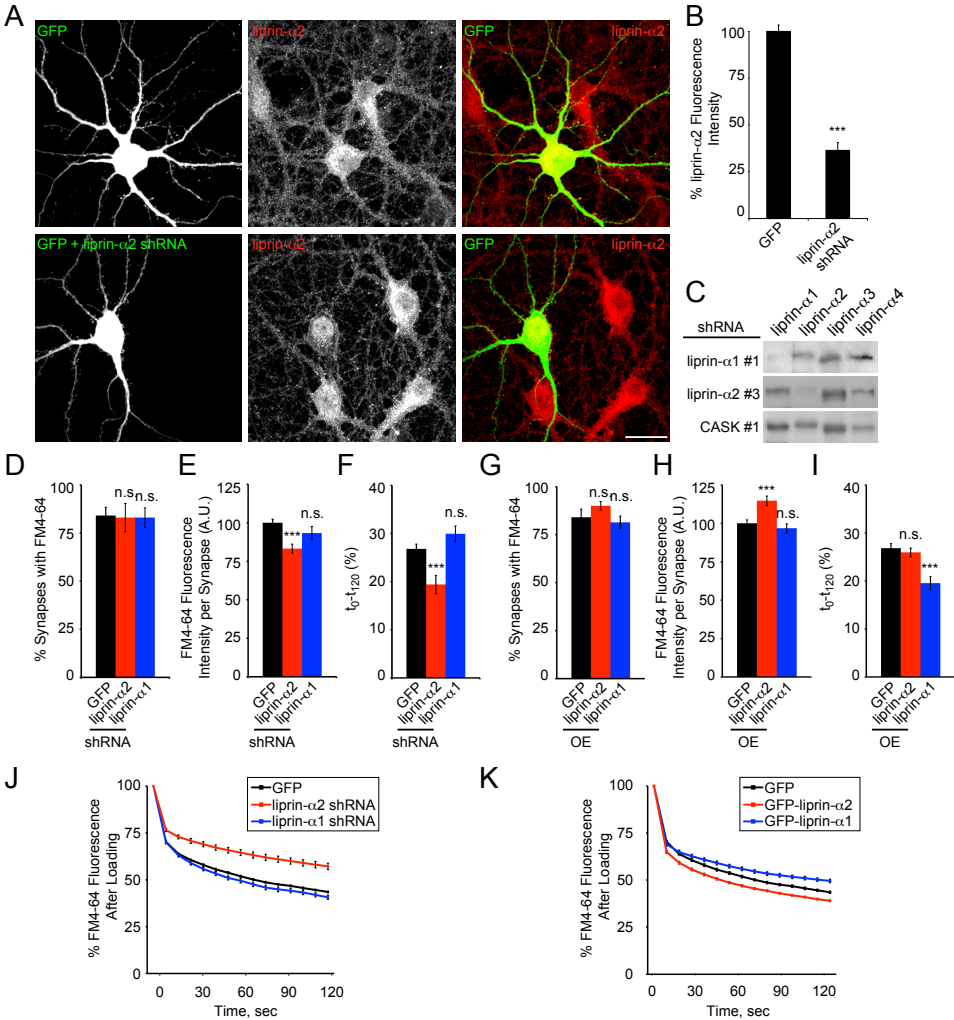
Figure 5.5. *Liprin-α proteins differentially regulate SV exocytosis.*

(A) Representative images of neurons transfected with GFP with and without liprin-α2 shRNA and imaged for GFP (green) and endogenous liprin-α2 (red). Scale bars, 10 μm.

(B) Quantification of knockdown of endogenous liprin-α2 staining in neuronal cell bodies by liprin-α2 shRNA#3. Fluorescence intensity of liprin-α2 staining in GFP transfected cells was set to 100% (n=5 images per group).

(C) Western blots of GFP expression in extracts of HeLa cells cotransfected with GFP-liprin-α and either liprin-α1, liprin-α2 or CASK shRNA constructs.

(D) Quantification of the number of presynaptic sites transfected with liprin shRNA constructs that were loaded with FM4-64 dye (n=5-15 sets of 20 synapses per group).

(E) Quantification of the fluorescence intensity of FM4-64 dye loading of presynaptic sites transfected with liprin shRNA constructs (n=100 synapses per group).

(F) Quantification of difference between the first frame after unloading stimulation (t_0) and the last frame imaged (t_{120}) for presynapses transfected with liprin shRNA constructs (n=25-82 synapses per group).

duction of FM4-64 fluorescence intensity compared to control, while FM4-64 fluorescence was increased in synapses of cells overexpressing GFP-liprin-α2 (GFP: 100 ± 2.3%, liprin-α1 shRNA: 93 ± 3.3%, liprin-α2 shRNA: 83 ± 2.9%, GFP-liprin-α1: 97 ± 2.9%, GFP-liprin-α2: 115 ± 3.1%; Figure 5.5E,H), implying that liprin-α2 is important for the maintenance of the total recycling pool of SVs. We further compared the destaining kinetics of the TRP following a second stimulation with 70 mM KCl for 60 seconds. Selected axon segments were imaged every ~7 seconds for 2 minutes following destaining, and the FM4-64 fluorescence intensity at individual boutons was quantified and normalized to the labeling intensity at that particular bouton prior to the second stimulation. Neurons expressing liprin-α2 shRNA exhibited decreased FM4-64 unloading both in the frame immediately following the second stimulation (Figure 5.5J, second data point) and in the two minutes that followed relative to the initial release (GFP: 27 ± 1.0 %, liprin-α1 shRNA: 30 ± 1.7%, liprin-α2 shRNA: 19 ± 1.9%, GFP-liprin-α1: 20 ± 1.4%, GFP-liprin-α2: 26 ± 0.9%; Figure 5.5F,J). Again, synapses in neurons expressing liprin-α1 shRNA were not significantly different from control neurons (Figure 5.5F,J). Though overexpression of liprin-α2 did not alter the rate of fluorescence decay over time (Figure 5.5I), it did lead to greater destaining immediately following the second stimulation (Figure 5.5K). These data suggest that liprin-α2 is important not only for the maintenance of the TRP of vesicles, but also regulates the efficiency of SV release.

In contrast to liprin-α2, liprin-α1 is only present at low levels at active synapses (Figure 5.2)[108]. Overexpressing GFP-liprin-α1 in neurons did not significantly alter general presynaptic stability and SV retention (Figure 5.5G,H), and there was no

(G) Quantification of the number of presynaptic sites transfected with liprin overexpression constructs that were loaded with FM4-64 dye (n=5-15 sets of 20 synapses per group).

(H) Quantification of the fluorescence intensity of FM4-64 dye loading of presynaptic sites transfected with liprin overexpression constructs (n=100 synapses per group).

(I) Quantification of difference between the first frame after unloading stimulation (t_0) and the last frame imaged (t_{120}) for presynapses transfected with liprin overexpression constructs (n=55-75 synapses per group).

(J) Quantification FM 4-64 destaining following unloading of presynapses transfected with liprin shRNA constructs (n=75 (GFP), 25 (liprin-α1 shRNA), or 82 (liprin-α2 shRNA) synapses; for GFP v. liprin-α2 shRNA: ANOVA Repeated Measures: ***, $p < 0.0005$)

(K) Quantification FM 4-64 destaining following unloading of presynapses transfected with liprin overexpression constructs (n=75 (GFP), 70 (GFP-liprin-α1), or 55 (GFP-liprin-α2) synapses; for GFP v. GFP-liprin-α1: ANOVA Repeated Measures: **, $p < 0.001$; for GFP v. GFP-liprin-α2: ANOVA Repeated Measures: **, $p < p < 0.004$)

T-test: *, $p < 0.05$; **, $p < 0.005$; ***, $p < 0.0005$. All data are expressed as mean ± SEM.

significant difference in control boutons and those expressing GFP-liprin-α1 for the first 30 seconds after unloading (Figure 5.5K, first five data points, t-test: p>0.05). However, overexpression of GFP-liprin-α1 did cause a notable decrease of FM4-64 destaining over time compared to control (Figure 5.5I,K), indicating that liprin-α1 slows down SV exocytosis. These data show that liprin-α1 and liprin-α2 differentially regulate SV exocytosis, and imply an important distinction between liprin-α protein function at presynapses.

To understand the presynaptic function of liprin-α2 in greater detail, we performed whole-cell patch clamp recordings in cultured hippocampal autapses infected with liprin-α2-shRNA and GFP co-expressing lentiviruses. Evoked EPSC amplitude was decreased by ~46% in neurons lacking liprin-α2 (Figure 5.6A), though miniature EPSC (mEPSC) amplitude (Figure 5.6B) and mEPSC frequency (Figure 5.6C) were unchanged. These changes were not due to notable differences in neuronal morphology, as dendrite length and branching as well as synapse number were unaffected by liprin-α2 knockdown (data not shown). We investigated readily releasable pool (RRP) size in liprin-α2 knockdown cells by measuring responses to application of 500mM sucrose[154]. Indeed, liprin-α2 deficient neurons showed an ~51% decrease in RRP size (Figure 5.6E), arguing that in addition to regulating the TRP, liprin-α2 is an important factor in determining RRP size. The vesicular release probability (Pvr) was unchanged (data not shown), meaning that those vesicles left in the RRP in the absence of liprin-α2 are equally likely to undergo exocytosis as SVs in control boutons.

To investigate the effect of liprin-α2 deletion on short-term plasticity, cells were stimulated with paired pulses of varying interstimulus intervals. Interestingly, neurons expressing liprin-α2 shRNA exhibited paired pulse facilitation, especially at low interstimulus intervals (Figure 5.6F), indicating that synaptic release probability is decreased in the absence of liprin-α2. Consistently, responses to high frequency (40Hz) stimulation also show less depression during the initial pulses (Figure 5.6G, inset). Although the initial release probability is smaller, kinetics of the rundown during high frequency stimulation are not affected by liprin-α2 knockdown. The rate of RRP replenishment (tested with single action potentials every 5 seconds) was not affected by liprin-α2 knockdown (Figure 5.6G). Furthermore, we observed no difference in the ratio of synchronous to asynchronous release in both groups (Figure 5.6D) indicating that the reduction in evoked release amplitude in the absence of liprin-α2 cannot be attributed to a shift towards slower asynchronous release but has an underly-
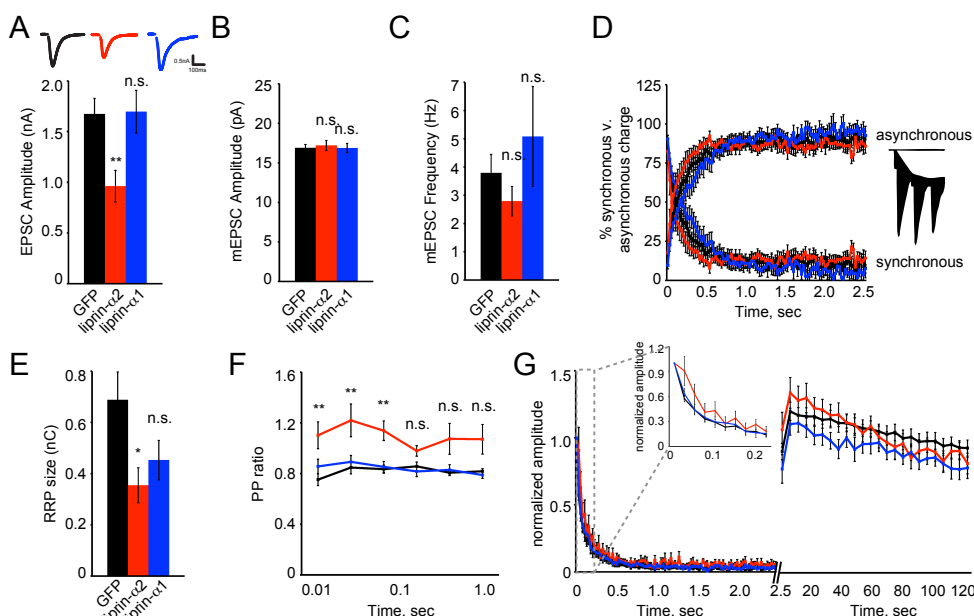
Figure 5.6. *Liprin-α2 regulates synaptic vesicle release and presynaptic plasticity.*
(A) Evoked EPSC size in hippocampal autapses infected with liprin shRNA viruses (GFP: 1.77 ± 0.21 nA, n=46; liprin-α2 shRNA: 0.96 ± 0.16 nA, n=39; liprin-α1 shRNA: 1.70 ± 0.21 nA, n=51; **, Kruskal-Wallis test, p =0.007).
(B) Miniature EPSC amplitude in hippocampal autapses infected with liprin shRNA viruses (GFP: 16.9 ± 0.4 pA, n=58; liprin-α2 shRNA: 17.2 ± 0.6, n=37; liprin-α1 shRNA: 16.9 ± 0.6, n=31).
(C) Miniature EPSC frequency in hippocampal autapses infected with liprin shRNA viruses (GFP: 3.8 ± 0.7 Hz, n=43; liprin-α2 shRNA: 2.8 ± 0.5 Hz, n=40; liprin-α1 shRNA: 5.1 ± 0.8 Hz, n=40).
(D) Mean contribution of synchronous and asynchronous release to the total charge transfer during an action potential train (40 Hz) as a function of time. (GFP, n = 21; liprin-α2 shRNA, n=5; liprin-α1 shRNA, n=12). The two components were measured as defined in the inset.
(E) RRP size as assessed with single hyperosmotic sucrose application (500 mM sucrose) in hippocampal autapses infected with liprin shRNA viruses (GFP: 0.69 ± 0.11 nC, n=11; liprin-α2 KD, 0.35 ± 0.07 nC, n=9; liprin-α1 KD, 0.45 ± 0.08 nC, n=8; *, ANOVA, p=0.0368).
(F) Paired-pulse ratio (ratio of the second to the first synaptic response plotted as a function of the stimulus interval) in hippocampal autapses infected with liprin shRNA viruses. (n = 30 (GFP), 19 (liprin-α2 shRNA), 35 (liprin-α1 shRNA); **, Kruskal-Wallis test, p<0.005).
(G) Mean normalized EPSC amplitudes during high-frequency stimulation stimulation (100AP, 40Hz) and subsequent recovery period (0.2 Hz). The inset shows the first ten responses at higher time resolution (GFP, n = 28; liprin-α2 shRNA, n=12; liprin-α1 shRNA, n=12; n.s.).

ing reduction of the total amount of both release components (data not shown).Thus liprin-α2 levels control the size of the RRP without affecting its depletion and replenishment. Importantly, in all electrophysiological parameters, no significant differences were observed in neurons lacking liprin-α1 (Figure 5.6A-G), further confirming that liprin-α2 is specifically required for normal presynaptic function in the hippocampus.
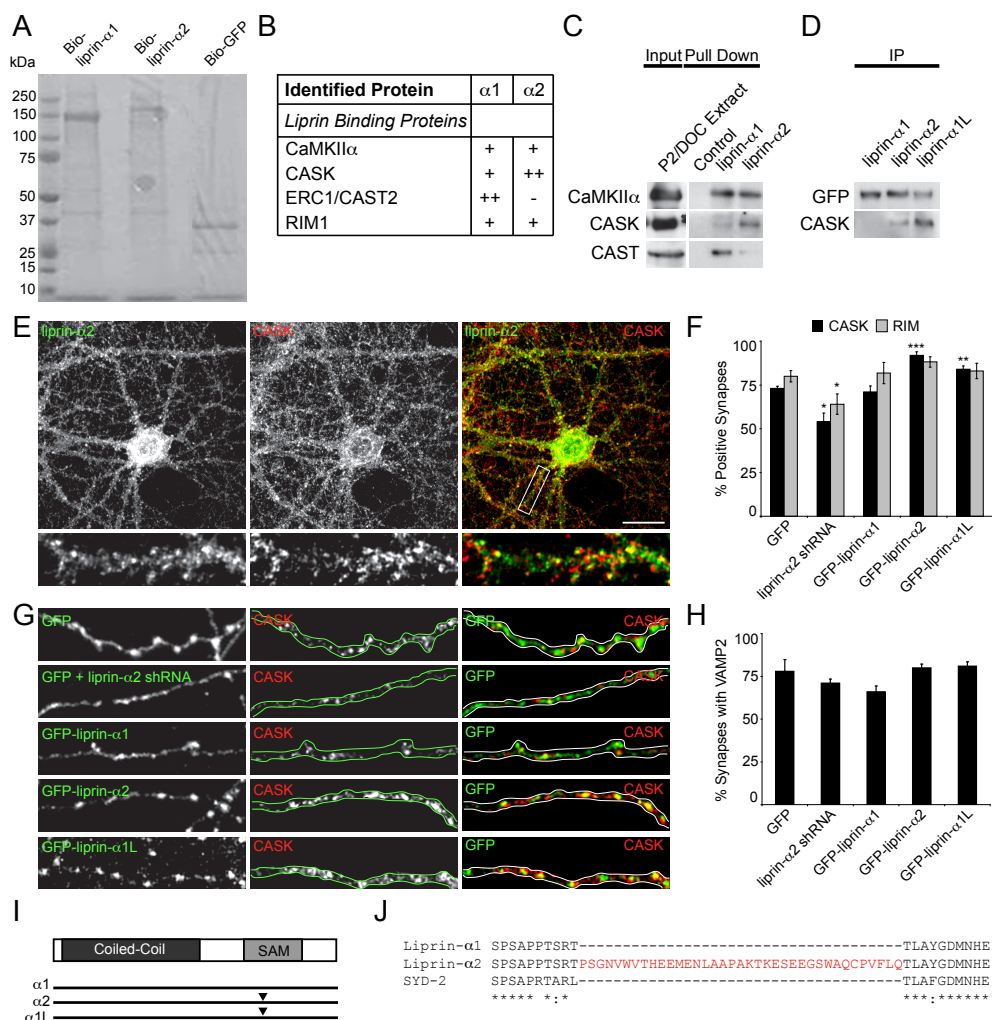
Figure 5.7. *Liprin-α2 recruits CASK and RIM to presynaptic sites.*

(A) Colloidal Blue stained 4-12% Bis-Tris gel containing samples of biotin pull downs from P2/DOC brain extracts for mass spectrometry.

(B) Table of mass spectrometry results from biotin pull downs. For each indicated protein, the list is filtered for duplicates and shows the number of unique peptides: "-", no peptides; "+", 1-4 peptides; "++", > 5 peptides.

(C) Western blots of liprin-α binding partners identified from biotin pull downs. Equal volumes of total pull down are loaded in each lane.

(D) Western blots of immunoprecipitation of GFP-liprin-α1/α2/α1L and coimmunoprecipitation of endogenous CASK protein from HEK293 cell extracts.

(E) Colocalization of endogenous liprin-α2 (green) and CASK (red) proteins in hippocampal neuron cultures. Box indicates zoomed in region. Scale bar, 10 μm.

(F) Quantification of endogenous CASK and RIM at presynaptic sites transfected with liprin expression constructs (n=5-15 sets of 20 synapses per group).

(G) Representative images of cells transfected with indicated expression constructs and imaged for GFP (green) and endogenous CASK (red).

5.2.4 Liprin-α1 and liprin-α2 selectively interact with different presynaptic proteins

To investigate the mechanism by which liprin-α proteins differentially influence presynaptic function, we next searched for distinct liprin-α1 and liprin-α2 binding partners using pull down assays combined with mass spectrometry. Biotinylation-tagged liprin-α1 and liprin-α2 (bio-liprin-α1 and bio-liprin-α2) and control bio-GFP were transiently coexpressed in HEK293 cells with the protein-biotin ligase BirA and isolated with streptavidin beads (Figure 5.7A). Additional bio-liprin-α mass spectrometry experiments were performed using crude synaptosome (P2) fractions from rat brain (see Ch. 6). Mass spectrometry analysis of the complete bio-liprin-α1 and bio-liprin-α2 lanes revealed several synaptic proteins that were not present in the control lane (Table 5.1). Some of the identified synaptic proteins, such as CASK, CaMKIIα, RIM1, and CAST, have previously been shown to directly interact with liprin-α proteins[58], while others are associated with liprin binding partners and could indirectly bind liprin-α, such as MALS and neurexins via CASK and rab3 via RIM1[53, 144]. In addition, several potentially new liprin-α binding partners were identified, such as actinin-α, AKAP9, and SNAP23 (Table 5.1). Next, we screened the mass spectrometry data for specific presynaptic proteins that showed particular affinity for either liprin-α1 or liprin-α2. Interestingly, although mass spectrometry in itself is a semi-quantitative technique, the number of proteolytic peptides identified suggests that the presynaptic scaffolding proteins CASK and CAST have remarkable preferences for individual liprin-α proteins; CASK was highly enriched in the liprin-α2 pull down and CAST was more prominently present in the liprin-α1 pull down (Figure 5.7B and Table 5.1). In contrast, CaMKIIα and RIM1 came down to a similar degree with both liprin-α proteins (Figure 5.7B and Table 5.1). These mass spectrometry results were confirmed by Western blotting (Figure 5.7C), suggesting that different liprin-α family members bind to distinct synaptic proteins, which may lead to specific regulation of

(H) Quantification of endogenous VAMP2 at presynaptic sites transfected with liprin expression constructs (n=5-15 sets of 20 synapses per group).

(I) Schematic diagram of the liprin-α1, α2, and mutant α1L expression constructs. Arrowhead indicates the presence of a 37-aa linker region (L) between the first and second SAM domains in liprin-α2 and mutant liprin-α1L.

(J) Alignment of the region between the first and second SAM domains of human liprin-α1, α2, and C.elegans SYD-2. The 37-aa linker region present in liprin-α2 and added to liprin-α1L is indicated in red. ".", semi-conserverd substitutions; ":", conserved substitutions; "*", identical.

T-test: *, $p<0.05$; **, $p<0.005$; ***, $p<0.0005$. All data are expressed as mean ± SEM.

Identified Protein	Bio-GFP-liprin-α1		Bio-GFP-liprin-α2			
	HEK	brain	HEK	brain		
liprin family proteins					binding	reference
α-*subfamily*						
liprin-α1 (PPFIA1)	50	33	13	7	Y2H, IP	79
liprin-α2 (PPFIA2)	13	10	53	41	Y2H, IP	79
liprin-α3 (PPFIA3)	10	8	8	5		
liprin-α4 (PPFIA4)	-	4	17	8		
β-*subfamily*						
liprin-β1 (PPFIBP1)	-	2	11	8	Y2H, IP	79
liprin-β2 (PPFIBP2)	-	-	-	-		
synaptic proteins					binding	reference
actinin-α2	6	-	-	-		
actinin-α3	5	-	-	-		
actinin-α4	22	-	2	-		
AKAP9 (yotiao)	7	-	5	-		
N-cadherin	-	-	2	1	IP	96
CaMKIIα	-	4	-	4	IP	108
CaMKIIβ	-	3	-	3	IP	108
CASK (lin-2)	3	-	14	10	Y2H, IP	104
β-catenin	9	-	11	8	IP	96
CAST1/ERC2	6	3	-	-	Y2H, IP	97
GIT1	5	-	-	-	Y2H, IP	107
LIN7C (MALS3)	6	-	-	5		
munc18-1	0	3	-	3		
neurexin 2	0	-	-	4		
neurexin 3	0	-	-	3		
rab3A	0	3	-	1		
RIM1	4	3	5	-	Y2H	99
SNIP/p140Cap	0	-	-	4		
SNAP23A	9	1	8	3		

Table 5.1. *Binding partners of bio-GFP-liprin-α proteins from HEK293 cells and brain extracts identified by mass spectrometry*

This table shows liprin-α binding proteins identified with a significant Mascot score in the biotin-streptavidin pull down from extracts of HEK293 cells co-expressing each of the bio-GFP-liprin-α and biotin ligase BirA (column HEK293). The number of unique peptides identified from bio-GFP-liprin-α pull downs using the P2 fraction from total rat brain is indicated (column brain). For each identified protein, the list is filtered for duplicates and shows the number of unique peptides. The list is corrected for background proteins which were identified in a control pull down from HEK293 cells expressing bio-GFP and BirA. Proteins previously reported as liprin-α binding partners by immunoprecipitation (IP) or yeast two-hybrid assay (Y2H) are indicated in the reference list.

the presynaptic machinery.

5.2.5 Liprin-α2 recruits CASK to presynaptic boutons

Since CASK was enriched in the liprin-α2 pull down, we next explored the effect of altered liprin-α levels on synaptic CASK localization by expressing liprin-α2 shRNA, GFP-liprin-α1, or GFP-liprin-α2 in hippocampal neurons. Four days after transfection, neurons expressing liprin-α2 shRNA showed a marked reduction of CASK (54 ± 4.8%; Figure 5.7F,G) positive synapses compared to control neurons (73 ± 1.2%; Figure 5.7F,G). In contrast, a robust increase in synaptic CASK was observed in neurons overexpressing liprin-α2 (92 ± 1.9%; Figure 5.7F,G). No significant effect on CASK localization was observed by overexpressing liprin-α1 (71 ± 3.5%; Figure 5.7F,G). Additionally, neurons expressing liprin-α2 shRNA showed a reduction of synapses containing the liprin-α binding protein RIM (64 ± 5.6%; Figure 5.7F) compared to control neurons (80 ± 3.2%, Figure 5.7F), though RIM labeling at presynapses was not significantly increased with liprin-α1 (82 ± 6.1%; Figure 5.7F) or liprin-α2 overexpression (88 ± 3.0%, Figure 5.7F). For all conditions, the number of presynapses containing VAMP2 (Figure 5.7H) and CAST (Figure 5.8E) was not significantly changed. These data reveal that liprin-α2 is necessary for synaptic CASK and RIM localization and, in particular, recruits CASK to presynaptic sites.

How do liprin-α1 and liprin-α2 differentially affect synaptic CASK recruitment? Endogenous CASK and liprin-α2 colocalize at synapses (Figure 5.7E), the C-terminal SAM domains of liprin-α2 bind to CASK[104], and cdk5-dependent phosphorylation of CASK regulates this interaction[151]. We compared the SAM domains of liprin-α1 and liprin-α2 and found a unique 37-amino acid linker region (L) between the first and second SAM domain of liprin-α2 that was absent in liprin-α1 (Figure 5.7I,J). Interestingly, the *C. elegans* liprin-α/SYD-2 protein does not contain the linker sequence (Figure 5.7J). We next investigated whether this linker domain of liprin-α2 is important for synaptic CASK localization by introducing the same 37 amino acid sequence between the first and second SAM domains of liprin-α1. Expression of the chimeric construct, GFP-liprin-α1L, in hippocampal neurons resulted in a significant increase of CASK positive synapses compared to control neurons; CASK is present in 84 ± 1.9% of the GFP-liprin-α1L-containing presynaptic boutons versus 73 ± 1.2% in control neurons (Figure 5.7F,G). Consistently, GFP-liprin-α1L showed increased binding to CASK in immunoprecipitation experiments (Figure 5.7D). As RIM binds to
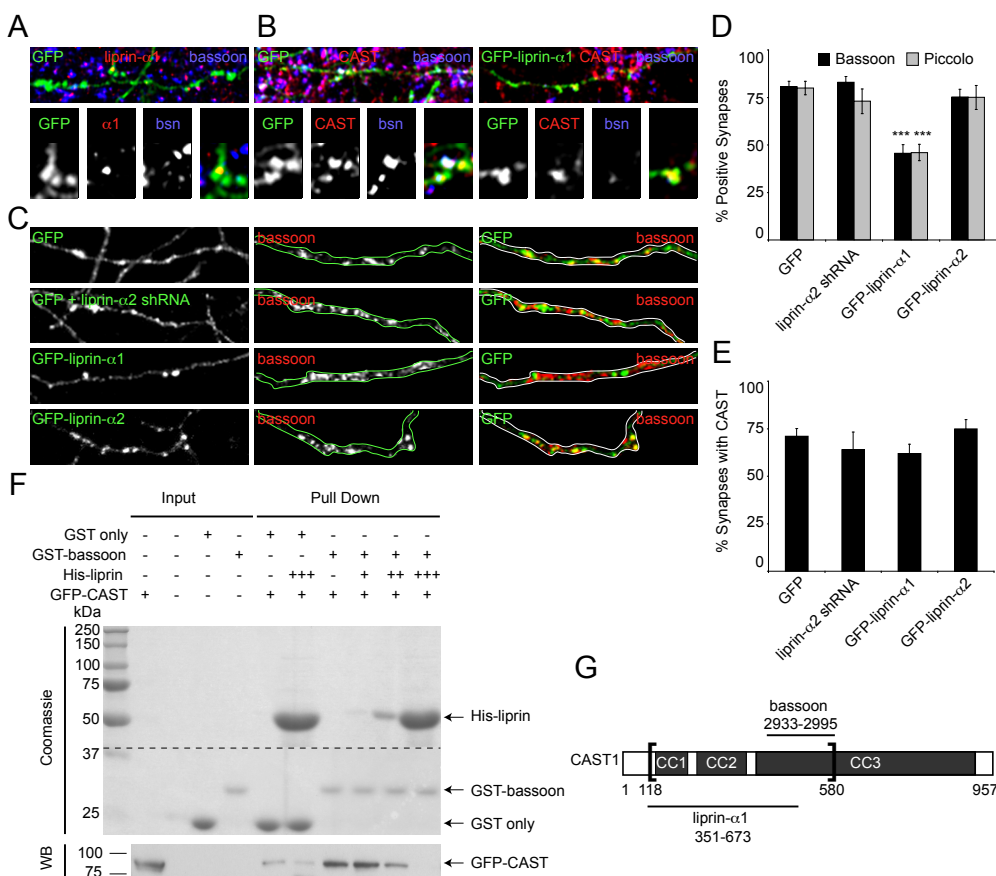
Figure 5.8. *Liprin-α1 competes with bassoon for binding to presynaptic CAST.*
(A) Image of an axon visualized for transfected GFP (green) and endogenous liprin-α1 (red) and bassoon (blue).
(B) Image of an axon visualized for transfected GFP (left) or GFP-liprin-α1 (right, green) and endogenous pan-CAST (red) and bassoon (blue).
(C) Representative images of cells transfected with indicated expression constructs and imaged for GFP (green) and endogenous bassoon (red).
(D) Quantification of endogenous bassoon and piccolo at presynaptic sites transfected with liprin expression constructs (n=5-15 sets of 20 synapses per group).
(E) Quantification of endogenous pan-CAST at presynaptic sites transfected with liprin expression constructs (n=5-15 sets of 20 synapses per group).
(F) *In vitro* competition assay between liprin-α1, CAST1, and bassoon. Presence and amount of protein are indicated by "-" and "+". "+"=1:1 ratio bassoon: liprin; "++"=1:10, "+++"=1:100. Coomassie stained gels are loaded with inputs into the experiment and Western blot is loaded with equal amounts of either input or pull down.
(G) Domain structure of rat CAST1 and indication of expression constructs used in the competition assay. Brackets indicate the region of CAST1, and lines indicate the identified sufficient binding regions for the respective proteins.
T-test: *, $p<0.05$; **, $p<0.005$; ***, $p<0.0005$. All data are expressed as mean ± SEM.

the coiled coil region of liprin-α proteins[99] and was not significantly recruited to bou-tons by liprin-α overexpression (Figure 5.7F), no change was seen in RIM localization at presynapses with overexpression of GFP-liprin-α1L (Figure 5.7F). Consistently, VAMP2 was also unchanged (Figure 5.7H). Together these data indicate that CASK is specifically recruited to presynapses by liprin-α2, and that this recruitment is depen-dent on the linker region between the first two liprin SAM domains.

5.2.6 Liprin-α1 reduces bassoon and piccolo localization at presynaptic boutons

Since overexpression of liprin-α1 slows down SV exocytosis, we wanted to gain a bet-ter understanding of the underlying mechanism by which this occurs. When carefully examining the synaptic localization and enrichment of liprin-α proteins, we noticed that, in contrast to other liprin-α proteins, many of the bright synaptic liprin-α1 puncta do not coincide with bassoon staining (Figure 5.2A). While the less intense puncta colocalized with bassoon (Figure 5.2A), some of the bright liprin-α1 clusters at GFP-positive boutons contained little or no bassoon staining (Figure 5.8A), though they do colocalize with endogenous VAMP2 (data not shown). Upon further examination, we found a robust reduction of both bassoon and piccolo positive synapses in hippocam-pal neurons transfected with GFP-liprin-α1 compared to control neurons (46 ± 4.5% of positive synapses versus 80 ± 2.8% in control, Figure 5.8B-D), while the synaptic localization of CAST was unaffected (Figure 5.8B,E). Furthermore, manipulating the levels of presynaptic liprin-α2 did not affect bassoon and piccolo localization (Figure 5.8C-D), indicating that presynaptic bassoon and piccolo are specifically and nega-tively regulated by liprin-α1.

5.2.7 Liprin-α1 competes with bassoon for binding to presynaptic CAST

How does liprin-α1 regulate the distribution of synaptic bassoon and piccolo? Although there is no evidence of a direct interaction between liprin-α proteins and bassoon/pic-colo, liprin-α and bassoon/piccolo do share a common binding partner, CAST[97, 155]. Both liprin-α and bassoon/piccolo interact with the central region of CAST, which is comprised of mostly coiled coil domains (Figure 5.8G). Since CAST localization at presynaptic sites is unchanged upon liprin-α1 overexpression (Figure 5.8B,E), and liprin-α1 showed increased binding to CAST compared to liprin-α2 (Figure 5.7B,C and Table 5.1), we hypothesized that bassoon/piccolo may compete with liprin-α1 for binding to CAST.

To test for competition between liprin-α1 and bassoon for CAST binding, we performed in vitro pull down assays with GST-bassoon(2933-2995), His-liprin-α1(351-673), and GFP-CAST1(118-580) constructs containing the minimal binding domain of each protein necessary to mediate interaction (Figure 5.8G)[97, 155]. The GST-bassoon fragment, which is highly similar to the corresponding region of piccolo[155], was purified from bacteria and used to pull down GFP-CAST1(118-580) from transfected HEK293 cell extracts (Figure 5.8F). We next determined the amount of GFP-CAST1(118-580) coming down with GST-bassoon(2933-2995) in the presence of varying amounts of purified His-liprin-α1(351-673). As the amount of His-liprin-α1(351-673) was increased, the level of GFP-CAST1(118-580) detected in the bound fraction decreased (Figure 5.8F), confirming the ability of liprin-α1 to out compete bassoon for binding to CAST.

5.2.8 CAST is critical for bassoon localization at membrane structures

To further investigate the mechanism of maintaining proper bassoon localization, we used heterologous cells containing endogenous CAST and examined the effects of liprin-α1 on GFP-bassoon targeting. When GFP-bassoon is introduced into HeLa cells, it is expressed in a punctate fashion and targets to the previously described endogenous CAST-containing clusters at the cell cortex (Figure 5.9A)[156, 157]. Overexpression of mCherry-CAST1 in conjunction with GFP-bassoon caused a marked increase in the cortical localization of bassoon, while overexpression of mRFP-liprin-α1 to the same structures disrupts the localization of bassoon at the cell cortex (Figure 5.9A).

To gain insight into the dynamics of GFP-Bassoon within the clusters at the cell cortex, we performed fluorescence recovery after photobleaching (FRAP) experiments (Figure 5.9B-D). First, we analyzed the mobility of GFP-bassoon clusters and observed in most cases that the peripheral bassoon patches displayed no significant motility (data not shown), consistent with published observations that proteins in these clusters are reasonably stagnant for as long as 30 minutes[156]. Next, time lapse images of GFP-bassoon were acquired every 3 seconds and the difference between the FRAP of the bleached clusters and the fluorescence loss in photobleaching (FLIP) of neighboring, unbleached clusters were quantified for 7 minutes (Figure 5.9C). FRAP analysis of GFP-bassoon cortical clusters in control cells showed a fluorescence recovery of ~51%, while cells co-expressing mCherry-CAST1 showed significantly lower recovery (~38%), suggesting that bassoon is more stably bound at the cell cortex in the pres-
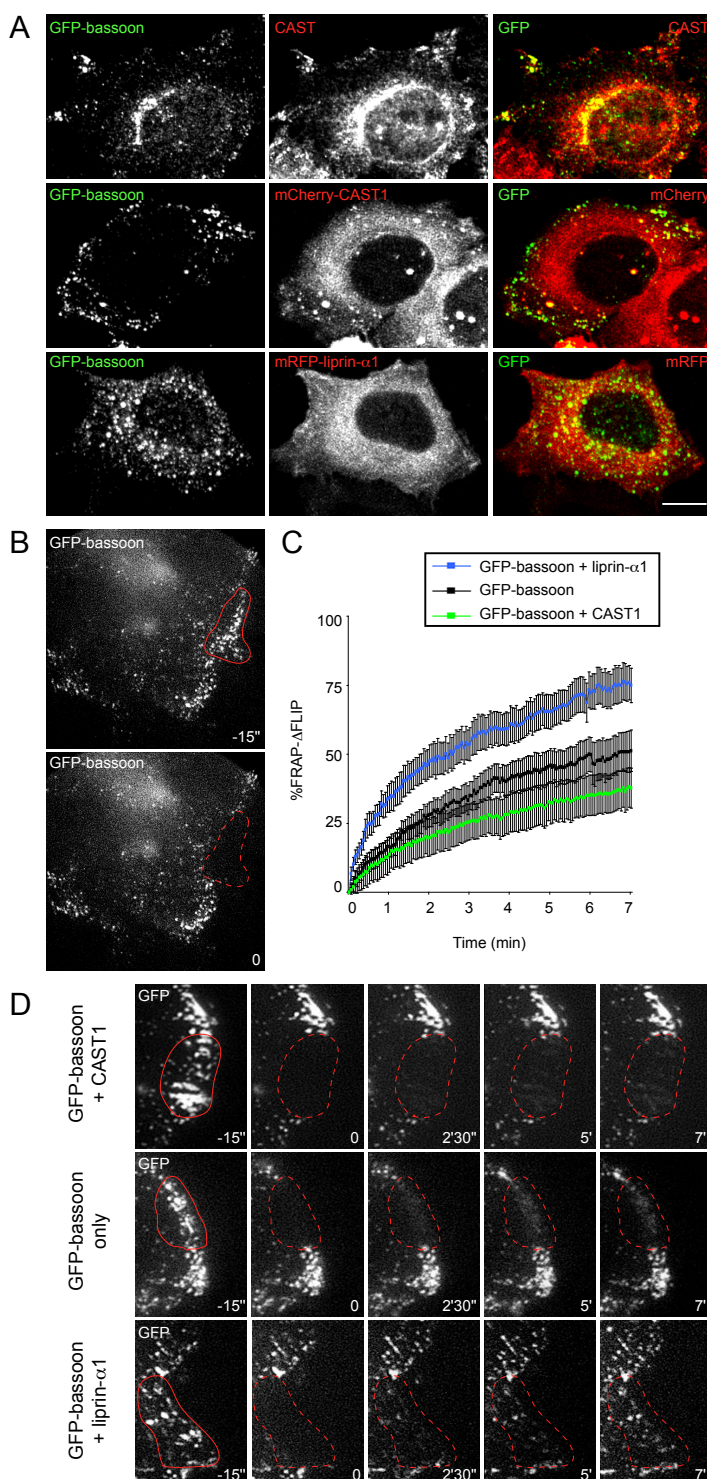
Figure 5.9. *CAST is critical for bassoon localization at membrane structures.*

(A) Representative images of HeLa cells transfected with either GFP-bassoon 95-3938 alone, or cotransfected with mCherry-CAST1 or mRFP-liprin-α1 and imaged for GFP (green) and either endogenous CAST2 or exogenous mCherry or mRFP (red). Scale bars, 10 μm.

(B) Representative images of GFP-bassoon 95-3938 in HeLa cells from a time-lapse movie indicating the region bleached for FRAP analysis. Time "0" represents the first image acquired following bleaching of the selected region.

(C) Quantification of FRAP-ΔFLIP for HeLa cells transfected with either GFP-bassoon 95-3938 alone, or cotransfected with mCherry-CAST1 or mRFP-liprin-α1 (n=12 cells per group).

(D) Representative images of HeLa cells transfected with either GFP-bassoon 95-3938 alone, or cotransfected with mCherry-CAST1 or mRFP-liprin-α1 from a time-lapse movie indicating the region bleached for FRAP analysis. Time "0" represents the first image acquired following bleaching of the selected region.

All data are expressed as mean ± SEM.

ence of high levels of CAST. In contrast, cells co-expressing mRFP-liprin-α1 showed greater degree of recovery (~75%) (Figure 5.9C,D). These data imply that presence of CAST at the cell cortex is important for the targeting of GFP-bassoon, and that interfering with the interaction between CAST and bassoon by expressing high levels of liprin-α1 disrupts the ability of bassoon to stably bind to cortical membrane structures.

Consistently, the localization of endogenous bassoon in hippocampal neurons is also directly affected by CAST. Overexpression of GFP-CAST1 causes a robust increase in bassoon positive synapses (98 ± 0.8% vs. 80 ± 2.8% in control neurons; Figure 5.8D and data not shown), while simultaneous knockdown of CAST1 and CAST2 leads to a significant decrease of presynaptic bassoon (60 ± 2.7%; data not shown). These results demonstrate that, while neither manipulation of liprin-α1 or CAST completely ablated the presynaptic staining of bassoon, both proteins are important for proper bassoon levels at presynaptic boutons.

5.3. Discussion

In this study, we demonstrate that liprin-α family proteins are key regulators of presynaptic protein composition and SV recycling at mature synapses. These findings are in line with genetic studies in *C. elegans*, where liprin-α/SYD-2 is one of the first proteins to arrive at a nascent synapse and is necessary for the subsequent recruitment of other AZ proteins during presynaptic development[87, 88]. Interestingly, mammalian liprin-α family proteins differentially regulate presynaptic protein composition and SV recycling. We propose that liprin-α proteins are key parts of the presynaptic targeting machinery which differentially organizes presynaptic structures along the axon.

5.3.1 Liprin-α2 is a molecular organizer of hippocampal presynapses

Numerous studies have established that the strength of synaptic connections between neurons is critically dependent on the orderly assembly of a vast number of presynaptic components[62, 144]. Studies in invertebrates suggest that liprin-α/dliprin-α/SYD-2 proteins play a role in these processes, however, due to the complexity of the vertebrate liprin-α family, previous knowledge of the presynaptic role of liprin-α was limited to observance of its presynaptic localization by electron microscopy[94] and understanding of its ability to bind to many AZ proteins[53, 58].

Here, we show that liprin-α2 is an important regulator of presynaptic com-

position in mature hippocampal synapses. First, liprin-α2 is localized at presynaptic boutons even in the absence of other major components of the AZ, including the large structural proteins bassoon and piccolo. These data are consistent with liprin-α being an upstream regulator of other presynaptic proteins[104, 151] and suggest that liprin-α2 targets to presynaptic terminals independently of piccolo-bassoon transport vesicles (PTVs)[158]. Second, liprin-α2 interacts with many presynaptic proteins, including several potentially novel liprin-α binding partners (Table 5.1). Third, liprin-α2 is responsible for the targeting of the presynaptic scaffolding proteins CASK and RIM, both of which were notably decreased in liprin-α2 deficient synapses. Fourth, CASK, in particular, is strongly recruited to boutons by liprin-α2, dependent on a 37-amino acid linker region between the first and second SAM domains of liprin-α2 which is spliced out in liprin-α1[80] and absent from SYD-2, which likely explains why liprin-α/SYD-2 had no effect on the synaptic localization of the *C. elegans* CASK homolog lin-2[88].

   In the absence of liprin-α2, SV exocytosis is markedly impaired, while the selective addition of liprin-α2 to neurons increased the rate of SV release. This is, in part, due to a decrease in the total releasable pool of vesicles in synapses lacking liprin-α2, similar to that which is seen in *Drosophila* dliprin-α mutants[129]. Further echoing the phenotypes of invertebrate liprin-α mutants[86, 89], loss of liprin-α2 disrupts the ability of the neuron to release SVs in response to chemical stimulation. This effect is likely explained by the depletion of both CASK and RIM at liprin-α2 deficient synapses. Both CASK and RIM have been shown to regulate cycling of SVs[53, 159]. CASK interacts with core presynaptic machinery such as neurexins, synCAM, and voltage-gated calcium channels[151, 159, 160], and is a part of the CASK/mint/MALS complex that regulates presynaptic munc18 levels[150] and SV cycling and release[104, 149, 150], and RIM binds to rab3, synaptotagmin, and munc13 and links SVs to the SV release machinery[99, 161, 162]. Consistent with the high levels of liprin-α2 protein found at presynaptic terminals *in vivo*, mossy fiber LTP in the hippocampus is abolished in mice lacking RIM1[162]. We propose a model in which liprin-α2 coordinates the targeting of RIM and CASK-complex to mature synapses, thereby regulating RIM- and CASK-dependent SV recycling (Figure 5.10). Additional studies are required to determine the factor(s) upstream of liprin-α2 which restrict AZ assembly to appropriate locations.

5.3.2 Liprin-α1 negatively regulates SV recycling

We found low liprin-α1 levels throughout the brain and in hippocampal cultures.
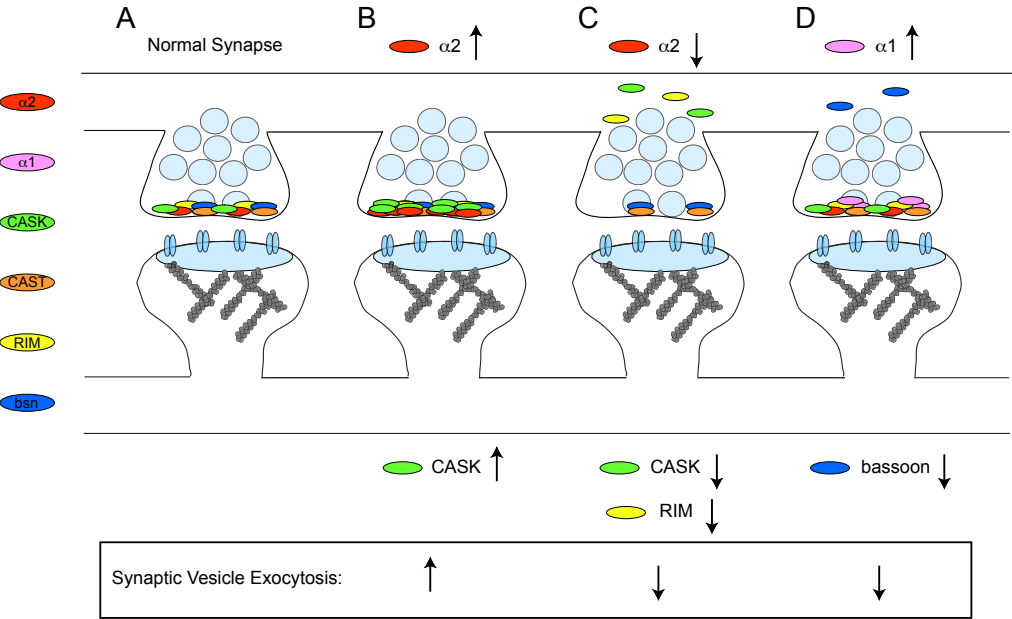
Figure 5.10. *Model of liprin-α mediated composition of presynapses.*
Schematic representation of a glutamatergic synapse. Glutamate is present within synaptic vesicles (SVs, light blue) at the presynaptic terminals. Fusion of SVs with the plasma membrane at the active zone (AZ) releases glutamate which results in activation of several different types of glutamate receptors (blue) anchored at the postsynaptic density (PSD, light blue) in the postsynaptic terminal. The actin filaments within the postsynaptic spines are shown (grey). Several families of structural and scaffolding proteins have been identified within AZs, including piccolo, bassoon, RIM, CAST1/2, CASK, and liprin-α. The diagram demonstrates the molecular and cellular changes at a presynaptic terminal regulated by liprin-α family proteins.
(A) The scaffolding proteins liprin-α2 (red), CASK (green), CAST1/2 (orange), RIM (yellow), and bassoon (blue) are represented by colored discs.
(B) Increased amounts of liprin-α2 (red) at a presynaptic bouton result in an increase in CASK (green) at that same bouton and, consequently, an increase in SV exocytosis.
(C) Depletion of liprin-α2 (red) from a presynaptic bouton results in a loss of both CASK (green) and RIM (yellow) from that same bouton and, consequently, a decrease in SV exocytosis.
(D) Increased amounts of liprin-α1 (pink) at a presynaptic bouton result in the loss of bassoon (blue) from that same bouton due to competition for binding to CAST1/2 (orange) and, consequently, a decrease in SV exocytosis.

These data are consistent with previous data showing that liprin-α1 is present in low levels at active synapses due to degradation by active CaMKII and in response to neuronal activity[108], which is important at the postsynapse for proper LAR targeting and dendrite development[108]. In *Drosophila*, dliprin-α levels, and through that, synapse size are regulated by the ubiquitin-proteasome system (UPS) via the anaphase promoting complex (APC)[130]. In hippocampal neurons, liprin-α1 is also degraded by the APC complex[108]. Here, we found substantial synapse-to-synapse variation in liprin-α1 stain-

ing, with single synapses that contained high levels of endogenous liprin-α1 showing decreased amounts of the AZ protein bassoon. Furthermore, overexpression of exogenous liprin-α1 eliminated both bassoon and its homolog piccolo from presynapses. This is most likely due to the selective competition of bassoon and piccolo with liprin-α1 for binding to CAST. Surprisingly, in spite of the fact that all four liprin-α proteins possess the ability to interact with CAST *in vitro*[97], in live cells expressing full length proteins, liprin-α1 displayed a significantly higher binding affinity for CAST than liprin-α2 and only liprin-α1 interfered with the localization of bassoon. These cellular experiments imply that the specificity of CAST binding relies on some unique feature within full length liprin-α1. Additional studies are needed to determine whether structural properties, post-translational modifications or additional cellular factors specify CAST/liprin-α interactions[163].

FRAP experiments revealed that high liprin-α1 levels prevent Bassoon targeting to CAST positive membrane structures. In the presence of liprin-α1, SV exocytosis is strongly impaired, likely because of the depletion of bassoon and piccolo from presynaptic terminals, since both bassoon[147] and piccolo[148] have been shown to regulate SV exocytosis. Together these data demonstrate that liprin-α1 levels are highly regulated and increased levels of liprin-α1 inhibit the targeting of bassoon and piccolo to mature synapses, thereby negatively regulating SV release (Figure 5.10). It is tempting to speculate that single synapses, by altering liprin-α1 levels, can switch between more or less active states. Local upregulation of liprin-α1, for example due to decreased neuronal activity[108], may result in the redistribution of bassoon[69] and therefore cause the synapse to lapse into a silent, nonfunctional state or even be eliminated, while leaving neighboring synapses unaffected[164]. This mechanism allows activity dependent fine-tuning of synaptic connectivity at a single synapse level by controlling the turnover of liprin-α1 proteins.

5.3.3 Liprin-α family proteins are not functionally redundant

Adhesion proteins and components assembled at synapses often have a high degree of functional redundancy[165, 166]. Interestingly, we found this not to be the case for liprin-α family proteins. Although all four liprin-α proteins are highly homologous (~70% amino acid identity)[79], especially within their protein binding domains, they each displayed distinct expression patterns in the brain and subcellular staining in cultured hippocampal neurons. It seems that short but unique amino acid regions within liprin-

α family proteins, such as the PEST domain in liprin-α1[108] and the short linker region in the SAM domains of liprin-α2, convey profound differences in liprin-α function at synapses. While some redundancy within the liprin-α family most likely occurs, it is clear that, at least, liprin-α1 and liprin-α2 have distinct synaptic functions.

The core components that carry out SV recycling at the AZ are present at all presynapses. However, AZs of different sizes and shapes have evolved to achieve the diverse physiological tasks of different neurons. We propose that liprin-α family proteins differentially organize the molecular composition of presynaptic terminals in order to locally regulate SV recycling along axons. In our model, liprin-α family proteins may dictate specificity, types, and strength of neuronal connections, which ultimately determine the functional properties of neural circuits.

ACKNOWLEDGMENTS

Chapter 6

Materials and Methods

6.1. Antibodies and Reagents

Rabbit anti-liprin-α "1069"[94], rabbit anti-p140Cap[114], mouse anti-CASK[167], rabbit anti-GRIP "1756"[134], rabbit anti-BICD2 "2293"[168] and guinea pig and mouse anti-PSD95[169] were previously described. The following antibodies were obtained from commercial sources: mouse anti-α-tubulin, mouse anti-synaptophysin and mouse anti-CaMKIIα (Sigma), mouse anti-CaMKIIβ (Zymed), mouse anti-β-catenin (BD Transduction Laboratories), mouse anti-GluR2 (Chemicon), mouse anti-bassoon (StressGen Biotechnologies), rabbit anti-calreticulin (Affinity BioReagents), mouse anti-CD8 (Covance), mouse anti-β-galactosidase (Promega), rabbit anti-cortactin, rabbit anti-HA, rabbit anti-cortactin, mouse anti-myc, and mouse-anti-CD8 (Santa Cruz), mouse anti-VAMP2 and rabbit anti-piccolo (Synaptic Systems), guinea pig anti-vGluT1 (Millipore), rabbit anti-GFP (Medical and Biological Laboratories), mouse anti-GFP (Quantum), rabbit anti-GFP (Abcam), Alexa488- and Alexa568- conjugated secondary antibodies (Molecular Probes) and CY5-conjugated secondary (Jackson ImmunoResearch Labs). Rabbit polyclonal liprin-α, LAR, and pan-CAST antibodies were made against GST-fusion proteins containing the following sequences: amino acids 480-614 of liprin-α1 (accession no. NM_177423.1), 498-635 of liprin-α2 (NM_003625.2), 187-286 of liprin-α3 (NM_003660.2), 461-564 of liprin-α4 (EF428334), 1294-1880 of LAR (Y00815), 118-580 of CAST1 ("GZT7") (AY049038); and affinity-purified on CN-Br-activated Sepharose columns coupled to His-fusion proteins containing the same sequences and tested by Western blotting and immunofluorescence using HeLa cells expressing individual GFP-tagged constructs. Rabbit polyclonal CAST2 antibody was a generous gift from Drs. Katarzyna Chmielarska and Frauke Melchior.

Antibodies were diluted for experimental use as follows: rabbit anti-liprin-α1 (WB-3μg/ml; ICC-1:50; IHC-1:500-1:5000), rabbit anti-liprin-α2 (WB-2μg/ml; ICC-1:250; IHC-1:500-1:5000), rabbit anti-liprin-α3 (WB-2μg/ml; ICC-1:100; IHC-1:500-1:5000), rabbit anti-liprin-α4 (WB-2μg/ml; ICC-1:100; IHC-1:500-1:5000), rabbit anti-pan-CAST/ERC "GZT7" (ICC-1:150), rabbit anti-liprin-α "1069" (WB-1:1000; ICC-1:100), rabbit anti-LAR (ICC-1:100), rabbit anti-p140Cap (ICC-1:500), mouse anti-CD8 (Covance, ICC-1:300), mouse anti-CD8 (Santa Cruz, ICC-1:50), rabbit anti-cortactin (WB-1:1000, ICC-1:500), mouse anti-CASK (WB-1:1000, ICC-1:200), guinea pig anti-PSD95 (ICC-1:800), rabbit-anti-GFP (WB-1:5000), mouse anti-α-tubulin (WB-1:10,000), mouse anti-CaMKIIα (WB-1:5000), mouse anti-bassoon

(ICC-1:500), mouse anti-VAMP2 (ICC-1:1000), rabbit anti-piccolo (ICC-1:200), mouse-anti-synaptophysin (IHC-1:500), guinea pig anti-VGluT1 (IHC-1:2000), rabbit anti-CAST2 (WB-1:2500; ICC-1:300), mouse anti-PSD95 (WB-1:2000).

Reagents used include MG132, lactacystin, KN92, KN93 (Calbiochem), TTX, bicuculline, calpain inhibitor I and II (ALLN, ALLM) (Sigma).

6.2. DNA Constructs

The following mammalian expression plasmids have been described: myc-liprin-α1, myc-liprin-α2, HA-liprin-β1[94], FLAG-CaMKIIα constructs[132], myc-PSD-95[169], GRIP1-HA[134], pSuper vector[170], pSuper-Cdh1-shRNA[131], pSuper-LAR-shRNA, myr-HA-LAR-D2[96], p140Cap[114] and CaMKIIβ constructs[124].

To generate GW1-GFP, GFP was ligated in the HindIII and AscI sites in a modified GW1 vector (British Biotechnology). GFP-liprin-α1 and HA-liprin-α1 were generated by cloning human liprin-α1 (U22816) cDNA in frame with N-terminal GFP or HA epitope tag (YPYDVPDYA). Deletion mutants of liprin-α1 were cloned by PCR. Mutating the CaMKII phosphorylation sites in liprin-α1 was done by site-directed mutagenesis leading to the exchange of Ser$^{1139/1168/1194/1201}$ to Ala$^{1139/1168/1194/1201}$. To generate doxycycline inducible CaMKII expression constructs, CaMKII was cloned in the pTRE vector (Clontech). pTETon containing the reverse tetracycline-controlled transcription activator (pTETon-rtTA, Clontech) was used to regulate transcription of pTRE-CamKII plasmids. CD8-LAR-C and CD8-LAR-CΔD2 were generated by PCR cloning the intracellular C-terminal tail with and without the D2 domain of human LAR in frame with the extracellular and transmembrane domain of CD8[134]. All cDNAs were subcloned in pGW1 or pβactin expression vectors for optimal neuronal expression[108]. Liprin-α3 constructs were generated by PCR from full length human cDNA sequences (IMAGE:8069024) and liprin-α4 constructs was assembled from three overlapping cDNAs; IMAGE:51967495 (aa 1-1930), IMAGE 1539820 (aa 1931-2382), and KIAA0897 (aa 2383-3555). The three segments of liprin-α4 were then cloned into pGW1, and the full length construct digested with AscI and BamHI and inserted into pGW1-GFP digested with AscI and BglII. The IMAGE cDNA clones were purchased from Geneservice. Bio-GFP-liprin-α constructs were generated by PCR subcloning liprin-α cDNA into a modified pEGFP-C2 vector containing the biotin tag (MASGLNDIFEAQKIEWHEGGG) upstream of GFP. GFP-liprin-α1L was cloned by creating an AgeI site at amino acid 955 of liprin-α1 by PCR and replacing

amino acid 955-1008 of liprin-α1 with amino acid 1029-1118 of liprin-α2. For the in vitro competition assay, CAST1 (aa 118-580) was PCR cloned into pGW1-GFP. GST- and His-fusion constructs for antibody production (see above) and competition assay were cloned into pGEX-4T (Pharmacia) and pET-32A (Novagen), respectively. Liprin-α1, CAST1, and bassoon fragments were amplified by PCR; liprin-α1 (aa 351-673), CAST1 (aa 118-580), bassoon (aa 2933-2995). All pSuper-shRNA sequences are in Table 6.1. The complementary oligonucleotides were annealed and inserted into pSuper vector[170].

GFP-bassoon 95-3938 was a gift from Dr. Eckart Gundelfinger[171]. CAST1 and CAST2 constructs were a gift from Dr. Toshihisa Ohtsuka[155, 157].

6.3. Biochemical Analysis

6.3.1 Heterologous cell transfection and immunoprecipitation

HeLa and HEK293 cells were cultured in DMEM/HAMF10 (50/50%) medium containing 10% FCS and 1% penicillin/streptomycin. For biochemistry, HeLa or HEK293 cells were plated at 1:15 or 1:5, respectively, in 10 cm dishes two days before transfection. Cells were transfected with Lipofectamine 2000 (Invitrogen) and grown for 24 hours after transfection. Cells were harvested in 1x PBS and lysed in PBS + 1% Triton X-100 (for Western blot) or 25mM Tris/50mM NaCl/0.5% Triton X-100 (for immunoprecipitation). IPs were performed using 3 μg of GFP antibody (Roche) conjugated to Protein A Sepharose beads (Sigma), incubated for 4 hours at 4ºC, and washed three times in lysis buffer. Proteins were eluted by boiling in 4x sample buffer and analysed by Western blotting.

6.3.2 Brain extracts and fractionations, immunoprecipitations, pull-downs, and mass spectrometry

For analysis of liprin protein expression in different brain regions, brains were obtained from adult female rats and dissected into appropriate regions as defined anatomically. The regions were homogenized in 10x volume/weight 20mM Tris/150mM NaCl/1% Triton X-100 (pH 7.4) and spun for 5 minutes at 13,200 rpm at 4ºC. The supernatant was collected and protein concentration was measured using a bicinchoninic acid (BCA) assay (Pierce). Equal amounts of protein were used for Western blotting (10 μg for liprin-α2, liprin-α3, and α-tubulin; 100 μg for liprin-α1 and liprin-α4).

Protein	shRNA sequence	Species	Effectiveness	Reference
LAR				
#1 *	gaaagtcagctcccagcgc	rat	++	96
p140Cap				
#1 *	cagccgaaacagacttcag	rat	++	114
CaMKIIα				
#1 *	gtaccagctcttcgaggaa	rat	++	108
CaMKIIβ				
#1 *	ccatgagtatgcagctaag	rat	++	108
APC2				
#1 *	gaaggtccgagaccagcag	rat	++	108
#2 *	ccgaatgtttgtaatgact	rat	++	108
liprin-α1				
#1 *	tctgtgcatgacctcaatg	rat/mouse/human	++	OligoEngine
#2	tgaccaagaaagaccttcg	rat/human	+	OligoEngine
liprin-α2				
#1	agaccgcttagcagctctt	rat	+	OligoEngine
#2	agccagtctgattacagaa	rat/mouse/human	++	OligoEngine
#3 *	gcatgaacttcttgaagaa	rat/mouse/human	++	OligoEngine
#4	gaaacaacacaagactgtt	rat/mouse	+	OligoEngine
CASK				
#1 *	gcactgaatcacccatggc	rat/mouse/human	++	OligoEngine
#2	aacggaactgcaggtctca	rat	++	OligoEngine
#3	ggtcctgagaactgcagag	rat/human	+	OligoEngine
CAST1/ERC2				
#1 *	catcaacaacttacccaaa	rat/mouse	++	siRNA at Whitehead
#2	cctttcatatacggatcaa	rat	+	siRNA at Whitehead
#3	gagatagaatcctttcgaa	rat/mouse	+	siRNA at Whitehead
CAST2/ERC1				
#1 *	atgctgcctatgctacatc	rat/mouse	++	siRNA at Whitehead
RIM1				
#1	cctcaagttgagattattg	rat	++	siRNA at Whitehead
#2 *	agtccagacggtaaagttc	rat/mouse/human	++	siRNA at Whitehead
bassoon				
#1	gccagagagcaacttctccaa	rat	+	based on h-TRC library
#2	cctaacgccttcctctgacat	rat	+	based on h-TRC library
bassoon16*	aacacctgcacccagtgtcac	rat/mouse/human	++	149
piccolo				
#1	ggtcagagcagaagctgcc	rat/mouse	+	based on h-TRC library
#2	agcaaggacaagtgaagga	rat	+	based on h-TRC library
piccolo28	aagtgctgtctcctctgttgt	rat/mouse	++	149

For immuoprecipitations of endogenous proteins from brain extracts, sodium deoxycholate extracts of rat cortex or transfected COS-7 cells were immunoprecipitated with non-immune rabbit immunoglobulins (IgG) or with antibodies to liprin-α[94] and CaMKII (Sigma) as previously described[94]. Precipitated proteins were analyzed on Western blot.

For biotin-streptavidin pull-down experiments, brains were harvested from adult female rats and P2 fractions were isolated as described[172] and extracted with 1% Sodium Deoxycholate (DOC) in 500mM Tris (pH 9.0) by incubation for 30 minutes at 36ºC. Extracts were dialyzed overnight into a 50mM Tris (pH 7.4)/0.1% Triton X-100 solution and spun down at 13,200 rpm for 40 minutes. The resulting supernatant is referred to as the P2/DOC extract. Streptavidin pull down experiments and mass spectrometry were performed as described[156], with the following modifications. Following pull down, beads were washed alternately with high and low salt washings and incubated with a P2/DOC fraction for two hours at 4ºC. Beads were washed with low salt buffer and retained for analysis on a 4-12% Bis-Tris gel (Invitrogen). The gel was stained with the Colloidal Blue Staining Kit (Invitrogen). Mass spectrometry was performed as described[156].

PSD preparations were performed as follows. Cytosol, synaptosome, synaptosomal membrane and PSD fractions from cultured hippocampal neurons were prepared using a small-scale modification of the procedure described[173, 174]. In brief, six 10 cm dishes containing 10^6 hippocampal neurons were grown for 3 weeks and scraped into 500 µl of HEPES-buffered sucrose (0.32 M sucrose, 4 mM HEPES pH7.4), homogenized with a motor driven glass-teflon homogenizer at 900 rpm (10-15 strokes) and centrifuged at 800-1000 x g 10 min at 4ºC results to yield the nuclear fraction (P1). Supernatant (S1) was centrifuged at 10,000 x g for 15 min to yield the crude synaptosomal pellet (P2) and washed 1x in 1 ml HEPES buffered sucrose. P2 was lysed by hypoosmotic shock in 1 ml ice cold 4 mM HEPES, pH 7.4, homogenized by an Eppendorf homogenizer and mixed for 30 min at 4ºC. The lysate was centrifuged at 25,000 x g for 20 min to yield supernatant (S3, crude synaptic vesicle fraction) and pellet (P3, lysed synaptosomal membrane fraction). To prepare the PSD fraction, P3

Table 6.1. *pSuper-shRNA sequences used in the study.*
This table shows the pSuper-shRNA sequences that showed significant knock-down of the indicated target protein. The asterisk denotes the sequence that was determined to be most effective and used in the experiments described. siRNA at Whitehead refers to the website: jura.wi.mit.edu/bioc/siRNAext/, h-TRC library refers to the human Sigma-Aldrich TRC shRNA libraries (MISSION libraries) and OligoEngine refers to the website:www.oligoengine.com

was resuspended in 500 ul of ice cold 50 mM HEPES, pH 7.4, 2 mM EDTA, plus complete inhibitors and 0.5% Triton X-100, rotated for 15 min at 4ºC and centrifuged at 32,000 x g for 20 min to obtain the PSD-1 pellet. Pellets were resuspended in 100 ul ice-cold 50 mM HEPES pH7.4, 2 mM EDTA plus complete inhibitors.

For Western blotting, protein samples were diluted with 4x Sample Buffer (8% SDS/25% Glycerol/0.05M Tris pH 6.8/200mM DTT/Bromophenol Blue/H_2O) and loaded onto 8% SDS-PAGE gels and subjected to Western blotting. Blots were blocked with 2% Bovine Serum Albumin/0.005% Tween20/PBS and incubated with the appropriate antibody overnight at 4ºC. Blots were washed with 0.05% Tween20/ PBS 3 times for 5 minutes at room temperature and incubated with either anti-rabbit or anti-mouse IgG antibody conjugated to HorseRadish Peroxidase (Dako). Blots were developed with Enhanced Chemiluminescent Western Blotting Substrate (Pierce).

6.3.3 *In vitro* competition assay

GST-bassoon (aa 2933-2995) and His-liprin-α1 (aa 351-673) constructs were trans-formed into BL21 and Rosetta *E.coli*, respectively, and grown to an OD_{600} of 0.6. Pro-tein expression was induced with 0.5mM IPTG (Sigma) and proteins were purified us-ing Glutathione Sepharose 4B (GST, Amersham) or Nickel-NTA (His, Qiagen) beads. GFP-CAST1/ERC2(118-580) was transfected into HEK293 cells using Lipofectamine 2000, expressed for one day, and lysed in 10mM HEPES/150mM NaCl/1% NP40 (pH 7.4). HEK293 cell lysates were incubated with Glutathione Sepharose 4B beads conjugated to GST alone (control) or GST-bassoon in the presence of either no liprin or 1:1, 1:10, or 1:100 concentration ratios of bassoon protein to liprin-α1 protein, as determined by Coomassie staining of protein products run on a 10% SDS-PAGE gel, for 1 hour at 4ºC. Samples were washed three times in lysis buffer, supplemented with 4x Sample Buffer, run on a 10% SDS-PAGE gel and Western blotted for GFP.

6.4. Heterologous Cell Culture, Transfection, and Immunocytochemsitry

HeLa and COS-7 cells were cultured in DMEM/HAMF10 (50/50%) medium con-taining 10% FCS and 1% penicillin/streptomycin. For immunocytochemistry, HeLa and COS-7 cells were plated at 1:50 in Lab-Tek chamber slides (Nunc) the day be-fore transfection. Cells were transfected with SuperFect (Qiagen) according to the

manufacturer's protocol and grown for 24 hours after transfection. Cells were serum-stimulated with fresh medium two hours prior to fixation. Cells were fixed in 4% paraformaldehyde (10 minutes at room temperature), followed by 5 minutes in 0.1% Triton X-100/PBS. Slides were blocked in 0.5% BSA/0.02% glycine/PBS and labeled with primary antibody for 2 hours at room temperature. After washing with 0.05% Tween-20/PBS, sections were incubated with secondary antibody for 1 hour at room temperature. Slides were mounted using Vectashield mounting medium (Vector Laboratories). All signals were captured with a Leica DMRBE fluorescence microscope equipped with a Hamamatsu Orca camera.

6.5. Primary Hippocampal Neuron Culture, Transfection, and Immunocyto-chemistry

Primary hippocampal cultures were prepared from embryonic day 19 (E19) rat brains. Neurons were plated on coverslips coated with poly-L-lysine (37.5 μg/ml) and laminin (2.5 μg/ml) at a density of 75,000/well. Hippocampal cultures were grown in Neuro-basal medium (Invitrogen) supplemented with B27 (Invitrogen), 0.5 mM glutamine, 12.5 μM glutamate, and penicillin/streptomycin mix.

Neurons were transfected with various DNA constructs using lipofectamine 2000 (L2K) (Invitrogen). Per well of a 12-well culture plate, 1.8 μg of DNA was added to 100 μl of Neurobasal medium (NB) and mixed with 3.3 μl of L2K which was diluted in 100 μl of NB. During the incubation period, the coverslips containing the neurons are transferred from the original plate into a plate containing the incubation medium (NB supplemented with 0.5 mM glutamine). After 30 minute incubation at room temperature, the DNA/L2K mixture was applied dropwise to the culture well containing 1 ml of incubation medium at 37°C in 5% CO_2 for 45 min. Next, the coverslips are rinsed by swirling in NB and returned to the original medium at 37°C in 5% CO_2 for 2-4 days.

For immunocytochemistry, cultured hippocampal neurons were fixed either with 4% paraformaldehyde and 4% sucrose in PBS for 10 minutes at room temperature or with ice-cold 100% methanol + 1mM EGTA for 10 minutes at -20ºC, washed three times with PBS for 5 minutes at room temperature and incubated with primary antibodies in GDB buffer (0.2% gelatin, 0.8 M NaCl, 0.5% Triton X-100, 30 mM phosphate buffer, pH 7.4) overnight at 4°C. Cells were then washed three times in PBS for 5 minutes at room temperature. Secondary antibodies were applied in GDB for 1

hour at room temperature and washed three times in PBS for 5 min. Secondary anti-bodies conjugated to Alexa488 and Alexa568 were used for double labeling. Slides were mounted using Vectashield mounting medium (Vector Laboratories). Confocal images were acquired using a LSM510 confocal microscope (Zeiss) with either 10x or 20x air objective, or 40x or 63x oil objective.

For surface staining, live cells were incubated with CD8 N-terminal antibod-ies (10 µg/ml) at 37°C for 15 min. After washing in DMEM medium (Invitrogen), the cells were fixed for 5 minutes with 4% formaldehyde/4% sucrose in PBS. The primary antibodies were detected by Alexa488or Alexa568 secondary antibodies in GDB buf-fer without TritonX-100.

6.6. Immunohistochemistry on Brain Sections

For immunohistochemistry mice were anesthetized with pentobarbital and perfused transcardially with 4% paraformaldehyde. The brain was carefully dissected out, in-cubated overnight in 30% sucrose for cryoprotection, and sectioned at 40µm with a freezing microtome. Sections were processed free floating, employing a standard avidinbiotin-immunoperoxidase complex method (ABC, Vector Laboratories) with diaminobenzidine (0.05%) as the chromogen. The specific liprin antibodies were di-luted at various concentration (1:1000 to 1:5000) in Tris buffered saline (TBS, pH7.6) containing 1% normal horse serum and 0.2% Triton X-100. For avidin–biotin–peroxi-dase immunocytochemistry, biotinylated secondary antibodies (Vector Laboratories) diluted 1:200 were used. FITC-, cyanine 3 (Cy3)-, and Cy5-conjugated secondary antibodies raised in donkey (Jackson ImmunoResearch) diluted 1:200 were used for immunofluorescence. Sections were analyzed and photographed using a Leica DM-RB microscope and a Leica DC300 digital camera. Sections stained for immunofluo-rescence were analyzed with a Zeiss LSM 510 confocal laser-scanning microscope.

6.7. Image Analysis and Quantification

6.7.1 Experiments described in chapter 3
Confocal images of transfected neurons were obtained with sequential acquisition set-tings at the maximal resolution of the microscope (1024 x 1024 pixels) using a Zeiss LSM510 confocal microscope, 20x (for morphology) or 63x (for fluorescence) objec-

tive with digital zoom 1. Each image was a z-series of 10-12 images each averaged 2 times that was chosen to cover the entire region of interest from top to bottom. The resulting z-stack was 'flattened' into a single image using maximum projection. Images were not processed further and were of similar high quality to the original single planes. The confocal settings were kept the same for all scans when fluorescence intensity was compared. Morphometric analysis, quantification and colocalization were performed using MetaMorph software (Universal Imaging Corporation). Acquisition of images as well as morphometric quantification were performed under "blinded" conditions. Statistical analysis was performed with student's t-test assuming a two-tailed and unequal variation. N was defined as the number of transfected neurons.

Quantification of fluorescence intensity. Confocal images of hippocampal neurons surface labeled with CD8 and stained for endogenous proteins were analyzed using MetaMorph software. Fluorescence intensities were measured using confocal images taken with identical laser power and microscope settings and normalized to nontransfected neurons in the same field. CD8 clusters were identified around the cell body and a region was drawn around the outside of the cluster.

Quantification of axon morphology. Confocal images of hippocampal neurons transfected with various expression constructs and filled with either GFP or β-galactosidase were analyzed using MetaMorph software. Axon length measurements were obtained by tracing the entire length of axon visible in the field of view and averaging per neuron. Axon branching was determined by counting the number of branching points per axon of an individual neuron.

6.7.2 Experiments described in chapter 4

Confocal images of transfected COS-7 and HeLa cells were acquired with 10x objective with 0.3x electronic zoom, resulting in an image with an established area (1302 μm x 1302 μm) for every experiment. Quantification of the number of expressing cells per area was performed using MetaMorph software (Universal Imaging Corporation). Confocal images of transfected neurons were obtained with sequential acquisition settings at the maximal resolution of the microscope (1024 x 1024 pixels). Each image was a z-series of 6-10 images each averaged 2 times. The resulting z-stack was 'flattened' into a single image using maximum projection. The confocal settings were kept the same for all scans when fluorescence intensity was compared. Morphometric analysis and quantification were performed using MetaMorph software. Quantifica-

tion of the number of dendritic tips, primary dendrites, total dendrite length and Sholl analysis was done with images acquired with 40x objective and 0.7x electronic zoom. For dendrite length all dendrites of a single neuron were traced in MetaMorph and the number of pixels was automatically converted to μm. For Sholl analysis concentric circles with 15 μm differences in diameter were drawn around the cell body, and the number of dendrites crossing each circle was manually counted. For the protrusion and spine measurements, the number, length and width of protrusions and spines from 3-5 dendritic segments per neuron were traced in MetaMorph. For the quantification of antibody staining, images were acquired with use of a 63x objective with 0.7x electronic zoom and the number of clusters per length and average intensity of signals in the cell body, dendrites and Golgi region, by costaining with a Golgi marker, were measured in MetaMorph. The dendrites of GFP expressing neurons were identified based on their morphology and by immunostaining for the dendritic marker MAP2. Acquisition of images as well as morphometric quantification were performed under "blinded" conditions. Statistical analysis was performed with student's t test assuming a two-tailed and unequal variation. N was defined as the number of transfected neurons.

6.7.3 Experiments described in chapter 5

Confocal images of transfected neurons were obtained with sequential acquisition settings at the maximal resolution of the microscope (1024 x 1024 pixels) using a Zeiss LSM510 confocal microscope, 63x objective with digital zoom 1. Each image was a z-series of 10-12 images each averaged 2 times that was chosen to cover the entire region of interest from top to bottom. The resulting z-stack was 'flattened' into a single image using maximum projection. Images were not processed further and were of similar high quality to the original single planes. The confocal settings were kept the same for all scans when fluorescence intensity was compared. Morphometric analysis, quantification and colocalization were performed using MetaMorph software (Universal Imaging Corporation).

Quantification of synaptic targeting at presynaptic boutons. For analysis of presynaptic boutons we used GFP as an unbiased cell-fill. Because axons often crossed several z planes, we took series stacks from the bottom to the top of all axons and used the LSM software to generate image projections for quantitative analyses. Presynaptic boutons were morphologically identified as swellings along GFP labeled axon segments as

described[148, 175]. Hippocampal neurons were transfected with a plasmid encoding GFP at DIV15 and stained after four days with antibodies for several presynaptic proteins. As shown in Figure 2A, GFP-positive axon segments exhibit axonal varicosities that reliably colocalized with presynaptic marker VAMP2. Quantification demonstrated that ~80% of these swellings were positive for endogenous presynaptic proteins (Fig. 2A,B,C) and loaded with FM4-64 (Fig. 3D). To control for background and "false positive" colocalization at presynaptic boutons, we rotated the red-channel image of the VAMP2 staining by 90° and 180° (Fig. 2A) and found that ~20% of synaptic staining at axonal swelling is due to coincidental crossing or overlap of non-transfected axons in the culture (Fig. 2A,B). For quantitative analysis of synaptic targeting, twenty GFP-positive presynaptic boutons were "blindly" selected from each confocal image and quantified for presence or absence of synaptic protein staining. All results were verified in at least two independent experiments with an n>5 for individual experiments. Statistical analysis was performed with Student's t-test assuming two-tailed distribution and unequal variation. n was defined as the number of transfected cells.

Quantification of fluorescent intensity. Confocal images of hippocampal neurons filled with GFP and labeled for endogenous synaptic proteins were analyzed using Meta-Morph software. Fluorescence intensities were measured using confocal images taken with identical laser power and microscope settings and normalized to nontransfected neurons in the same field. Synaptic boutons were identified either morphologically in transfected neurons or by colabeling with synaptic markers in nontransfected neurons.

Colocalization of fluorescent signals. Colocalization of two fluorescent signals was determined by thresholding the bassoon (red) channel image and creating regions around the thresholded objects in MetaMorph. Those regions were then transferred onto the second (liprin-α, green) channel image and quantified for presence or absence of labeling with the second antibody. Statistical analysis was performed with Student's t test assuming two-tailed distribution and unequal variation. n was defined as the number of images.

Live cell image acquisition and FM4-64 loading and quantification. Time-lapse live cell imaging was performed on a Nikon Eclipse TE2000E microscope with Coolsnap and QuantEM cameras (Roper Scientific). Neurons were maintained at 37ºC with 5% CO_2 (Tokai Hit). FRAP experiments were performed using the scanning head 3 FRAP L5 D – CURIE (Curie Institute) as described[176]. For SV exocytosis experiments, transfected neurons were loaded with 10 μM FM4-64FX (Invitrogen) as described[152] and

areas containing transfected axons were selected. One image of the FM4-64-loaded synapses was taken prior to the second stimulation, and images were taken at an interval of ~7 seconds for 2 minutes immediately following the second stimulation.

Measurements of FM4-64 recycling at presynaptic boutons were performed as described[177]. Synapses from >5 neurons per experiment were identified in MetaMorph by morphology and overlaid onto the FM4-64 images for quantification of fluorescence intensity using MetaMorph software. The intensity of all points following unloading was normalized to the intensity of that synapse prior to unloading. Separate experiments were adjusted to control to allow for comparison and analyzed in a blind manner. Statistical significance was measured by ANOVA repeated measurements in SPSS 16.0 (SPSS, Inc.).

6.8. Electrophysiology

For electrophysiology, isolated hippocampal neurons were plated on astrocyte microislands[181]. Astrocytes and hippocampal neurons were prepared as described previously[182]. Only islands containing single neurons were examined 5-7 days after infection with Lentiviral vectors at DIV14-17.

Whole cell voltage-clamp (Vm=-70mV) recordings were acquired with an Axopatch 200A amplifier, Digidata 1322A and Clampex 9.0 software. The intracellular pipette solution contained (in mM): 125 K^+-gluconate, 10 NaCl, 4.6 $MgCl_2$, 4 K_2-ATP, 1 EGTA, 15 Creatine Phosphate, 20 U/ml phosphocreatine kinase (pH 7.30, 300 mOsm). The external medium contained (in mM): 140 NaCl, 2.4 KCl, 4 CaCl2, 4 MgCl2, 10 HEPES, 10 glucose (pH 7.30; 300 mOsm). Hypertonic sucrose (500mM) was applied using a fast barrel application system (Perfusion Fast-Step, Warner Instruments) to assess RRP size. Pvr was calculated as the response to a single stimulus divided by the response to hypertonic sucrose. All recordings were performed at room temperature. Custom made matlab routines and Minianalysis software was used for offline analysis.

Chapter 7

Discussion

In this thesis we investigated the role of liprin-α proteins in neuronal development and synapse function using primary hippocampal neuron cultures. By examining the expression patterns of the four liprin-α proteins in the brain using specific polyclonal antibodies, we determined that while all liprins show punctate staining throughout the brain, they each have unique distribution over the different regions of the brain. While liprin-α2 is enriched in the hippocampus, liprin-α3 is most highly expressed in the cerebral cortex and liprin-α4 in the cerebellum. Our studies focused on liprin-α1 and liprin-α2, however, further studies of the unique features of liprin-α3 and liprin-α4 will provide insight into the relevance of their different distribution patterns, while the generation of liprin knockout mice could yield interesting tools to study behaviors related to those particular regions of the brains.

7.1. Liprin-α in Axon Growth, Guidance, and Targeting

Liprin-α2 is enriched in mouse brain from late embryonic stages through maturity and expressed at similar levels throughout the development of hippocampal neurons in culture (Figure 7.1), implying that it is involved in multiple stages of neuronal development and function. The first of these to occur in cultured hippocampal neurons is the differentiation of the axon and its subsequent rapid growth and branching. In *Drosophila*, the liprin-α homolog *dliprin-α* is necessary for the proper targeting of R1-R6 photoreceptor axons in a LAR-dependent manner[91] and R7 photoreceptor axons independently of LAR[92]. In Chapter 3, we studied the importance of the LAR-liprin-α signaling pathway in axon growth and branching in mammalian neurons.

In immature hippocampal neurons, considerable amounts of endogenous liprin-α2 are found in the axonal growth cone (Figure 3.2), the structure at the tip of each axon branch that is responsible for promoting the directed growth of the axon[21]. Liprin-α2 is distributed throughout the growth cone in both the actin containing peripheral domain and the microtubule containing central domain (Figures 1.2 and 3.2). The experiments described in Chapter 3 suggest that liprin-α2 functions in the growth cone primarily as an integral member of a potential protein complex between LAR-RPTP, p140Cap, and cortactin that relays signals found in the extracellular matrix surrounding the cell to the actin and microtubule cytoskeleton within it, thereby contributing to axon outgrowth.

In this respect, we found that LAR acts as a positive regulator of axon growth

A

liprin-α2

actin

E13.5 E16 E18 P1 P5
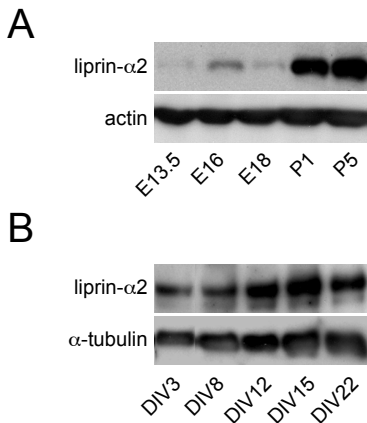
Figure 7.1. *Liprin-α2 is expressed in developing neurons* in vivo *and* in vitro.
(A) Western blots of liprin-α2 protein expression in extracts from developing mouse brains. Actin was used as a loading control.
(B) Western blots of liprin-α2 protein expression in extracts from hippocampal neuron cultures. α-tubulin was used as a loading control.

B

liprin-α2

α-tubulin

DIV3 DIV8 DIV12 DIV15 DIV22

and a negative regulator of axon branching by two molecular pathways. First, LAR promotes axon growth by signaling through liprin-α2 and p140Cap, likely due to regulation of MT growth and dynamics via EB3. It was previously shown that EB3 acts through p140Cap to control dendritic spine morphology[114]. We propose that this interaction could be important for controlling microtubule dynamics in the growth cones of developing axons, but further experiments are needed to verify this hypothesis. Second, LAR inhibits axon branching by negatively regulating cortactin. Local upregulation of cortactin is known to result in actin polymerization and the subsequent formation of new axon branches[115] and knocking down LAR enhances the increased branching seen with cortactin overexpression. In contrast to the role of LAR in axon growth, its control of axon branching seems to occur independently of liprin-α2. Interestingly, p140Cap is also capable of binding to and regulating cortactin[114], indicating that there may be some cross-talk between these pathways. Future experiments involving the direct manipulation of actin and microtubule dynamics as well as the role of LAR phosphatase activity are needed to foster a more complete understanding of the intracellular signaling mechanisms mediated by LAR to control axon development in hippocampal neurons.

While we clearly show in Chapter 3 that LAR is a key molecule in controlling the intracellular mechanisms of axon growth and branching in cultured neurons, these experiments largely ignore another important function of LAR in the hippocampus *in vivo*. In addition to its intracellular phosphatase domain, LAR contains an extensive extracellular region consisting of three Ig-like domain and 4-8 FNIII domains (see Figure 2.2) that allows it to function as a cell adhesion molecule[81]. *In vivo*, this likely

means that LAR not only controls axon growth and branching in general, but plays a critical role in the targeting of axons to their proper locations. The importance of the LAR extracellular domain in LAR clustering and phosphatase activity remains largely unknown, but LAR knockout mice do show disrupted innervation of the dentate gyrus, with some axons stopping prematurely and others growing past their intended targets[112, 113]. The importance of liprin-α2 in axon growth and guidance *in vivo* is also unknown, as to date there is no liprin-α2 knockout mouse. Future analysis of a liprin-α2 knockout mouse and comparison of the liprin and LAR knockouts will lead to greater understanding of the relevance of the liprin-LAR interaction in axon growth in the hippocampus.

7.2. Liprin-α in Dendrite Development

Following a period of rapid axonal outgrowth, axon growth slows and dendrite growth and branching commences[13]. During this time, the dendrites of pyramidal neurons take on a characteristic tapered shape, with each primary dendrite branching off into numerous secondary and tertiary dendrites, though they often lack the distinct apical and basal dendrites seen *in vivo*. In the later stages, dendritic filopodia and spines are also formed and become the sites of excitatory postsynaptic receptor clustering. Importantly, liprins are expressed throughout the neuron, both in axons and dendrites[94], and interact with multiple proteins that are important for dendrite development, including GRIP1[94, 134], LAR, and CaMKII (Ch. 4).

In Chapter 4 we show that liprin-α1 functions as a downstream target of CaMKII signaling in dendrites to control dendritic growth and branching. Activation of CaMKII due to synaptic activity causes the specific degradation of liprin-α1, which is necessary for the establishment of normal dendrite morphology. We observed that CaMKII-dependent liprin-α1 degradation is necessary for the dendritic targeting of LAR, loss of which resulted in a decrease in total dendrites, dendrite length, and dendrite branches. Our data suggests that LAR is transported into dendrites in a liprin-α1-dependent fashion, and that local degradation of liprin-α1 results in the unloading of LAR at synaptically active sites within the dendrite, resulting in activity-dependent growth at that particular site. This hypothesis is supported by the finding that liprin-α1 levels are indeed regulated on a local level by synaptic activity, and that liprins

interact with a variety of kinesin proteins (Table 7.1), including KIF1A[109], KIF5, and KIF21 (Figure 7.2 and data not shown). In *Drosophila*, the liprin-KIF1A interaction is important for synaptic vesicle trafficking, but the significance of that and the other liprin-KIF interactions is unclear in mammalian cells. Future experiments that further characterize the association between liprins and KIFs could greatly improve our knowledge of how liprins and other synaptic proteins are differentially trafficked to pre- and postsynaptic sites, and how the selection of different motor proteins affects the efficiency and specificity of MT-based transport.

7.3. Liprin-α in Formation and Function of Synapses

Thus far, liprin-αs have been best studied in the context of synaptogenesis and synaptic function. Invertebrate liprin mutants display notable presynaptic defects (see Ch. 2), and liprins are frequently identified in mass spectrometry analysis of biochemical synaptic fractions[178]. Furthermore, liprins have been shown to interact with a wide variety of pre- and postsynaptic proteins in invertebrates and mammals (see Ch. 2), and manipulation of those interactions has consequences for the trafficking of numerous synaptic proteins.

Cell adhesion molecules are of key importance not just in axon pathfinding, but in the establishment and stabilization of nascent synaptic sites. They are responsible for bridging the gap between the pre- and postsynaptic membranes and inducing the clustering of other major synaptic components. Our protein binding and mass spectrometry experiments, combined with previously published data, indicated that multiple cell adhesion molecules are associated with liprins in the brain, including LAR, β-catenin and N-cadherin (through LAR[96]), and neurexin 2 and 3 (likely through CASK), suggesting that liprins are closely associated with cell adhesion molecules and likely to be important in the early assembly of synaptic specializations. This is known to be true in *C. elegans*, where the liprin-α homolog SYD-2 is one of the first proteins to arrive at a newly formed synapse and is necessary for the hierarchical assembly of other synaptic proteins[87, 88]. Our data described in Chapter 5 also supports this conclusion, as the synaptic localization of liprin-α2 is not dependent on other major synaptic scaffolding proteins.

In Chapter 5, we show that liprin-α1 and liprin-α2 are capable of differentially regulating the composition of individual presynapses, due to their different binding

affinities for other synaptic scaffolding proteins. We found that liprin-α2 interacts preferentially with CASK and is both necessary for its synaptic localization and sufficient to recruit it to presynaptic sites, while liprin-α1 binds more strongly to CAST. The upregulation of liprin-α1 at presynapses due to low activity results in the specific loss of bassoon and piccolo at those individual synapses as a result of competition for binding to CAST. These data suggest that liprin-α1 and liprin-α2 control presynaptic composition in opposite directions, with liprin-α2 supporting synapse formation and liprin-α1 facilitating synapse elimination.

Moreover, we show that depletion of liprin-α2 causes a defect in synaptic vesicle release. Additionally, overexpressing liprin-α2 is sufficient to cause increased SV release, while overexpressing liprin-α1 results in decreased SV exocytosis. Therefore, we believe that liprins play critical roles in the control of synaptic transmission on both sides of the synapse, likely due to their ability to control the protein composition of individual synaptic sites.

7.4. Liprin-α in Maintenance and Plasticity of Synapses

Even in maturity, synapses in the hippocampus remain tremendously plastic. That is, the molecular composition and the strength of synaptic transmission at an individual
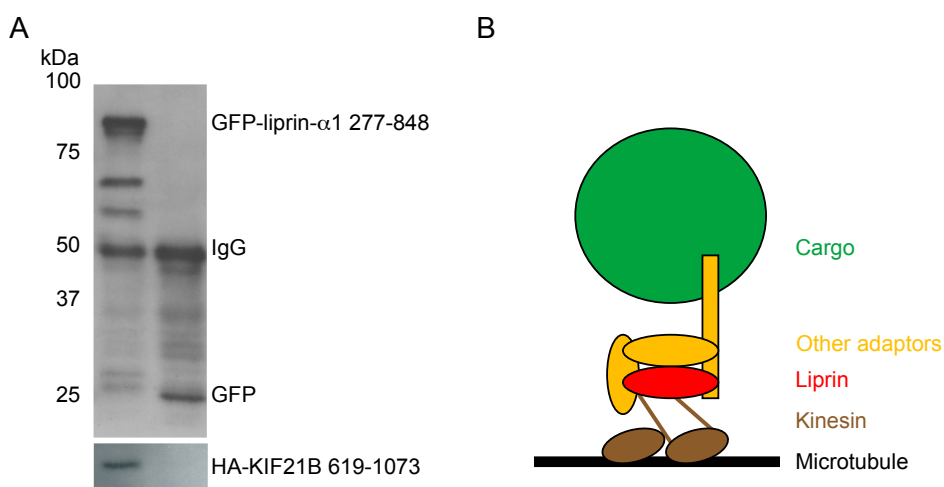
Figure 7.2. *Liprins interact with kinesins.*
(A) Western blots of immunoprecipitation of GFP-liprin-α1 aa 277-848 and coimmunoprecipitation of HA-KIF21B aa 619-1073 from HeLa cell extracts.
(B) Schematic diagram of interaction between liprins and kinesins to traffic cargo along microtubules.

Identified protein	α1		α2		α3		α4		β1		β2		
	H	B	H	B	H	B	H	B	H	B	H	B	
liprin family proteins													input
α-subfamily													
liprin-α1 (PPFIA1)	#	#	13	7	7	5	13	5	2	-	-	-	50
liprin-α2 (PPFIA2)	13	10	#	#	6	-	15	12	-	3	-	-	53
liprin-α3 (PPFIA3)	10	8	8	5	#	#	7	5	-	-	-	-	58
liprin-α4 (PPFIA4)	-	4	17	8	4	-	#	#	-	-	-	-	52
β-subfamily													
liprin-β1 (PPFIBP1)	-	2	11	8	6	5	7	5	#	#	5	4	79
liprin-β2 (PPFIBP2)	-	-	-	-	-	-	3	-	5	4	#	#	57
kinesin motor protein family													function
kinesin-1													
KIF5A	-	5	2	-	3	-	-	-	-	-	-	-	organelle
KIF5B	-	-	3	-	-	-	-	-	-	-	-	-	transport
KIF5C	3	-	2	-	-	-	-	-	-	-	-	-	
kinesin-2													
KIF3A	-	-	-	3	3	-	-	-	-	-	-	-	organelle
KIF3B	-	-	8	-	-	-	-	-	-	-	-	3	transport
kinesin-3													
KIF1A	-	2	-	3	3	3	-	3	-	3	-	-	
KIF13A	-	-	6	6	-	3	-	-	-	-	-	-	organelle
KIF13B	3	-	-	6	-	-	-	4	3	2	4	-	transport
KIF16B	-	-	-	-	-	3	-	-	-	-	-	2	
kinesin-4													
KIF7	12	5	12	9	2	-	5	12	-	3	-	-	
KIF21A	4	-	6	-	-	-	-	-	3	2	-	-	unknown/
KIF21B	-	-	2	2	3	-	2	-	-	-	-	-	multiple
KIF27	8	2	-	-	3	-	-	-	-	-	-	-	
kinesin-9													
KIF6	-	-	-	2	3	2	-	2	-	2	-	-	unknown
KIF9	-	-	-	-	-	-	-	3	-	4	-	-	
kinesin-11													
KIF26A	-	-	2	-	3	-	-	-	-	-	-	-	signal
KIF26B	3	-	-	-	6	-	-	-	-	-	6	-	trans.
kinesin-13													
KIF2A	3	-	-	-	-	-	-	-	-	1	-	-	MT depo-
KIF2B	-	-	3	-	-	-	-	-	-	-	2	-	lymeriza-
KIF2C (MCAK)	-	3	-	-	-	-	-	3	-	-	-	-	tion

Table 7.1. *Binding partners of bio-GFP-liprin proteins from HEK293 cells and brain P2 extracts identified by mass spectrometry.*
The table shows liprin binding proteins identified with a significant Mascot score in the pull down with streptavidin beads from extracts of HEK293 cells co-expressing each of the bio-GFP-liprin and biotin ligase BirA (column H). The number of unique peptides identified from bio-GFP-liprin pull downs using the P2 fraction from total rat brain is indicated (column B). For each identified protein, the list is filtered for duplicates and shows the number of unique peptides. The list is corrected for background proteins which were identified in a control pull-down from HEK293 cells expressing bio-GFP and BirA. Only proteins with at least 3 unique peptide hits in one of the liprin samples are shown.

synapse are constantly being modified in response to activity, even as its neighbors remain unchanged. In spite of the fact that liprins are known to be important for synaptogenesis and trafficking of synaptic proteins, their role in synaptic plasticity has not previously been explored. As in invertebrates, mammalian liprins are major components of the active zone and interact with and influence the distribution of numerous other active zone proteins. The findings in Chapters 4 and 5 represent exciting new knowledge about how liprins are regulated globally and locally, and provide a basis for the further study of liprins in synaptic plasticity.

Recently a tremendous amount of work has gone into determining the rates of protein turnover of synaptic scaffolding proteins and what role that plays in synaptic function. While some proteins, such as bassoon[69] are exchanged at relatively low frequencies (on the order of hours), others exchange almost continuously (on the order of minutes). In Chapters 4 and 5 we show that liprin-α1 and liprin-α2 are both highly dynamic and short-lived components of the synaptic machinery. Both mammalian liprin-α1 and liprin-α2 contain two APC destruction box motifs, and disrupting liprin-α degradation by the proteosome affects both total liprin levels and the stability of liprin at presynapses. Those sites are conserved from *Drosophila*, where the APC/C acts through *dliprin-α* to control synapse size[130]. Though we show that liprin-α1 APC- and CaMKII-dependent degradation is important for dendrite development in mammalian neurons, the significance of liprin-α2 degradation by APC is not yet known. The rapid turnover rates of presynaptic liprins, however, likely contribute to their ability to influence the activity levels of individual synapses through the recruitment and/or elimination of other synaptic proteins.

In addition to their general defect in synaptic vesicle release, liprin-α2 deficient hippocampal autapses also show a decrease in paired-pulse depression indicative of an impairment in short-term presynaptic plasticity. This is consistent with the idea that liprins act locally to rapidly influence synaptic composition and function and generally organize active zones to promote synaptic vesicle release. Comprehensive analysis of synaptic transmission and plasticity in the hippocampus liprin-α2 mutant mice would contribute greatly to our knowledge of the importance of liprins in these processes.

Liprin-α2 is expressed at very low levels in non-neuronal tissue, and at particularly high levels in the hippocampus (Ch. 2)[106], raising the possibility that the phenotype of a liprin-α2 knockout mouse may be specific to the hippocampus. Furthermore,
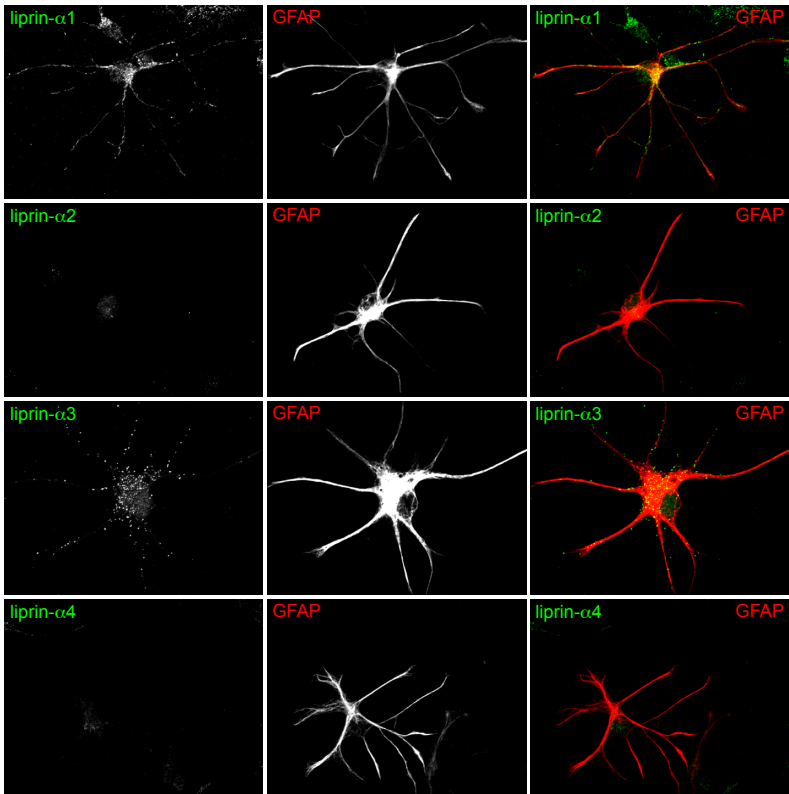
Figure 7.3. *Liprin-α1 and liprin-α3 are present in glial cells.* Representative images of endogenous liprin-α in glial cells. GFAP is used to identify astrocytes.
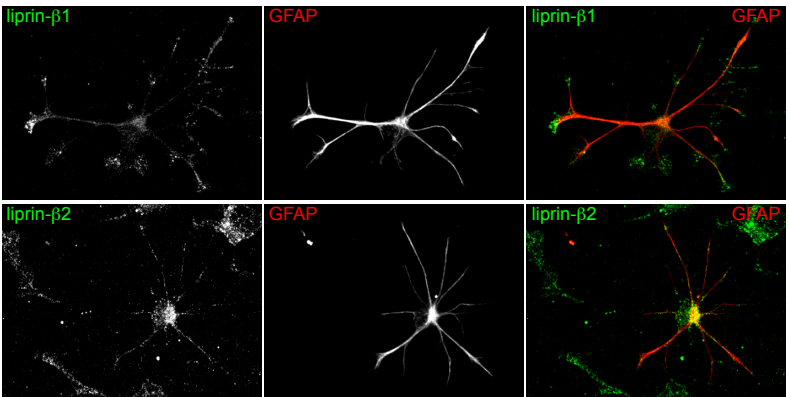
Figure 7.4. *Liprin-β1 and liprin-β2 are present in glial cells.* Representative images of endogenous liprin-β in glial cells. GFAP is used to identify astrocytes.

generation of liprin-α2 knockouts would further clarify the potential of other liprins to compensate for its loss *in vivo*, in spite of the fact that they do not seem to do so *in vitro*. However, since liprin-α2 is likely important for the expression of presynaptic and/or postsynaptic plasticity in the hippocampus, it stands to reason that liprin-α2 conditional knockout mice would also display defects in hippocampal learning and memory. Generation of these mice will be important for the understanding of the contribution of liprin-α2 to learning and memory processes in an *in vivo* setting.

7.5. Liprins in the Rest of the Brain – Future Directions

While the experiments presented in this thesis have focused on the roles of liprin-α1 and liprin-α2 in neuronal development and synaptic function in hippocampal neurons, these and other liprin family members likely function in similar processes in other regions of the brain. We believe that liprin-α1 function is probably conserved throughout the brain, as CaMKII activation is a significant hallmark of synaptic activity at a wide variety of synapses[179, 180]. However, based on general expression patterns and the amino acid sequences of liprin-α2, liprin-α3, and liprin-α4 proteins, it seems likely that they play similar roles in neurons, but in different brain regions. Additionally, the interactions between liprins and GRIP, GIT1, and LAR to control AMPAR surface expression[94, 96, 107] imply that they could play important roles in the expression of postsynaptic long-term potentiation and depression. The distribution of postsynaptic proteins in liprin-α2 knock down neurons has not yet been studied, and will be crucial to determining the complete role of liprins in postsynaptic development and plasticity.

In addition to their expression in neurons, some members of the liprin family are expressed in glial cells (Figure 7.3). Liprin-α2 and liprin-α4 seem to be neuron specific, while the others have moderate to high expression in cultured astrocytes from the hippocampus and the midbrain (Figure 7.3 and data not shown). Interestingly, the liprin-βs, which are less enriched at synapses than liprin-αs, are also found in glial cells (Figure 7.4). Of particular interest is liprin-β1, which is found in large amounts at astrocyte endfeet and can be seen colocalizing with astrocyte markers in clusters near synapses in neuron-glia co-cultures (Figure 7.4). The exploration of this and other liprin functions in different cell types and more *in vivo* model systems will lead to a more comprehensive understanding of the importance of liprin proteins in the mammalian nervous system.

1.   Kandel, E.R., Schwartz, J.H. & Jessell, T.M. Principles of neural science. xli, 1414 p. (2000).

2.   Nagerl, U.V., Willig, K.I., Hein, B., Hell, S.W. & Bonhoeffer, T. Live-cell imaging of dendritic spines by STED microscopy. *Proc Natl Acad Sci U S A* **105**, 18982-18987 (2008).

3.   Miesenbock, G. & Kevrekidis, I.G. Optical imaging and control of genetically designated neurons in functioning circuits. *Annu Rev Neurosci* **28**, 533-563 (2005).

4.   Feinberg, E.H*., et al.* GFP Reconstitution Across Synaptic Partners (GRASP) defines cell contacts and synapses in living nervous systems. *Neuron* **57**, 353-363 (2008).

5.   Sudhof, T.C. & Rothman, J.E. Membrane fusion: grappling with SNARE and SM proteins. *Science* **323**, 474-477 (2009).

6.   Hirokawa, N. & Takemura, R. Molecular motors and mechanisms of directional transport in neurons. *Nat Rev Neurosci* **6**, 201-214 (2005).

7.   Sheng, M. & Hoogenraad, C.C. The postsynaptic architecture of excitatory synapses: a more quantitative view. *Annu Rev Biochem* **76**, 823-847 (2007).

8.   Newpher, T.M. & Ehlers, M.D. Glutamate receptor dynamics in dendritic microdomains. *Neuron* **58**, 472-497 (2008).

9.   Bramham, C.R. Local protein synthesis, actin dynamics, and LTP consolidation. *Curr Opin Neurobiol* **18**, 524-531 (2008).

10.   Lin, A.C. & Holt, C.E. Function and regulation of local axonal translation. *Curr Opin Neurobiol* **18**, 60-68 (2008).

11.   Banker, G.A. & Cowan, W.M. Rat hippocampal neurons in dispersed cell culture. *Brain Res* **126**, 397-342 (1977).

12.   Banker, G. & Goslin, K. Developments in neuronal cell culture. *Nature* **336**, 185-186 (1988).

13.   Dotti, C.G., Sullivan, C.A. & Banker, G.A. The establishment of polarity by hippocampal neurons in culture. *J Neurosci* **8**, 1454-1468 (1988).

14.   Washbourne, P. & McAllister, A.K. Techniques for gene transfer into neurons. *Curr Opin Neurobiol* **12**, 566-573 (2002).

15.   Brummelkamp, T.R. & Bernards, R. New tools for functional mammalian cancer genetics. *Nat Rev Cancer* **3**, 781-789 (2003).

16.   Chalfie, M., Tu, Y., Euskirchen, G., Ward, W.W. & Prasher, D.C. Green fluorescent protein as a marker for gene expression. *Science* **263**, 802-805 (1994).

17.   Shimomura, O., Johnson, F.H. & Saiga, Y. Extraction, purification and properties of aequorin, a bioluminescent protein from the luminous hydromedusan, Aequorea. *J Cell Comp Physiol* **59**, 223-239 (1962).

18.   Tsien, R.Y. The green fluorescent protein. *Annu Rev Biochem* **67**, 509-544 (1998).

19.   Giepmans, B.N., Adams, S.R., Ellisman, M.H. & Tsien, R.Y. The fluorescent toolbox for assessing protein location and function. *Science* **312**, 217-224 (2006).

20.   Shaner, N.C*., et al.* Improved monomeric red, orange and yellow fluorescent proteins derived from Discosoma sp. red fluorescent protein. *Nat Biotechnol* **22**, 1567-1572 (2004).

21.   Goldberg, J.L. How does an axon grow? *Genes Dev* **17**, 941-958 (2003).

22.   Chilton, J.K. Molecular mechanisms of axon guidance. *Dev Biol* **292**, 13-24 (2006).

23.   Pasterkamp, R.J. & Verhaagen, J. Semaphorins in axon regeneration: developmental guidance molecules gone wrong? *Philos Trans R Soc Lond B Biol Sci* **361**, 1499-1511 (2006).

24.   Dent, E.W. & Gertler, F.B. Cytoskeletal dynamics and transport in growth cone motility and axon guidance. *Neuron* **40**, 209-227 (2003).

25.   Bray, D. & Chapman, K. Analysis of microspike movements on the neuronal growth cone. *J Neurosci* **5**, 3204-3213 (1985).

26.   Goldberg, D.J. & Burmeister, D.W. Stages in axon formation: observations of growth of Aplysia axons in culture using video-enhanced contrast-differential interference contrast microscopy. *J Cell Biol* **103**, 1921-1931 (1986).

27.   Lin, C.H. & Forscher, P. Growth cone advance is inversely proportional to retrograde F-actin flow. *Neuron* **14**, 763-771 (1995).

References

28.   Kalil, K. & Dent, E.W. Touch and go: guidance cues signal to the growth cone cytoskeleton. *Curr Opin Neurobiol* **15**, 521-526 (2005).

29.   Ensslen-Craig, S.E. & Brady-Kalnay, S.M. Receptor protein tyrosine phosphatases regulate neural development and axon guidance. *Dev Biol* **275**, 12-22 (2004).

30.   Spruston, N. Pyramidal neurons: dendritic structure and synaptic integration. *Nat Rev Neurosci* **9**, 206-221 (2008).

31.   McAllister, A.K. Cellular and molecular mechanisms of dendrite growth. *Cereb Cortex* **10**, 963-973 (2000).

32.   Sudhof, T.C. & Malenka, R.C. Understanding synapses: past, present, and future. *Neuron* **60**, 469-476 (2008).

33.   McAllister, A.K., Lo, D.C. & Katz, L.C. Neurotrophins regulate dendritic growth in developing visual cortex. *Neuron* **15**, 791-803 (1995).

34.   Polleux, F., Morrow, T. & Ghosh, A. Semaphorin 3A is a chemoattractant for cortical apical dendrites. *Nature* **404**, 567-573 (2000).

35.   Xu, B*., et al.* Cortical degeneration in the absence of neurotrophin signaling: dendritic retraction and neuronal loss after removal of the receptor TrkB. *Neuron* **26**, 233-245 (2000).

36.   Jan, Y.N. & Jan, L.Y. The control of dendrite development. *Neuron* **40**, 229-242 (2003).

37.   Urbanska, M., Blazejczyk, M. & Jaworski, J. Molecular basis of dendritic arborization. *Acta Neurobiol Exp (Wars)* **68**, 264-288 (2008).

38.   Hering, H. & Sheng, M. Dendritic spines: structure, dynamics and regulation. *Nat Rev Neurosci* **2**, 880-888 (2001).

39.   Fiala, J.C., Feinberg, M., Popov, V. & Harris, K.M. Synaptogenesis via dendritic filopodia in developing hippocampal area CA1. *J Neurosci* **18**, 8900-8911 (1998).

40.   Ziv, N.E. & Smith, S.J. Evidence for a role of dendritic filopodia in synaptogenesis and spine formation. *Neuron* **17**, 91-102 (1996).

41.   Bourne, J.N. & Harris, K.M. Balancing structure and function at hippocampal dendritic spines. *Annu Rev Neurosci* **31**, 47-67 (2008).

42.   Marrs, G.S., Green, S.H. & Dailey, M.E. Rapid formation and remodeling of postsynaptic densities in developing dendrites. *Nat Neurosci* **4**, 1006-1013 (2001).

43.   Okabe, S., Miwa, A. & Okado, H. Spine formation and correlated assembly of presynaptic and postsynaptic molecules. *J Neurosci* **21**, 6105-6114 (2001).

44.   Trachtenberg, J.T*., et al.* Long-term in vivo imaging of experience-dependent synaptic plasticity in adult cortex. *Nature* **420**, 788-794 (2002).

45.   Cheng, D*., et al.* Relative and absolute quantification of postsynaptic density proteome isolated from rat forebrain and cerebellum. *Mol Cell Proteomics* **5**, 1158-1170 (2006).

46.   McAllister, A.K. Dynamic aspects of CNS synapse formation. *Annu Rev Neurosci* **30**, 425-450 (2007).

47.   Scheiffele, P. Cell-cell signaling during synapse formation in the CNS. *Annu Rev Neurosci* **26**, 485-508 (2003).

48.   Murthy, V.N. & De Camilli, P. Cell biology of the presynaptic terminal. *Annu Rev Neurosci* **26**, 701-728 (2003).

49.   Yamagata, M., Sanes, J.R. & Weiner, J.A. Synaptic adhesion molecules. *Curr Opin Cell Biol* **15**, 621-632 (2003).

50.   Linhoff, M.W*., et al.* An unbiased expression screen for synaptogenic proteins identifies the LRRTM protein family as synaptic organizers. *Neuron* **61**, 734-749 (2009).

51.   Woo, J*., et al.* Trans-synaptic adhesion between NGL-3 and LAR regulates the formation of excitatory synapses. *Nat Neurosci* **12**, 428-437 (2009).

52.   Ziv, N.E. & Garner, C.C. Cellular and molecular mechanisms of presynaptic assembly. *Nat Rev Neurosci* **5**, 385-399 (2004).

53.   Schoch, S. & Gundelfinger, E.D. Molecular organization of the presynaptic active zone. *Cell Tissue Res* **326**, 379-391 (2006).

54. Zhen, M. & Jin, Y. Presynaptic terminal differentiation: transport and assembly. *Curr Opin Neurobiol* **14**, 280-287 (2004).

55. Wang, Z.W. Regulation of synaptic transmission by presynaptic CaMKII and BK channels. *Mol Neurobiol* **38**, 153-166 (2008).

56. Wayman, G.A., Lee, Y.S., Tokumitsu, H., Silva, A. & Soderling, T.R. Calmodulin-kinases: modulators of neuronal development and plasticity. *Neuron* **59**, 914-931 (2008).

57. Hsueh, Y.P. The role of the MAGUK protein CASK in neural development and synaptic function. *Curr Med Chem* **13**, 1915-1927 (2006).

58. Spangler, S.A. & Hoogenraad, C.C. Liprin-alpha proteins: scaffold molecules for synapse maturation. *Biochem Soc Trans* **35**, 1278-1282 (2007).

59. Han, K. & Kim, E. Synaptic adhesion molecules and PSD-95. *Prog Neurobiol* **84**, 263-283 (2008).

60. Ehrengruber, M.U., Kato, A., Inokuchi, K. & Hennou, S. Homer/Vesl proteins and their roles in CNS neurons. *Mol Neurobiol* **29**, 213-227 (2004).

61. Scannevin, R.H. & Huganir, R.L. Postsynaptic organization and regulation of excitatory synapses. *Nat Rev Neurosci* **1**, 133-141 (2000).

62. Sudhof, T.C. The synaptic vesicle cycle. *Annu Rev Neurosci* **27**, 509-547 (2004).

63. Verhage, M. & Sorensen, J.B. Vesicle docking in regulated exocytosis. *Traffic* **9**, 1414-1424 (2008).

64. Murthy, V.N. & Stevens, C.F. Reversal of synaptic vesicle docking at central synapses. *Nat Neurosci* **2**, 503-507 (1999).

65. Sudhof, T.C. The synaptic vesicle cycle revisited. *Neuron* **28**, 317-320 (2000).

66. Bredt, D.S. & Nicoll, R.A. AMPA receptor trafficking at excitatory synapses. *Neuron* **40**, 361-379 (2003).

67. Bingol, B. & Schuman, E.M. Synaptic protein degradation by the ubiquitin proteasome system. *Curr Opin Neurobiol* **15**, 536-541 (2005).

68. Ding, M. & Shen, K. The role of the ubiquitin proteasome system in synapse remodeling and neurodegenerative diseases. *Bioessays* **30**, 1075-1083 (2008).

69. Tsuriel, S., *et al.* Exchange and redistribution dynamics of the cytoskeleton of the active zone molecule bassoon. *J Neurosci* **29**, 351-358 (2009).

70. Ehlers, M.D. Activity level controls postsynaptic composition and signaling via the ubiquitin-proteasome system. *Nat Neurosci* **6**, 231-242 (2003).

71. Bingol, B. & Schuman, E.M. Activity-dependent dynamics and sequestration of proteasomes in dendritic spines. *Nature* **441**, 1144-1148 (2006).

72. Kavalali, E.T. Multiple vesicle recycling pathways in central synapses and their impact on neurotransmission. *J Physiol* **585**, 669-679 (2007).

73. Neher, E. & Sakaba, T. Multiple roles of calcium ions in the regulation of neurotransmitter release. *Neuron* **59**, 861-872 (2008).

74. Collingridge, G.L., Isaac, J.T. & Wang, Y.T. Receptor trafficking and synaptic plasticity. *Nat Rev Neurosci* **5**, 952-962 (2004).

75. De Roo, M., Klauser, P., Garcia, P.M., Poglia, L. & Muller, D. Spine dynamics and synapse remodeling during LTP and memory processes. *Prog Brain Res* **169**, 199-207 (2008).

76. Cui, Z., *et al.* Inducible and reversible NR1 knockout reveals crucial role of the NMDA receptor in preserving remote memories in the brain. *Neuron* **41**, 781-793 (2004).

77. Tang, Y.P., *et al.* Genetic enhancement of learning and memory in mice. *Nature* **401**, 63-69 (1999).

78. Serra-Pages, C., *et al.* The LAR transmembrane protein tyrosine phosphatase and a coiled-coil LAR-interacting protein co-localize at focal adhesions. *EMBO J* **14**, 2827-2838 (1995).

79. Serra-Pages, C., Medley, Q.G., Tang, M., Hart, A. & Streuli, M. Liprins, a family of LAR transmembrane protein-tyrosine phosphatase-interacting proteins. *J Biol Chem* **273**, 15611-15620 (1998).

References

80. Zurner, M. & Schoch, S. The mouse and human Liprin-alpha family of scaffolding proteins: Genomic organization, expression profiling and regulation by alternative splicing. *Genomics* (2008).

81. Pulido, R., Serra-Pages, C., Tang, M. & Streuli, M. The LAR/PTP delta/PTP sigma subfamily of transmembrane protein-tyrosine-phosphatases: multiple human LAR, PTP delta, and PTP sigma isoforms are expressed in a tissue-specific manner and associate with the LAR-interacting protein LIP.1. *Proc Natl Acad Sci U S A* **92**, 11686-11690 (1995).

82. Baron, M.K., *et al.* An architectural framework that may lie at the core of the postsynaptic density. *Science* **311**, 531-535 (2006).

83. Serra-Pages, C., Streuli, M. & Medley, Q.G. Liprin phosphorylation regulates binding to LAR: evidence for liprin autophosphorylation. *Biochemistry* **44**, 15715-15724 (2005).

84. Green, J.B., Gardner, C.D., Wharton, R.P. & Aggarwal, A.K. RNA recognition via the SAM domain of Smaug. *Mol Cell* **11**, 1537-1548 (2003).

85. Barrera, F.N., Poveda, J.A., Gonzalez-Ros, J.M. & Neira, J.L. Binding of the C-terminal sterile alpha motif (SAM) domain of human p73 to lipid membranes. *J Biol Chem* **278**, 46878-46885 (2003).

86. Zhen, M. & Jin, Y. The liprin protein SYD-2 regulates the differentiation of presynaptic termini in C. elegans. *Nature* **401**, 371-375 (1999).

87. Patel, M.R., *et al.* Hierarchical assembly of presynaptic components in defined C. elegans synapses. *Nat Neurosci* **9**, 1488-1498 (2006).

88. Dai, Y., *et al.* SYD-2 Liprin-alpha organizes presynaptic active zone formation through ELKS. *Nat Neurosci* **9**, 1479-1487 (2006).

89. Kaufmann, N., DeProto, J., Ranjan, R., Wan, H. & Van Vactor, D. Drosophila liprin-alpha and the receptor phosphatase Dlar control synapse morphogenesis. *Neuron* **34**, 27-38 (2002).

90. Kaufmann, N., Wills, Z.P. & Van Vactor, D. Drosophila Rac1 controls motor axon guidance. *Development* **125**, 453-461 (1998).

91. Choe, K.M., Prakash, S., Bright, A. & Clandinin, T.R. Liprin-alpha is required for photoreceptor target selection in Drosophila. *Proc Natl Acad Sci U S A* **103**, 11601-11606 (2006).

92. Hofmeyer, K., Maurel-Zaffran, C., Sink, H. & Treisman, J.E. Liprin-alpha has LAR-independent functions in R7 photoreceptor axon targeting. *Proc Natl Acad Sci U S A* **103**, 11595-11600 (2006).

93. Stepanek, L., Stoker, A.W., Stoeckli, E. & Bixby, J.L. Receptor tyrosine phosphatases guide vertebrate motor axons during development. *J Neurosci* **25**, 3813-3823 (2005).

94. Wyszynski, M., *et al.* Interaction between GRIP and liprin-alpha/SYD2 is required for AMPA receptor targeting. *Neuron* **34**, 39-52 (2002).

95. Dong, H., *et al.* GRIP: a synaptic PDZ domain-containing protein that interacts with AMPA receptors. *Nature* **386**, 279-284 (1997).

96. Dunah, A.W., *et al.* LAR receptor protein tyrosine phosphatases in the development and maintenance of excitatory synapses. *Nat Neurosci* **8**, 458-467 (2005).

97. Ko, J., Na, M., Kim, S., Lee, J.R. & Kim, E. Interaction of the ERC family of RIM-binding proteins with the liprin-alpha family of multidomain proteins. *The Journal of biological chemistry* **278**, 42377-42385 (2003).

98. Ohtsuka, T., *et al.* Cast: a novel protein of the cytomatrix at the active zone of synapses that forms a ternary complex with RIM1 and munc13-1. *J Cell Biol* **158**, 577-590 (2002).

99. Schoch, S., *et al.* RIM1alpha forms a protein scaffold for regulating neurotransmitter release at the active zone. *Nature* **415**, 321-326 (2002).

100. Wang, Y., Okamoto, M., Schmitz, F., Hofmann, K. & Sudhof, T.C. Rim is a putative Rab3 effector in regulating synaptic-vesicle fusion. *Nature* **388**, 593-598 (1997).

101. Wang, Y., Sugita, S. & Sudhof, T.C. The RIM/NIM family of neuronal C2 domain proteins. Interactions with Rab3 and a new class of Src homology 3 domain proteins. *J Biol Chem* **275**, 20033-20044 (2000).

102. Betz, A., *et al.* Functional interaction of the active zone proteins Munc13-1 and RIM1 in syn-

aptic vesicle priming. *Neuron* **30**, 183-196 (2001).

103.   Augustin, I., Rosenmund, C., Sudhof, T.C. & Brose, N. Munc13-1 is essential for fusion competence of glutamatergic synaptic vesicles. *Nature* **400**, 457-461 (1999).

104.   Olsen, O*., et al.* Neurotransmitter release regulated by a MALS-liprin-alpha presynaptic complex. *J Cell Biol* **170**, 1127-1134 (2005).

105.   Lein, E.S*., et al.* Genome-wide atlas of gene expression in the adult mouse brain. *Nature* **445**, 168-176 (2007).

106.   Zurner, M. & Schoch, S. The mouse and human Liprin-alpha family of scaffolding proteins: genomic organization, expression profiling and regulation by alternative splicing. *Genomics* **93**, 243-253 (2009).

107.   Ko, J*., et al.* Interaction between liprin-alpha and GIT1 is required for AMPA receptor targeting. *J Neurosci* **23**, 1667-1677 (2003).

108.   Hoogenraad, C.C*., et al.* Liprinalpha1 degradation by calcium/calmodulin-dependent protein kinase II regulates LAR receptor tyrosine phosphatase distribution and dendrite development. *Dev Cell* **12**, 587-602 (2007).

109.   Shin, H*., et al.* Association of the kinesin motor KIF1A with the multimodular protein liprin-alpha. *J Biol Chem* **278**, 11393-11401 (2003).

110.   Chagnon, M.J., Uetani, N. & Tremblay, M.L. Functional significance of the LAR receptor protein tyrosine phosphatase family in development and diseases. *Biochem Cell Biol* **82**, 664-675 (2004).

111.   Johnson, K.G. & Van Vactor, D. Receptor protein tyrosine phosphatases in nervous system development. *Physiol Rev* **83**, 1-24 (2003).

112.   Van Lieshout, E.M., Van der Heijden, I., Hendriks, W.J. & Van der Zee, C.E. A decrease in size and number of basal forebrain cholinergic neurons is paralleled by diminished hippocampal cholinergic innervation in mice lacking leukocyte common antigen-related protein tyrosine phosphatase activity. *Neuroscience* **102**, 833-841 (2001).

113.   Yeo, T.T*., et al.* Deficient LAR expression decreases basal forebrain cholinergic neuronal size and hippocampal cholinergic innervation. *J Neurosci Res* **47**, 348-360 (1997).

114.   Jaworski, J*., et al.* Dynamic microtubules regulate dendritic spine morphology and synaptic plasticity. *Neuron* **61**, 85-100 (2009).

115.   Mingorance-Le Meur, A. & O'Connor, T.P. Neurite consolidation is an active process requiring constant repression of protrusive activity. *EMBO J* **28**, 248-260 (2009).

116.   Paul, S. & Lombroso, P.J. Receptor and nonreceptor protein tyrosine phosphatases in the nervous system. *Cell Mol Life Sci* **60**, 2465-2482 (2003).

117.   Erturk, A., Hellal, F., Enes, J. & Bradke, F. Disorganized microtubules underlie the formation of retraction bulbs and the failure of axonal regeneration. *J Neurosci* **27**, 9169-9180 (2007).

118.   Tehrani, S., Tomasevic, N., Weed, S., Sakowicz, R. & Cooper, J.A. Src phosphorylation of cortactin enhances actin assembly. *Proc Natl Acad Sci U S A* **104**, 11933-11938 (2007).

119.   Kennedy, M.B., Beale, H.C., Carlisle, H.J. & Washburn, L.R. Integration of biochemical signalling in spines. *Nat Rev Neurosci* **6**, 423-434 (2005).

120.   Sheng, M. & Kim, M.J. Postsynaptic signaling and plasticity mechanisms. *Science* **298**, 776-780 (2002).

121.   Wong, R.O. & Ghosh, A. Activity-dependent regulation of dendritic growth and patterning. *Nat Rev Neurosci* **3**, 803-812 (2002).

122.   Lisman, J., Schulman, H. & Cline, H. The molecular basis of CaMKII function in synaptic and behavioural memory. *Nat Rev Neurosci* **3**, 175-190 (2002).

123.   Thiagarajan, T.C., Piedras-Renteria, E.S. & Tsien, R.W. alpha- and betaCaMKII. Inverse regulation by neuronal activity and opposing effects on synaptic strength. *Neuron* **36**, 1103-1114 (2002).

124.   Fink, C.C*., et al.* Selective regulation of neurite extension and synapse formation by the beta but not the alpha isoform of CaMKII. *Neuron* **39**, 283-297 (2003).

125.   Colbran, R.J. & Brown, A.M. Calcium/calmodulin-dependent protein kinase II and synaptic

References

plasticity. *Curr Opin Neurobiol* **14**, 318-327 (2004).

126.   Griffith, L.C. Regulation of calcium/calmodulin-dependent protein kinase II activation by intramolecular and intermolecular interactions. *J Neurosci* **24**, 8394-8398 (2004).

127.   Wu, G.Y. & Cline, H.T. Stabilization of dendritic arbor structure in vivo by CaMKII. *Science* **279**, 222-226 (1998).

128.   Gaudilliere, B., Konishi, Y., de la Iglesia, N., Yao, G. & Bonni, A. A CaMKII-NeuroD signaling pathway specifies dendritic morphogenesis. *Neuron* **41**, 229-241 (2004).

129.   Miller, K.E.*, et al.* Direct observation demonstrates that Liprin-alpha is required for trafficking of synaptic vesicles. *Curr Biol* **15**, 684-689 (2005).

130.   van Roessel, P., Elliott, D.A., Robinson, I.M., Prokop, A. & Brand, A.H. Independent regulation of synaptic size and activity by the anaphase-promoting complex. *Cell* **119**, 707-718 (2004).

131.   Konishi, Y., Stegmuller, J., Matsuda, T., Bonni, S. & Bonni, A. Cdh1-APC controls axonal growth and patterning in the mammalian brain. *Science* **303**, 1026-1030 (2004).

132.   Pak, D.T. & Sheng, M. Targeted protein degradation and synapse remodeling by an inducible protein kinase. *Science* **302**, 1368-1373 (2003).

133.   Rechsteiner, M. & Rogers, S.W. PEST sequences and regulation by proteolysis. *Trends Biochem Sci* **21**, 267-271 (1996).

134.   Hoogenraad, C.C., Milstein, A.D., Ethell, I.M., Henkemeyer, M. & Sheng, M. GRIP1 controls dendrite morphogenesis by regulating EphB receptor trafficking. *Nat Neurosci* **8**, 906-915 (2005).

135.   Murphey, R.K. & Godenschwege, T.A. New roles for ubiquitin in the assembly and function of neuronal circuits. *Neuron* **36**, 5-8 (2002).

136.   Hegde, A.N. & DiAntonio, A. Ubiquitin and the synapse. *Nat Rev Neurosci* **3**, 854-861 (2002).

137.   Kuo, C.T., Jan, L.Y. & Jan, Y.N. Dendrite-specific remodeling of Drosophila sensory neurons requires matrix metalloproteases, ubiquitin-proteasome, and ecdysone signaling. *Proc Natl Acad Sci U S A* **102**, 15230-15235 (2005).

138.   Garcia-Alai, M.M.*, et al.* Molecular Basis for Phosphorylation-Dependent, PEST-Mediated Protein Turnover. *Structure* **14**, 309-319 (2006).

139.   Liu, X. & Jones, E.G. Alpha isoform of calcium-calmodulin dependent protein kinase II (CAM II kinase-alpha) restricted to excitatory synapses in the CA1 region of rat hippocampus. *Neuroreport* **8**, 1475-1479 (1997).

140.   Cline, H.T. Dendritic arbor development and synaptogenesis. *Curr Opin Neurobiol* **11**, 118-126 (2001).

141.   Tang, F.*, et al.* Regulated degradation of a class V myosin receptor directs movement of the yeast vacuole. *Nature* **422**, 87-92 (2003).

142.   Atwood, H.L. & Karunanithi, S. Diversification of synaptic strength: presynaptic elements. *Nat Rev Neurosci* **3**, 497-516 (2002).

143.   Rosenmund, C., Rettig, J. & Brose, N. Molecular mechanisms of active zone function. *Curr Opin Neurobiol* **13**, 509-519 (2003).

144.   Jin, Y. & Garner, C.C. Molecular mechanisms of presynaptic differentiation. *Annu Rev Cell Dev Biol* **24**, 237-262 (2008).

145.   Siksou, L.*, et al.* Three-dimensional architecture of presynaptic terminal cytomatrix. *J Neurosci* **27**, 6868-6877 (2007).

146.   Zhai, R.G. & Bellen, H.J. The architecture of the active zone in the presynaptic nerve terminal. *Physiology (Bethesda)* **19**, 262-270 (2004).

147.   Altrock, W.D.*, et al.* Functional inactivation of a fraction of excitatory synapses in mice deficient for the active zone protein bassoon. *Neuron* **37**, 787-800 (2003).

148.   Leal-Ortiz, S.*, et al.* Piccolo modulation of Synapsin1a dynamics regulates synaptic vesicle exocytosis. *J Cell Biol* **181**, 831-846 (2008).

149.   Atasoy, D.*, et al.* Deletion of CASK in mice is lethal and impairs synaptic function. *Proc Natl Acad Sci U S A* **104**, 2525-2530 (2007).

150.   Ho, A.*, et al.* Genetic analysis of Mint/X11 proteins: essential presynaptic functions of a neu-

ronal adaptor protein family. *J Neurosci* **26**, 13089-13101 (2006).

151.   Samuels, B.A*., et al.* Cdk5 promotes synaptogenesis by regulating the subcellular distribution of the MAGUK family member CASK. *Neuron* **56**, 823-837 (2007).

152.   Fernandez-Alfonso, T. & Ryan, T.A. The kinetics of synaptic vesicle pool depletion at CNS synaptic terminals. *Neuron* **41**, 943-953 (2004).

153.   Pyle, J.L., Kavalali, E.T., Piedras-Renteria, E.S. & Tsien, R.W. Rapid reuse of readily releasable pool vesicles at hippocampal synapses. *Neuron* **28**, 221-231 (2000).

154.   Rosenmund, C. & Stevens, C.F. Definition of the readily releasable pool of vesicles at hippocampal synapses. *Neuron* **16**, 1197-1207 (1996).

155.   Takao-Rikitsu, E*., et al.* Physical and functional interaction of the active zone proteins, CAST, RIM1, and Bassoon, in neurotransmitter release. *J Cell Biol* **164**, 301-311 (2004).

156.   Lansbergen, G*., et al.* CLASPs attach microtubule plus ends to the cell cortex through a complex with LL5beta. *Dev Cell* **11**, 21-32 (2006).

157.   Inoue, E*., et al.* ELKS, a protein structurally related to the active zone protein CAST, is involved in Ca2+-dependent exocytosis from PC12 cells. *Genes Cells* **11**, 659-672 (2006).

158.   Shapira, M*., et al.* Unitary assembly of presynaptic active zones from Piccolo-Bassoon transport vesicles. *Neuron* **38**, 237-252 (2003).

159.   Olsen, O., Moore, K.A., Nicoll, R.A. & Bredt, D.S. Synaptic transmission regulated by a presynaptic MALS/Liprin-alpha protein complex. *Curr Opin Cell Biol* **18**, 223-227 (2006).

160.   Mukherjee, K*., et al.* CASK Functions as a Mg2+-independent neurexin kinase. *Cell* **133**, 328-339 (2008).

161.   Calakos, N., Schoch, S., Sudhof, T.C. & Malenka, R.C. Multiple roles for the active zone protein RIM1alpha in late stages of neurotransmitter release. *Neuron* **42**, 889-896 (2004).

162.   Castillo, P.E., Schoch, S., Schmitz, F., Sudhof, T.C. & Malenka, R.C. RIM1alpha is required for presynaptic long-term potentiation. *Nature* **415**, 327-330 (2002).

163.   Margeta, M.A., Shen, K. & Grill, B. Building a synapse: lessons on synaptic specificity and presynaptic assembly from the nematode C. elegans. *Curr Opin Neurobiol* **18**, 69-76 (2008).

164.   Ahmari, S.E. & Smith, S.J. Knowing a nascent synapse when you see it. *Neuron* **34**, 333-336 (2002).

165.   Lise, M.F. & El-Husseini, A. The neuroligin and neurexin families: from structure to function at the synapse. *Cell Mol Life Sci* **63**, 1833-1849 (2006).

166.   Yamada, S. & Nelson, W.J. Synapses: sites of cell recognition, adhesion, and functional specification. *Annu Rev Biochem* **76**, 267-294 (2007).

167.   Hsueh, Y.P. & Sheng, M. Regulated expression and subcellular localization of syndecan heparan sulfate proteoglycans and the syndecan-binding protein CASK/LIN-2 during rat brain development. *J Neurosci* **19**, 7415-7425 (1999).

168.   Hoogenraad, C.C*., et al.* Mammalian Golgi-associated Bicaudal-D2 functions in the dynein-dynactin pathway by interacting with these complexes. *EMBO J* **20**, 4041-4054 (2001).

169.   Kim, E., Niethammer, M., Rothschild, A., Jan, Y.N. & Sheng, M. Clustering of Shaker-type K+ channels by interaction with a family of membrane-associated guanylate kinases. *Nature* **378**, 85-88 (1995).

170.   Brummelkamp, T.R., Bernards, R. & Agami, R. A system for stable expression of short interfering RNAs in mammalian cells. *Science* **296**, 550-553 (2002).

171.   Dresbach, T*., et al.* Assembly of active zone precursor vesicles: obligatory trafficking of presynaptic cytomatrix proteins Bassoon and Piccolo via a trans-Golgi compartment. *J Biol Chem* **281**, 6038-6047 (2006).

172.   Lee, S.H., Valtschanoff, J.G., Kharazia, V.N., Weinberg, R. & Sheng, M. Biochemical and morphological characterization of an intracellular membrane compartment containing AMPA receptors. *Neuropharmacology* **41**, 680-692 (2001).

173.   Carlin, R.K., Grab, D.J., Cohen, R.S. & Siekevitz, P. Isolation and characterization of postsynaptic densities from various brain regions: enrichment of different types of postsynaptic densities. *J*

References

Cell Biol **86**, 831-845 (1980).

174.   Cho, K.O., Hunt, C.A. & Kennedy, M.B. The rat brain postsynaptic density fraction contains a homolog of the Drosophila discs-large tumor suppressor protein. *Neuron* **9**, 929-942 (1992).

175.   Bamji, S.X., *et al.* Role of beta-catenin in synaptic vesicle localization and presynaptic assembly. *Neuron* **40**, 719-731 (2003).

176.   Grigoriev, I., *et al.* Rab6 regulates transport and targeting of exocytotic carriers. *Dev Cell* **13**, 305-314 (2007).

177.   Murthy, V.N., Sejnowski, T.J. & Stevens, C.F. Heterogeneous release properties of visualized individual hippocampal synapses. *Neuron* **18**, 599-612 (1997).

178.   Peng, J., *et al.* Semiquantitative proteomic analysis of rat forebrain postsynaptic density fractions by mass spectrometry. *J Biol Chem* **279**, 21003-21011 (2004).

179.   Hansel, C., *et al.* alphaCaMKII Is essential for cerebellar LTD and motor learning. *Neuron* **51**, 835-843 (2006).

180.   van Woerden, G.M., *et al.* betaCaMKII controls the direction of plasticity at parallel fiber-Purkinje cell synapses. *Nat Neurosci* (2009).

181.   Bekkers, J.M. & Stevens, C.F. Excitatory and inhibitory autaptic currents in isolated hippocampal neurons maintained in cell culture. *Proc Natl Acad Sci U S A* **88**, 7834-7838 (1991).

182.   Wierda, K.D., Toonen, R.F., de Wit, H., Brussaard, A.B. & Verhage, M. Interdependence of PKC-dependent and PKC-independent pathways for presynaptic plasticity. *Neuron* **54**, 275-290 (2007).

Summary

Human thoughts and behaviors result from communication between the cells in our brains, and inside each one of these cells lies an entire world where things are built, packaged, transported, and delivered according to the needs of the cell at any given moment. Contrary to most other cells, a neuron is built to last a lifetime, and as such, the significance of each of its pieces can vary as the neuron progresses from infancy to maturity. The work presented in this thesis describes the way the liprin-α family of proteins, in particular liprin-α1 and liprin-α2, contributes to neuronal development and ultimately synapse function in the hippocampus. We began by examining how the entire liprin-α family (liprin-α1, α2, α3, and α4) was expressed in the brain. While liprin-α2 is expressed at high levels in the hippocampal neurons, we found very little liprin-α1 in the brain, although it is the predominant liprin-α in the rest of the body. From there, we investigated the importance of liprin-α2 as a component of the LAR signaling pathway that is critical for axon development in immature hippocampal neurons. We found that LAR acts through liprin-α2 to control axon growth and regulates axon branching through a liprin-α2-independent pathway. We described a novel link between LAR and the actin cytoskeleton via cortactin and suggest that liprin-α2 connects LAR to microtubules by interacting with p140Cap and EB3. Following axon outgrowth, neurons begin to develop an extensive dendritic tree. Here, we identified the mechanism by which liprin-α1 is degraded by CaMKII and the proteasome, explaining its low expression in the nervous system. Furthermore, liprin-α1 degradation is necessary for proper dendrite development, as the introduction of stably expressed liprin-α1 results in dysfunctional LAR trafficking, impaired dendrite growth, abnormal dendritic tree shape, and decreased synapse density. Finally, we examined the ways in which liprin-α1 and liprin-α2 differentially affect presynaptic function in mature neurons. We found that while liprin-α2 was essential for efficient synaptic transmission, liprin-α1 was detrimental to it. This seems to be due to discrepancies in protein binding between the two liprin-αs, and highlights the fact that liprin-α proteins are not functionally redundant in mammalian neurons. These experiments represent a considerable step towards understanding liprin-α function in the brain, and provide the basis for future study of liprin-α as well as neuronal development and synapse function in general.

Samenvatting

De gedachten en het gedrag van de mens komen tot stand door communicatie tussen de cellen van onze hersenen. Binnen iedere cel bevindt zich een wereld waar dingen worden gemaakt, verpakt, getransporteerd, en geleverd waar ze op dat moment nodig zijn. In tegenstelling tot de meeste andere cellen, is een neuron gebouwd om een heel leven lang mee te gaan, en daardoor, kan het belang van elk onderdeel van het neuron in de loop der tijd variëren. Het werk dat is gepresenteerd in dit proefschrift beschrijft de manier waarop de liprin-α familie van eiwitten, in het bijzonder liprin-α1 en liprin-α2, bijdragen aan de neuronale ontwikkeling en de uiteindelijke synaps functie in de hippocampus. We zijn begonnen met te onderzoeken waar de liprin-α familie (liprin-α1, α2, α3, en α4) tot expressie komt in het brein. Ondanks dat liprin-α2 in hoge mate tot expressie wordt gebracht in hippocampale neuronen, hebben wij erg weinig liprin-α1 in het brein gevonden, terwijl het de meest voorkomende liprin-α is in de rest van het lichaam. Vervolgens hebben wij onderzocht wat het belang is van liprin-α2 als onderdeel van de LAR signalerings route, die noodzakelijk is voor axonale ontwikkeling van nog niet volgroeide hippocampale neuronen. Wij ontdekten dat LAR via liprin-α2 werkt om axonale groei te controleren en axonale vertakkingen reguleert via een liprin-α2-onafhankelijk route. Wij beschrijven een nieuwe verbinding tussen LAR en het actine cytoskelet via cortactine en suggereren dat liprin-α2 LAR verbindt met microtubuli door een interactie aan te gaan met p140Cap en EB3. Na de groei van het axon begint een neuron aan de ontwikkeling van de dendritische boom. Hier onthullen we het mechanisme waarbij liprin-α1 wordt afgebroken door CaMKII en het proteasoom, wat de lage expressie in het zenuwstelsel verklaart. Bovendien is de afbraak van liprin-α1 nodig voor de juiste ontwikkeling van een dendriet, omdat de introductie van een stabiele vorm van liprin-α1 leidt tot verkeerde LAR verdeling, aangetaste dendriet groei, abnormale vorm van de dendritische boom en een verlaagde synaps dichtheid. Tot slot hebben we onderzocht waarin liprin-α1 en liprin-α2 een differentieel effect hebben op de presynaptische functie in volgroeide neuronen. We vonden dat hoewel liprin-α2 essentieel is voor efficiënte synaps transmissie, liprin-α1 nadelig is. Dit lijkt te komen door de tegenstrijdigheid in eiwit binding tussen de twee liprin-αs en benadrukt het feit dat liprin-α eiwitten niet functioneel in overvloed aanwezig zijn in zoogdier neuronen. Deze experimenten vormen een aanzienlijke stap in het begrijpen van de liprin-α functie in de hersenen, en vormen een basis voor toekomstige studies over liprin-α en de neuronale ontwikkeling en synaps functies in het algemeen.

Curriculum Vitae

<u>Name</u>   Samantha Ann Spangler

<u>Born</u>   November 15, 1981, Charlotte, NC, USA

<u>Education</u>

2003   BS (Biology, minor: Chemistry)
College of Arts and Sciences, University of North Carolina at Chapel Hill, Chapel Hill, NC, USA

2006   MS (Neuroscience)
Department of Neuroscience, Erasmus MC, Rotterdam, The Netherlands

<u>Positions held</u>

2001   Undergraduate student.
Endocrinology Branch, Reproductive Toxicology Divison. United States Environmental Protection Agency. (Dr. Michael G. Narotsky)

2001-2002   Undergraduate student.
Department of Biochemistry and Biophysics, University of North Carolina at Chapel Hill. (Dr. Patricia F. Maness)

2002-2003   Undergraduate student.
Neuroscience Center, University of North Carolina at Chapel Hill. (Dr. Eva S. Anton)

2003-2005   Research Technician.
Picower Institute for Learning and Memory, Department of Brain and Cognitive Sciences, Massachusetts Institute of Technology. (Dr. Morgan Sheng)

2005-Present   PhD Student.
Department of Neuroscience, Erasmus MC. (Dr. Casper C. Hoogenraad)

2009   Visiting PhD Student.
Department of Chemistry and Biochemistry, University of California at San Diego. (Dr. Terunaga Nakagawa)

List of Publications

1. Jaworski J, **Spangler S**, Seeburg DP, Hoogenraad CC, Sheng M. Control of dendritic arborization by the phosphoinositide-3'-kinase-Akt-mammalian target of rapamycin pathway. *J Neurosci.* 2005 Dec 7:25(49):11300-12.

2. Hoogenraad CC, Feliu-Mojer MI, **Spangler SA**, Milstein AD, Dunah AW, Hung AY, Sheng M. Liprinalpha1 degradation by calcium/calmodulin-dependent protein kinase II regulates LAR receptor tyrosine phosphatase distribution and dendrite development. *Dev Cell.* 2007 Apr:12(4):587-602.

3. **Spangler SA**, Hoogenraad CC. Liprin-alpha proteins: scaffold molecules for synapse maturation. *Biochem Soc Trans.* 2007 Nov:35(Pt 5):1278-82. Review.

4. Jaworski J, Kapitein LC, Gouveia SM, Dortland BR, Wulf PS, Grigoriev I, Camera P, **Spangler SA**, Di Stefano P, Demmers J, Krugers H, Defilippi P, Akhmanova A, Hoogenraad CC. Dynamic microtubules regulate dendritic spine morphology and synaptic plasticity. *Neuron.* 2009 Jan 15:61(1):85-100.

5. **Spangler SA**, Schmitz SK, Jaarsma D, de Graaff E, Sheng M, Toonen RF, Hoogenraad CC. Liprin-α2 influences presynaptic plasticity by targeting CASK and RIM. *Submitted.*

6. Malik A, Urbanska M, Macias M, **Spangler SA**, Sheng M, Jaworski J. p70S6K is not sufficient for control of dendritic arborization of hippocampal neurons. *Submitted.*

7. **Spangler SA**, Grigoriev I, de Graaff E, Demmers J, Akhmanova A, Hoogenraad CC. Local upregulation of liprin-α1 causes depletion of presynaptic bassoon. *Submitted.*

Scientific Meetings Attended

April, 2006	7th Joint MGC-Cancer Research UK Graduate Student Conference, Oxford, United Kingdom
June, 2007	6th Dutch Endo-Neuro-Psycho Meeting, Doorwerth, The Netherlands
August, 2007	2nd Westerburg Symposium on "Molecular Dynamics of the Chemical Synapse," Westerburg, Germany (poster presentation)
March, 2008	SILS-CNS Masterclass, Amsterdam, The Netherlands (oral presentation)
June, 2008	7th Dutch Endo-Neuro-Psycho Meeting, Doorwerth, The Netherlands
July, 2008	6th FENS Forum of European Neurosciences, Geneva, Switzerland (poster presentation)
November, 2008	38th Society for Neuroscience Annual Meeting, Washington, DC, USA (oral presentation)
May, 2009	10th Anniversary of the International Institute of Molecular and Cell Biology, Warsaw, Poland (oral presentation)

Acknowledgements

As anyone who has ever written a PhD thesis knows, the polished and smooth finished product betrays very few signs of the rocky road traveled to get there. At every stage of my career thus far, I have been extremely fortunate to have the support of a tremendous number of people, whether they taught me how do experiments, did experiments themselves, or simply offered moral support. This, of course, means that I have a lot of people to thank, so here goes…

First, I'd like to thank my promotor, Chris de Zeeuw, as well as the rest of my thesis committee for taking the time to participate in a day that is certainly much more important for me than it is for any of them. Chris, thank you in particular for your assistance in facilitating my move to the Netherlands, as well as for providing me with a productive place to work for the past four years. Gerard, Ype, and Anna, my reading committee, thank you for your constructive comments on the original draft of this thesis as well as your patience in dealing with a PhD candidate who was off spending the summer halfway around the world at the beach!

To my copromotor and supervisor, Casper, goes the biggest thank you of all. No other person was as influential as you were in every phase of my last four years. Thank you for inviting me on what has been the wildest roller coaster ride of my life… even if both of us would have rather jumped off headfirst at times than stay the course. I especially appreciate your scientific guidance and criticism and hope to one day be able to emulate your uncanny ability to find all the money in the room and stuff it in your pockets.

Naturally, along with Casper comes the rest of the "Casper Lab." I'd like to thank all my fellow lab members for countless lab meetings, practice talks, stolen snacks, and not-always-stolen beers. It's been an explosive four years, as I'm sure the next four (plus) will continue to be in my absence.

Two other labs played a significant role in my time as a PhD student, those of Anna Akhmanova and Teru Nakagawa. I'd like to thank Anna for serving as a second supervisor of sorts (in spite of my hopeless preference for neuronal cells) and the rest of the Akhmanova lab for listening to innumerable stories about my non-Rab6 or plus end-binding protein, as well as lots of "we got another paper published"-cakes. To Teru, thank you for welcoming me into your lab this summer and showing me how to do some "real" biochemistry. And to the rest of the Nakagawa lab, thanks for accepting me as a full-fledged member of the lab, even if I was only around for three months. It's unlikely I'll ever be a true biochemist or EM specialist, but I'll always cherish my time at UCSD.

I'd also like to thank the many people who were influential in my life and career prior to my time in the Netherlands. First, to my family, thank you for your constant support and belief in me, as well as putting up with my decision to pursue my PhD on the other side of the ocean. I promise, this was the last time! And second, to the multitude of people who have fostered my scientific development up to this

point: Mike Narotsky, Susan Bielmeier, Debbie Best, Patricia Maness, Bentley Midkiff, Mona Buhusi, Galina Demyanenko, Eva Anton, Ralf Schmid, Troy Ghashghaei, Morgan Sheng, Zheng Li, and Jacek Jaworski. Each of you spent significant time and effort teaching me, and it is my sincere hope that I have lived up to your expectations of me and will someday be able to do for someone else what you have done for me.

A significant portion of the work in this thesis was done in collaboration with a number of other scientists. For that, I would like to thank Dick Jaarsma, Jeroen Demmers, Linde Kegel, Monica Feliu-Mojer, Aaron Milstein, Anthone Dunah, Morgan Sheng, Sabine Schmitz, Ilya Grigoriev, Esther de Graaff, Anna Akhmanova, Ruud Toonen, and Phebe Wulf. Additionally, I'd like to thank those of you whose experiments, for one reason or another, did not end up in the final version of this thesis and say a special thanks to Nanda Keijzer and Marijn Kuipers for relieving me of my neuron culture duties. I also owe a tremendous debt of gratitude to Linde Kegel, my first (and thus far only) student. Thank you for all of your hard work and enthusiasm. I learned a great deal from working with you, and I am extremely proud that you are continuing your scientific career as a PhD student…I wish you the best of luck!

I'd like to thank a few groups of people who made my time here much more enjoyable/livable. To my first year masters class, thank you for showing me Rotterdam (even if it was from the back of a bike) and teaching me my first (non-obscene) Dutch words. Thank you to the entire administrative staff at the Department of Neuroscience for handling lots of things that no scientist wants to deal with, and especially to Kenneth for your constant cheerfulness and efficiency in taking care of anything, large or small. Also thanks to Edith, Jennifer, Roelof, Jeanette, Patricia, and Petra for making sure that I always had a roof over my head.

On the big day itself, two people will play a particularly important part in my PhD defense, my two paranimfs, and for that, they deserve a special acknowledgement. Papa, very few PhD candidates are lucky enough to have their grandfather by their side for their graduations, much less their entire lives. You (and Grams) have been more important to my siblings and I than I can possibly tell you, and for that I will always be grateful. Joël, I have been lucky to have you as a friend from the time I arrived in Holland to the time I will leave. Such friends are difficult to come by, and I appreciate your supportive shoulder and listening ear. Thank you for all the hard work you've put into making graduation day a success, and I look forward to congratulating Dr. Joël soon as well.

Lastly, I have had the good fortune of having many friends during my stay in the Netherlands. I won't attempt to name you all, as I'll inevitably leave someone out inadvertently, but please know that I am grateful for the time I spent with each one of you, and you will always have a place to stay in the US! Three ladies, though, stand out above the crowd, especially over the past year, so Aleksandra, Petra, and Mary Jo, thank you from the bottom of my heart for late-night phone calls and tequila shots, Friday night dinners, and sojourns to Amsterdam…and the more serious stuff. I owe you!